ASSESSING EPIGENETIC THERAPY IN PRECLINICAL MODELS OF NON-SMALL CELL LUNG CANCER

by
Frank P. Vendetti III

A dissertation submitted to Johns Hopkins University in conformity with the requirements for the degree of Doctor of Philosophy

Baltimore, Maryland
October, 2013

© 2013 Frank P. Vendetti III
All Rights Reserved

Abstract

Epigenetic dysregulation, including aberrant DNA hypermethylation and histone deacetylation, and associated silencing of tumor suppressor genes, is critically involved in the development of non-small cell lung cancer (NSCLC). Targeting key regulators of these processes, DNA methyltransferases and histone deacetylases, can promote re-expression of silenced genes, can produce major clinical responses, and may alter responsiveness to subsequent chemotherapy. Still, the mechanisms responsible for clinical efficacy remain controversial.

To characterize the effects of azacitidine (Aza) and entinostat in preclinical models of NSCLC, we treated cell lines and assessed cytotoxicity and potential synergy at the end of treatment, sustained effects on proliferation, cell cycle progression, and colony formation days later, and effects on tumorigenic potential of xenografts initiated one week after treatment. We also assessed the effects of epigenetic therapy on chemosensitivity of cell lines in viability and colony formation assays. Furthermore, we examined response of cell line and patient derived xenografts to chemotherapy following epigenetic therapy.

Following Aza treatment, proliferation and colony formation were inhibited in H358, H460, and H2170, while proliferation was less affected in H838 and H1299. Tumorigenicity of H358 and H1299 xenografts was also impaired. In cell viability assays, Aza and entinostat were generally not synergistic, or in H1299 cells, were antagonistic. However, the combination of Aza and entinostat at non-toxic doses significantly impaired tumorigenicity of H1299 xenografts compared to either agent alone. To a lesser degree, combinatorial benefit was observed in H460 xenografts, and in

H358 xenografts at higher dose entinostat. Pretreatment with epigenetic therapy did not alter chemosensitivity of H358, H838, H1299, or A549 *in vitro*, but sensitized A549 xenografts and worsened response of H460 xenografts to irinotecan therapy *in vivo*. Combination epigenetic therapy *in vivo* also improved sensitivity of LX7 to repeat treatment with irinotecan following tumor regrowth.

These results indicate that epigenetic therapy can produce durable anti-tumor effects in NSCLC at relatively non-cytotoxic doses, and suggest these effects are, at least in part, mediated through epigenetic mechanisms. In addition, our data demonstrating sensitization of select xenografts to irinotecan provide preclinical support for clinical observations that suggest the potential for epigenetic therapy to sensitize NSCLC to subsequent chemotherapy.

Thesis Advisor/First Reader: Dr. Charles Rudin

Second Reader: Dr. Michael Carducci

Acknowledgements

First and foremost I need to thank my advisor, Dr. Charles Rudin, for his exceptional mentorship, which has been vital to my advancement as a scientist. Dr. Rudin has always encouraged me to explore my scientific interests, but has also provided the needed guidance to keep my research focused. Working in his lab has been an incredibly rewarding experience, and I cannot thank him enough for all of the time and effort he has devoted to my training and my research projects.

I would also like to thank: Dr. Christine Hann, as well as past and present members of the Rudin and Hann labs, for the productive discussions and constructive criticisms regarding this thesis work; my thesis committee members, Dr. Stephen Baylin, Dr. Michael Carducci, and Dr. William Nelson, for their willingness to serve on my advisory committee, and for all of the valuable advice that has helped develop this work; The Stand Up 2 Cancer Epigenetics Dream Team members, many of whom have been collaborators in some capacity, for the hard work and valuable input that has in any way furthered my own research; Dr. James Herman for the project guidance and troubleshooting advice provided during the early part of my thesis work; the Department of Pharmacology for the opportunity to be a part of the graduate program and pursue a doctoral degree; Pharmacology administrative staff who have assisted me through this process; anyone who I may not mentioned who has participated in any way in my scientific advancement.

I also need to acknowledge individuals who have contributed to particular aspects of this work: Dr. John Poirier for his assistance with analysis of the synergy matrix assays; Dr. Cynthia Zahnow for her advice and assistance facilitating the xenograft

tumorigenicity studies; Kirsten Harbom and Robert Beaty of the Zahnow lab for performing tumor cell injections and tumor volume measurements for the xenograft tumorigenicity experiments; Dr. Peng Huang for statistical analysis of A549 and LX7 xenograft data from priming studies; Irina Dobromilskaya for her help with a number of xenografts experiments; Bill Schuler for help with the LX7 and LX14 xenograft experiments; Dr. Jason Howard for assistance with the Matrigel™ colony formation assays; Dr. Tim Burns for help with the cell cycle assay and shRNA knockdown techniques; Michael Topper, who as a rotation student, contributed substantially to the *in vitro* epigenetic "priming" research studies.

Finally, I would like to thank all colleagues, friends, and family who have supported me in my pursuit of this achievement.

Table of Contents

I. Introduction 1

1. Lung cancer background and significance 1

2. Overview of cancer epigenetics 2

3. Epigenetic dysregulation in NSCLC 4

3.1 Aberrant DNA hypermethylation and gene silencing 4

3.2 DNA methyltransferases 7

3.3 Histone deacetylases 9

4. Targeting the NSCLC epigenome 11

4.1 DNMT inhibitors 11

4.2 HDAC inhibitors 14

4.3 Combination epigenetic therapy 17

5. Epigenetic therapy for sensitization and reversal of drug resistance 20

6. Discussion 21

II. Epigenetic therapy alters proliferative and tumorigenic potential of NSCLC 25

1. Introduction 25

2. Results 27

2.1 NSCLC cell lines exhibit differential sensitivity to Aza in cell viability assays 27

2.2 Dose combinations of Aza and entinostat generally do not synergistically impair cell viability in NSCLC cell lines 29

2.3 Epigenetic therapy exerts differential sustained effects on proliferation of NSCLC lines 37

2.4 The cytotoxic effects of overlapping and sequential combination treatment are transient and peak at unique times in H358 43

2.5 Epigenetic therapy *in vitro* reactivated the key tumor suppressor gene, *p16*, and produced durable effects on tumorigenicity *in vivo* 48

2.6 Reactivation of *p16* is not critical for anti-tumor efficacy of epigenetic therapy in H358 xenografts 52

2.7 Epigenetic therapy exerts differential effects on tumorigenicity of NSCLC xenografts 56

3. Discussion 60

4. Materials and Methods 62

III. Epigenetic therapy as a primer for subsequent chemotherapy 71

1. Introduction 71

2. Results 74

2.1 Epigenetic therapy does not sensitize NSCLC cell lines to subsequent chemotherapy in acute cytotoxicity assays 74

2.2 Epigenetic therapy does not augment inhibition of colony growth by subsequent chemotherapy in NSCLC cell lines 82

2.3. *in vitro* combinatorial epigenetic therapy exerts differential effects on *in vivo* chemosensitivity of NSCLC cell line xenografts 87

2.4 *in vivo* combinatorial epigenetic therapy does not sensitize H358 xenografts to cisplatin or irinotecan 92

2.5 Combination epigenetic therapy has utility as a priming therapy in a patient-derived NSCLC xenograft model 95

3. Discussion 102

4. Materials and Methods 105

IV. Conclusions and Future Directions 112

V. References 117

VI. Biographical Sketch 134

List of Tables

Table 1. Histone deacetylases (HDAC) 10

Table 2. Common HDAC inhibitors 14

Table 3. IC50 values for NSCLC cell lines treated with azacitidine. 28

Table 4. Calculated IC50 values for chemotherapy following epigenetic priming. 76

List of Figures

Figure 1. Epigenetic changes in cancer and combinatorial epigenetic therapy. 17

Figure 2. Sensitivity of NSCLC cell lines to azacitidine. 28

Figure 3. The combination of Aza and entinostat does not synergistically inhibit cell viability in NSCLC cell lines. 31

Figure 4. Overlapping, but not sequential, administration of the combination of Aza and entinostat has combinatorial activity against proliferation of H358 cells. 35

Figure 5. Differential effects on proliferation of NSCLC cell lines following epigenetic therapy. 38

Figure 6. Effects of epigenetic therapy on colony growth parallel effects on proliferation. 41

Figure 7. Overlapping and sequential combination treatment exert transient cytotoxic effects on H358 cells, but do not induce cell cycle arrest. 45

Figure 8. Azacitidine does not induce G1 arrest in H358 cells. 47

Figure 9. Epigenetic therapy *in vitro* reactivates the tumor suppressor gene p16 and exerts durable anti-tumor effects against H358 xenografts *in vivo*. 50

Figure 10. Reactivation of p16 is not critical for anti-tumor efficacy of epigenetic therapy in H358. 53

Figure 11. Effects of *in vitro* epigenetic therapy on tumorigenicity of NSCLC xenografts. 57

Figure 12. Maximal change in tumor size in response to subsequent chemotherapy following combinatorial epigenetic therapy. 72

Figure 13. Epigenetic priming does not alter chemosensitivity of NSCLC cell lines 79

Figure 14. Epigenetic therapy does not enhance the effects of chemotherapy on colony growth on Matrigel™. 83

Figure 15. Methylcellulose colony formation following chemotherapy is not altered by epigenetic priming. 86

Figure 16. Response of A549 xenografts to irinotecan, but not cisplatin, is augmented by epigenetic therapy. 88

Figure 17. Epigenetic therapy desensitizes H460 xenografts to subsequent chemotherapy. 90

Figure 18. Epigenetic therapy *in vivo* does not sensitize H358 xenografts to immediate subsequent chemotherapy. 93

Figure 19. Epigenetic therapy does not extend duration response to gemcitabine in a patient derived xenograft model of squamous cell carcinoma. 96

Figure 20. Epigenetic therapy sensitizes a patient derived model of adenocarcinoma to repeat treatment with irinotecan, but does not sensitize to cisplatin. 99

I. Introduction

1. Lung cancer background and significance

Lung cancer remains one of the most commonly diagnosed cancers worldwide, and the leading cause of cancer related death [1]. More than 228,000 new cases are expected in 2013 in the United States alone [2]. Approximately 80% of cases are non-small cell lung cancer (NSCLC), comprised of several histological subtypes, predominantly adenocarcinoma (AdC) and squamous cell carcinoma (SqCC), and to a lesser extent, large cell carcinoma (LCC). In the past decade, identification of *EGFR* mutations and ALK fusions has led to advances in the treatment of NSCLC, particularly AdC, through the use of targeted therapies [3-5]. While other driver mutations may also represent viable therapeutic targets, they occur at low frequency in AdC, with nearly half of cases still lacking a defined driver mutation, and have been less well defined in SqCC [6]. As a result, therapeutic options are limited for many patients. In addition, acquired resistance to existing targeted agents and disease recurrence present further challenges, and highlight the need for alternative treatment strategies [7-9].

One such strategy of interest involves pharmacological modulation of the NSCLC epigenome, since, unlike genetic alterations, epigenetic modifications can be reversed through inhibition of mediating enzymes. This introductory chapter discusses the underlying epigenetic landscape and the therapeutic utility of targeting DNA methyltransferases (DNMTs) and histone deacetylases (HDAC) to reverse aberrant gene silencing in NSCLC.

2. Overview of cancer epigenetics

Human cancers contain widespread epigenetic abnormalities, including global DNA hypomethylation, region-specific DNA hypermethylation, global histone hypoacetylation, and other aberrant histone modification patterns, that alter gene expression and disrupt normal cell behavior [10-12]. The first of these to be described was global hypomethylation, which is known to cause activation of repetitive elements, genomic instability, and expression of oncogenes, all of which contribute to carcinogenesis [13-15]. Loss of both histone H4 lysine 16 acetylation (H4K16ac) and lysine 20 trimethylation (H4K20me3) appears to be another hallmark of early epigenetic dysregulation in cancer, and is associated with hypomethylated repetitive DNA regions [16]. In the last few years, emerging data has suggested several large scale epigenetic alterations in cancer, that have as of yet not been fully characterized. It appears that differentiation-specific H3K9me2 across large chromatin regions is lost in many cancer cells. These regions are characterized by a relatively low density of genes, which are generally CpG-poor. It has been suggested that these alterations may contribute to phenotypic plasticity in cancer [17]. DNA methylation occurs primarily (but not exclusively) at the cytosine residue of CpG dinucleotides, which are unevenly distributed in the genome, clustering in "CpG islands" often located in the vicinity of gene promoters and other regulatory elements, flanked by so-called "shores." Studies in several tumor types provide evidence that a significant portion of differential methylation in cancer occurs outside of CpG islands, in conserved CpG island shore regions and in large blocks of general hypomethylation. Methylation across the cancer genome is quite variable, and may contribute to tumor heterogeneity [18, 19].

The most extensively studied epigenetic abnormality in cancer is hypermethylation of CpG island promoter regions and associated transcriptional repression of genes. It is well established that aberrant methylation, which can affect hundreds of genes in a given cancer, including numerous tumor suppressor genes (TSGs), plays a critical role in carcinogenesis. Hypermethylated and transcriptionally silenced genes are associated with compact heterochromatin characterized by loss of active H3K9ac and H3K4me3 and gain of repressive H3K27me3 and H3K9me2/me3 histone marks [11, 12]. While this has been known for some time, only in recent years have we begun to better understand the complexity of *de novo* methylation and gene silencing in cancer. In stem cells, genes involved in regulation of development and differentiation normally exhibit a poised transcriptional state in which surrounding chromatin is maintained in a bivalent state manifest by coexistence of both repressive H3K27me3 and activating H3K4me3 marks. In cancer cells, these genes often lose this plasticity and become more stably repressed by addition of repressive H3K9me2 and H3K9me3 marks and DNA promoter region methylation [20-25]. While it has become evident that aberrant gene silencing in cancer is a complex process involving histone methylation and multiple mediating enzymes [26], it remains clear that removal of histone acetylation by HDAC enzymes plays a critical role in transcriptional repression of TSGs, particularly considering laboratory findings that histone deacetylation and methylation can trigger chromatin inactivation and gene silencing prior to DNA methylation [27-29]. A recent report by Coolen et al. further highlights the important of HDACs in gene silencing. The authors identified, in prostate cancer, regions of long-range epigenetic silencing (LRES), approximately 2Mb in size, that typically contain silenced tumor suppressor and miRNA

genes. These regions contained distinct subdomains of different silencing marks, including DNA methylation, H3K9me2, and H3K27me3, but the common feature through LRES was loss of H3K9ac, emphasizing the importance of deacetylation in establishing and maintaining these silenced regions [30].

3. Epigenetic dysregulation in NSCLC

3.1 Aberrant DNA hypermethylation and gene silencing

Loss of gene function, whether by genetic alteration or epigenetic silencing, results in disruption of a variety of critical cellular processes, providing the framework for oncogenic transformation. In NSCLC, focal hypermethylation and silencing of TSGs affects numerous key biological processes, including cell cycle regulation (*p16*), DNA repair (*MGMT*), apoptosis (*DAPK*), regulation of RAS (*RASSF1A*) and Wnt (*APC*) signaling, and suppression of invasion (*CDH13*, *TIMP3*), among many others [11, 31-33]. Indeed, TSG silencing contributes to virtually all of the hallmarks of cancer [34]. Candidate gene based studies have demonstrated that hypermethylation of TSGs including *p16*, *MGMT*, *RASSF1A*, and *APC*, often occurs early during neoplasia and increases during progression to carcinoma, pointing to the involvement of these events in both initiation and progression of disease [33, 35-37]. Clinically, candidate gene approaches have linked methylation and silencing of TSGs, including genes methylated during the earliest stages of disease, to recurrence after surgical resection. For example, one study found that methylation of *p16* and concomitant loss of p16 protein expression correlated with shorter survival after resection [38]. Another study noted that concurrent methylation of *p16* and *CDH13*, or with *APC* or *RASSF1A*, is strongly associated with

recurrence following resection of stage I NSCLC [39]. It has been suggested that early silencing events may facilitate abnormal expansion of precancerous cells and allow for accumulation of genetic and epigenetic abnormalities needed to drive tumorigenesis [12, 40]. The existence of abnormal clones harboring early TSG silencing in adjacent, nonresected tissue may contribute to increased risk of recurrence.

As new approaches and technologies have been developed in recent years, a shift from candidate gene based approaches to genome-wide methylation profiling has occurred, allowing for more comprehensive interrogation of DNA methylation patterns in NSCLC. Using the Illumina Infinium HumanMethylation27K array platform, Selamat et al. identified more than 700 common differentially methylated genes among 59 AdC and matched normal tissues. Hierarchical clustering revealed the existence of two distinct subgroups within the AdC tumors, with one subgroup exhibiting greater DNA methylation and a higher likelihood of concomitant mutation in *Kras*. Differential methylation of these genes correlated with altered expression of 221 genes involved in pathways including cell cycle control, differentiation, epithelial-to-mesenchymal transition, and proliferation. Roughly 75% of these altered genes were frequently hypermethylated and silenced in tumors [41].

Shinjo et al. recently classified AdC tumors based on the presence of a CpG island methylator phenotype (CIMP), originally defined in colon cancer following observation of tumors with consistent, dense, cancer-specific hypermethylation of multiple loci [42]. Using methylated CpG island amplification microarray (MCAM) analysis, the authors identified a novel six gene CIMP marker panel. The authors then assessed methylation status of their CIMP markers in 85 AdC data sets from The Cancer

Genome Atlas (TCGA) database, which were generated using the Infinium HumanMethylation27K array platform. Interestingly, while this array contained promoter region probes for only three CIMP markers (*ACAN*, *CCNA1* and *GFRA1*), methylation of one or two markers correlated with increased overall methylation of the most variable probes in the TCGA data sets [43]. However, the value of these CIMP markers as predictors of overall methylation in AdC is currently unclear.

A recent study by Lockwood et al. incorporated genome-wide methylation, expression, and copy number analysis to compare AdC and SqCC primary tumors. Subtype-specific gene expression patterns resulting from both copy number disparity and differential methylation were discovered, and correlated with disruption of distinct pathways. SqCC tumors exhibited altered expression of histone modifying enzymes as a result of copy number alteration and greater overall hypomethylation. The authors noted several genes, including the tumor suppressor *FHIT*, silenced in SqCC due to both copy number loss and hypermethylation [44].

Taken together, these data both add to the wealth of existing evidence that aberrant DNA hypermethylation is critically involved in malignancy, and highlight that, like genetic alterations, epigenetic abnormalities are highly variable in NSCLC, both within and across histological subtypes. While tumor heterogeneity presents major challenges for the use of targeted agents, due to the potential for variable compensatory mechanisms and modes of resistance, modulation of epigenetic abnormalities, such as aberrant hypermethylation, may provide advantages through the ability to broadly reprogram the epigenetic landscape, simultaneously affecting multiple cellular pathways.

3.2 DNA methyltransferases

Three catalytically active DNA methyltransferases, DNMT1, DNMT3a, and DNMT3b, mediate the methylation of cytosine residues in CG dinucleotides in mammalian cells. DNMT1 is primarily involved in maintenance of methylation following replication and DNA repair. DNMT3a and DNMT3b facilitate *de novo* methylation, and appear to have a maintenance role as well [45, 46]. In cancer cells, hypermethylation of genes may be particularly dependent on both DNMT1 and DNMT3b [47, 48], and DNMT1 may have a cancer-specific role in *de novo* CpG island hypermethylation [49].

Dysregulated expression of these enzymes has been implicated as a cause of aberrant methylation in cancer. All three DNMTs are overexpressed in NSCLC, and DNMT1 overexpression in particular has been correlated with poor prognosis [50-53]. Dysregulation of expression may occur through various mechanisms. One study showed that loss of p53 function accompanied by overexpression of Sp1, a known transcriptional activator of DNMT1, is associated with DNMT1 overexpression in NSCLC tumors [52]. Another demonstrated that MDM2 overexpression and concurrent low Rb expression correlate with upregulated DNMT3a [53]. Both studies associated elevated DNMT levels with increased methylation of candidate TSGs. Several microRNAs are also known to modulate DNMT expression [54]. For example, miR-29 family members downregulate DNMT3a and DNMT3b directly, and DNMT1 indirectly, through interaction with the 3' untranslated region and Sp1, respectively [55, 56]. Decreased miR-29 has been associated with increased DNMT3a and DNMT3b expression in NSCLC [55]. Loss of temporal control of DNMT1 protein stability has been observed in breast cancer, resulting in elevated protein levels independent of transcript upregulation [57]. This impaired

proteasomal degradation of DNMT1 results, at least in part, from association with the chaperone Hsp90, maintained in a deacetylated state by HDAC1 [58]. The histone demethylase LSD1 has also been reported to stabilize DNMT1 by removal of SET7/9 mediated lysine methylation [59]. Overexpression of HDAC1 and LSD1, which occurs in NSCLC and has been associated with poor prognosis [60-62], may also contribute to the dysregulation of DNMT1 by promoting protein stability. In addition, variant forms of DNMT3b, resulting from alternative promoters and alternative transcript splicing, have been identified and are commonly expressed in NSCLC but not in normal lung. Expression of these variants has been associated with TSG methylation and poor clinical outcome [63, 64].

While overexpression has implicated all three DNMTs as contributors to oncogenesis in NSCLC, the actual role of DNMT3a is less clear. A recent study found loss of DNMT3a expression in 13/28 NSCLC patient tumors, resulting from loss of heterozygosity (LOH) in five cases, and unknown mechanisms in the remaining eight. In addition, three tumors harbored previously unreported mutations in DNMT3a, however none were associated with loss of expression [65]. While the consequences of DNMT3a loss in NSCLC are not yet understood, recent preclinical evidence suggests a paradoxical tumor suppressor role for this enzyme. Work using a conditional *Kras* mutant AdC mouse model demonstrated that loss of DNMT3a was associated with altered expression of nearly 2000 genes, decreased methylation across the majority of differentially methylated regions, including gene bodies, and enhanced proliferation and progression of more poorly differentiated tumors. Mechanistic studies were lacking, but the authors speculated that DNMT3a-mediated gene body methylation may promote expression of

differentiation genes, and that DNMT3a loss impairs differentiation of tumor initiating cells [66]. This model is supported by reports that differentiation of certain cell types requires DNMT3a, both for gene body methylation and associated expression of differentiation genes, as well as silencing of genes critically involved in stem cell maintenance [67, 68]. However, this appears contrary to the findings that DNMT3a-mediated gene body non-CpG methylation, which is present in embryonic stem cells, is lost in differentiated fibroblasts, with concurrent reduction in DNMT3a expression [69]. While the exact functions may be tissue and context dependent, these recent findings have important implications, given the occurrence of DNMT3a mutations and dysregulated expression in cancer. Since strategies aimed at reversal of hypermethylation and gene silencing utilize agents that target all enzymatically active DNMTs, it is important to further define the role of DNMT3a in NSCLC.

3.3 Histone deacetylases

Chromatin structure is governed by the dynamic interplay of a multitude of histone modifying enzymes and the post translational modifications they mediate. Histone deacetylases (HDACs) catalyze the removal of acetyl groups from lysine residues on histone tails to induce chromatin compaction and transcriptional repression. There are 18 identified human HDAC isoforms, separated into four classes (Table 1). Classes I, II, and IV contain metalloenzymes that require Zn^{2+} for catalytic activity, whereas class III, or sirtuins, use an NAD^{+} dependent mechanism. Discussion here will be restricted to zinc metalloenzymes, as these are the targets of the majority of investigational and all FDA approved HDAC inhibitors (HDIs). Class I HDACs (1, 2, 3,

8) are ubiquitously expressed in normal tissues and preferentially located in the nucleus, whereas class II (4, 5, 6, 7, 9, 10) and IV HDACs (11) have tissue-specific expression patterns, and move between the nucleus and cytoplasm, or in the case of HDAC6 and HDAC10, are preferentially found in the cytoplasm [70].

Table 1. Histone deacetylases (HDAC)

Class	Isoform	Cofactor	Localization	Expression
I	HDAC1, HDAC2, HDAC3, HDAC8	Zn^{2+}	Primarily in nucleus; HDAC3 and HDAC8 also in cytoplasm	Ubiquitous
IIa	HDAC4, HDAC5, HDAC7, HDAC9	Zn^{2+}	Nucleus and cytoplasm	Tissue specific
IIb	HDAC6, HDAC10	Zn^{2+}	Primarily in cytoplasm; HDAC10 also in nucleus	Tissue specific
III	SIRT1-7	NAD+	Varies with enzyme	Varies with enzyme
IV	HDAC11	Zn^{2+}	Nucleus and cytoplasm	Tissue specific

Class I enzymes are generally involved in proliferation and survival, while class II HDACs have been implicated in differentiation and development [70]. As reviewed elsewhere, HDACs alter the activity of many non-histone targets through deacetylation [70, 71]. One example, previously mentioned, is the chaperone Hsp90, whose deacetylation by HDAC1 or HDAC6 allows it to interact with DNMT1, which prevents proteasomal degradation of the methyltransferase [58, 71].

HDAC expression is commonly altered in cancer, and overexpression has been noted in multiple cancer types [70, 71]. As mentioned previously, HDAC1 is highly overexpressed in NSCLC [60, 61]. In addition, one study found upregulation of HDAC3

protein in 92% of squamous cell tumors [72]. Interestingly, it has been reported that several class II enzymes, particularly HDAC5 and HDAC10, are downregulated in NSCLC, and downregulation of either is a negative prognostic factor [73]. In addition to expression alterations, HDAC activity may be dysregulated due to existing aberrant methylation. HDACs can be recruited to sites of hypermethylation through interaction with methyl-binding proteins, DNMT, and co-repressors such as mSin3A [10, 12], resulting in the targeting of HDACs to inappropriate chromatin sites, and aberrant patterns of deacetylation. Finally, HDACs, through their integral role in heterochromatin formation, may indirectly contribute to increased genetic variation in cancer, as regions of repressive chromatin have been associated with increased mutation rates in lung, colon, melanoma, and leukemia cells [74].

4. Targeting the NSCLC epigenome

4.1 DNMT inhibitors

The significance of aberrant hypermethylation cancer in general, along with the frequent dysregulation of DNMTs levels in lung cancer, certainly makes these enzymes attractive drug targets. Ironically, agents that target DNMTs have existed for more than 40 years, long before hypermethylation in cancer was discovered. It was not until 1980 that Taylor and Jones discovered that azacitidine (5-azacytidine, Vidaza®) and decitabine (5-aza-2'-deoxycytidine, Dacogen®), which were originally developed as cytotoxic drugs, could induce loss of DNA methylation and differentiation of cells [75]. The generally accepted mechanism involves incorporation of these azanucleosides into DNA, followed by the covalent trapping of DNMTs to the DNA, and subsequent proteasomal

degradation of the enzymes [76-80]. DNA damage and impaired DNA synthesis resulting from these DNA-DNMT adducts is likely responsible for much of the cytotoxicity induced by these agents, particularly at higher doses [77, 78, 80-83]. While decitabine is specific to DNA, azacitidine is also incorporated into RNA, which may explain differential effects of these agents with regard to toxicity and gene reactivation [78, 84, 85].

The hypomethylating effects of these agents are best realized at doses below the cytotoxic range [75], and it was not until lower dose, prolonged treatment regimens were employed that this was appreciated clinically. As a result, testing of low dose regimens resulted in FDA approval of both agents in the mid-2000s for treatment of myelodysplasia (MDS), and of decitabine for acute myelogenous leukemia (AML) [80]. The value of lowered doses has been further defined in the laboratory. Tsai et al. demonstrated that relatively low doses of demethylating agents could impair the clonogenic and tumorigenic capacity of leukemia and breast cancer cell lines, and induce reactivation of tumor suppressor genes to restore critical regulatory pathways. In addition, the authors showed *in vivo* that lower doses of azacitidine were as or more effective than higher doses at inhibiting growth of breast cancer xenografts in mouse models [86].

Early trials using demethylating agents in advanced lung cancer showed limited success. In a pilot phase I/II study, three of 15 stage IV NSCLC patients treated with high-dose decitabine (200-660mg/m^2) demonstrated evidence of prolonged survival, with one individual surviving a surprising 81 months. However, only six patients received more than one decitabine infusion because 5-7 week intervals were needed to manage

hematopoietic toxicities, no doubt limiting the potential for efficacy in this trial [87]. Schrump et al. conducted a phase I dose escalation study of decitabine, starting at lower doses, in 35 patients with solid tumors, including 20 NSCLC patients. No objective responses were noted, and stable disease was achieved in only four patients, including three SqCC patients, and one patient with small cell lung cancer. Decitabine-induced expression of p16, MAGE-3, or NY-ESO-1 protein (assessed by immunohistochemistry) was observed in approximately one-third of patients. Consistent with repeated exposure to decitabine, one patient with prolonged stable disease exhibited progressive increases in MAGE-3 and NY-ESO-1 mRNA, with markedly increased expression at six and eight months. Interestingly, no patients receiving the highest dose of decitabine ($30mg/m^2/day$) achieved stable disease [88], consistent with the suggestion from myeloid malignancies that lower doses are more effective [80]. While early studies like these caused many to believe demethylating agents were of little use in solid tumors, future studies employing regimens successfully used in MDS and AML may provide different results.

While not as extensively studied as azacitidine and decitabine, other demethylating agents, such as the anti-hypertensive hydralazine and the cytidine analog zebularine, have been tested in the clinic, but with limited success. One promising agent is SGI-110, a dinucleoside containing decitabine with improved stability [89] that is currently being tested in a phase I/II trial in MDS and AML. It remains to be seen whether this agent will be useful for the treatment of NSCLC.

4.2 HDAC inhibitors

Since the discovery that trichostastin A (TSA) inhibited HDACs and caused differentiation and cell cycle arrest in mammalian cells [90], numerous HDAC inhibitors (HDIs) have been synthesized and studied for their potential as anti-cancer agents [71, 91]. To date, only two have been FDA approved: vorinostat (SAHA, Zolinza®) and romidepsin (depsipeptide, Istodax®). Both drugs are approved for use in cutaneous T cell lymphoma, while romidepsin is also approved for treatment of peripheral T cell lymphoma. Current HDIs encompass several chemical classes, and differ in the HDAC isoforms they target (Table 2) [71, 91].

Table 2. Common HDAC inhibitors

Chemical Category	Compound	Deacetylase selectivity
Aliphatic acid	Phenylbutyrate	Class I, IIa
	Valproic Acid (VPA)	Class I, IIa
Hydroxamate	Trichostatin A (TSA)	Class I, II, IV
	Vorinostat (SAHA, Zolinza)	Class I, II, IV
	Panobinostat (LBH589)	Class I, II, IV
	Belinostat (PDX101)	Class I, II, IV
Benzamide	Entinostat (MS-275)	Class I
	Mocetinostat (MGCD0103)	Class I
Cyclic tetrapeptide	Romidepsin (Depsipeptide, Istodax)	Class I

It is currently unknown whether increased selectively of HDIs for specific HDAC isoforms limits toxicities or increases anti-tumor efficacy. Targeting nuclear specific

class I HDACs may have a more specific effect on histone acetylation with fewer effects on "off-target" non-histone cytoplasmic proteins. The relative benefits of narrow vs. broad targeting may be tissue and context dependent, influenced by the roles of epigenetic modulation and of the non-histone HDAC target proteins in a given cancer. One study defined a nine-gene panel in NSCLC cells predictive of sensitivity to TSA and vorinostat, but did not explore whether this panel would be predictive of benefit from a class I-specific HDI [92].

A wide array of phenotypic effects caused by HDI treatment of cancer cells has been documented [70, 91]. HDIs cause G_1-phase cell cycle arrest through activation of p21 and repression of cyclin expression. These agents have been shown to activate both the extrinsic and intrinsic apoptotic pathways by altering expression of death receptors and ligands, as well as the balance of key intracellular pro- and anti-apoptotic regulators [70, 91]. Preclinical studies in NSCLC cell lines have demonstrated that induction of apoptosis in response to HDIs also involves downregulation of checkpoint kinase 1 (Chk1) [93]. HDIs induce generation of reactive oxygen species (ROS) and cause DNA damage, and can downregulate expression of DNA repair genes. In addition, HDIs have been shown to downregulate pro-angiogenic and matrix remodeling genes, suggesting that these agents may be useful in suppressing angiogenesis and metastasis. HDIs also impair glucose metabolism through targeting of the glucose transporter 1 and hexokinase 1 [70]. Finally, HDIs may modulate immunogenicity of cancer cells through upregulation of molecules involved in T-cell and NK cell activation, such as MHC class I and II, CD80/CD86, and MICA/MICB [70, 91].

Due to the small number of NSCLC patients in many of the trials, clinical data for HDI monotherapy in NSCLC is limited. In general, the results in advanced, solid tumors have been disappointing. While well tolerated, these agents typically produce only stable disease as the best response, with rates varying from 15-75% depending on the clinical context and the HDI tested [94-102]. In a small phase II study of vorinostat in patients with relapsed NSCLC, stable disease ranging from 1.4-19.4 months was achieved in 8/14 patients [101]. In another phase II study of vorinostat, 4 of 8 evaluable NSCLC patients achieved stable disease lasting 44-98 days [100]. In a phase II trial of romidepsin, disease stabilization was achieved in 5/15 evaluable NSCLC patients, however this lasted more than four months in only three patients. Interestingly, correlative studies demonstrated that romidepsin induced *p21* expression, H4 acetylation, and a general shift toward expression patterns in adjacent normal bronchial epithelial cells, demonstrating epigenetic modulation in patients [98]. While the available data does indicate that current HDIs alone are unlikely to provide substantial benefit to unselected NSCLC patients, they may have utility in combination with other agents. Vorinostat has been shown to improve response rate to first-line therapy with carboplatinum and paclitaxel in advanced NSCLC, although no survival benefit was seen [103]. Addition of entinostat to erlotinib provided no overall benefit relative to erlotinib alone in advanced, chemo-refractory NSCLC, but appeared to improve survival in a subset of patients with high tumor E-cadherin levels at diagnosis [104].

4.3 Combination epigenetic therapy

Elucidation of the involvement of HDACs in TSG silencing in cancer led to the hypothesis that combined DNMT and HDAC inhibition might result in enhanced or sustained TSG reactivation (Figure 1).

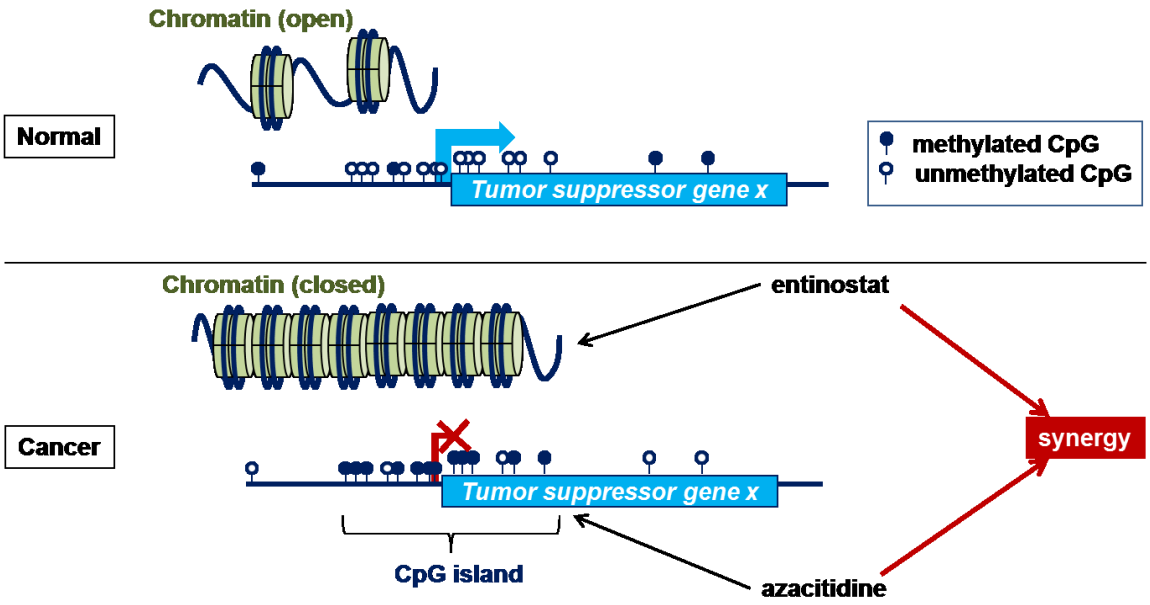

Figure 1. Epigenetic changes in cancer and combinatorial epigenetic therapy.

Upper panel shows a typical tumor suppressor gene in a normal cellular context, with increased density of CpG dinucleotides (defining a CpG island) surrounding the transcriptional start site indicated in the blue arrow. Chromatin in the region of an actively transcribed gene is typically in a relatively open configuration, as shown, with space between nucleosomes allowing access by transcription factors. **Lower panel** shows typical changes associated with epigenetic silencing of a tumor suppressor gene in cancer. DNA methylation is markedly increased within the CpG islands, and chromatin has assumed a closed configuration with tightly packed nucleosomes. Combined epigenetic therapy attempts to reverse these changes: azacitidine results in demethylation of the DNA, and entinostat inhibits histone deacetylase, shifting the chromatin to a

more open configuration. Targeting both of these levels of epigenetic silencing concurrently may lead to synergistic re-expression of tumor suppressors.

This idea does have support from preclinical data. In 1999, Cameron et al. demonstrated that the combination of decitabine and TSA synergistically reactivated silenced TSGs in colon and leukemia cell lines [105]. This was a pivotal paper at the time because it demonstrated that the functional link between DNA methylation and histone deacetylation in gene silencing could be exploited pharmacologically. Shortly after, studies *in vitro* showed additive to synergistic inhibition of DNA synthesis, loss of clonogenicity, and induction of apoptosis in NSCLC cell lines treated with the combination of decitabine and an HDI (phenylbutyrate, depsipeptide, TSA) [106-108]. In addition, the combination of decitabine and phenylbutyrate was shown to synergistically inhibit development of lung lesions following exposure of mice to the carcinogen, NNK [108].

Recently, Belinsky et al. reported efficacy of combined azacitidine and entinostat therapy in immunocompromised rat orthotopic models of AdC. Combination therapy was roughly twice as effective as azacitidine alone in reducing growth of *Kras* mutant Calu-6 tumors, and also markedly reduced growth of two additional *Kras* (A549) and *EGFR* (H1975) mutant tumors. Both therapies induced demethylation and reexpression of numerous genes, including the tumor suppressors *p16* and *p21*, pro-apoptotic genes, and Polycomb (PRC2) target genes, and downregulated expression of the histone methyltransferase and PRC2 component, EZH2. A clear trend toward greater effect on gene expression was seen with combination over azacitidine alone [109]. In addition to showing efficacy against NSCLC models, these studies provide mechanistic insights into

the anti-tumor effects of epigenetic therapy. Not surprisingly, these involved reactivation of key regulators of apoptosis and cell cycle progression, including TSGs commonly hypermethylated in NSCLC.

Despite preclinical evidence supporting the utility of combined epigenetic therapy and successful use of combination regimens in the treatment of AML and MDS [110, 111], initial trial results in solid tumors were underwhelming. The combination of azacitidine and phenylbutyrate lacked evident clinical benefit [112], whereas the combination of azacitidine and valproic acid yielded only stable disease in 14/55 solid tumor patients [113]. However, a very recent phase I/II trial of the combination of azacitidine and entinostat in advanced, chemo-refractory NSCLC patients has renewed substantial interest in this therapeutic strategy. The patient population enrolled in this trial had a median of three prior therapies, and achieved a 6.4 month median survival, similar to that of erlotinib in second and third line therapy (the only FDA approved therapy in this context). While only 2/34 evaluable patients had objective response (1 CR for 14 months, 1 PR for 8 months), another 10 had disease stabilization for at least 12 weeks, with durations of 14 and 18 months in two patients [114]. The durability of these responses was particularly striking. Uncovering biomarkers that predict which patients are likely to derive benefit is important for any therapy. Exploratory results from this cohort suggest that reduction in promoter methylation of two or more of four genes previously associated with disease recurrence [39] in circulating tumor DNA from the peripheral blood may correlate with improved progression free and overall survival.

5. Epigenetic therapy for sensitization and reversal of drug resistance

Another intriguing observation from this trial, which we are continuing to explore, was the observed responses to subsequent chemotherapy following epigenetic therapy in this heavily pretreated population. Several patients, including patients who progressed quickly on epigenetic therapy, seemed to respond surprisingly well to their next therapy. Notably, two patients that received only one subsequent treatment regimen survived 44 and 52 months after epigenetic therapy [114]. Interestingly, the previously mentioned decitabine treated patient that survived 81 months had also received chemotherapy roughly six months after decitabine [87]. While these represent a small number of patients, this certainly raises the question as to whether epigenetic therapy reprograms cancers in a manner that increases susceptibility to later therapies.

Epigenetic mechanisms have been previously implicated in drug resistance [115], providing potential mechanisms for epigenetic therapy priming subsequent response. One study demonstrated decitabine-induced sensitization of mismatch repair-deficient ovarian and colon cancer xenografts to cisplatin, carboplatin, temozolomide, and epirubicin following demethylation and reactivation of the DNA repair gene, *hMLH1* [116]. Another reported that TSA treatment sensitized a cisplatin-resistant AdC cell line to cisplatin by restoring DAPK protein expression [117]. A particularly insightful recent paper described the expansion of drug tolerant clones following treatment of an *EGFR* mutant NSCLC line with an EGFR inhibitor as a result of increased expression of the histone demethylase, JARID1A/KDM5A, loss of H3K4me2/me3 histone marks, and altered IGF1-R signaling [118]. Cells with this altered chromatin were highly sensitive to HDI mediated DNA damage, and treatment with HDIs prevented or suppressed the drug

tolerant phenotype. This study directly implicated a reversible epigenetic mechanism in drug resistance, and demonstrated the ability to revert the phenotype through epigenetic modulation. Finally, Cooper et al. demonstrated that reactivation of the Wnt pathway antagonist *sFRP1* by the combination of decitabine and romidepsin led to synergistic growth inhibition and apoptosis in renal cell carcinoma and triple-negative breast cancer lines [119]. These data are intriguing given the direct involvement of TSG reactivation in response to therapy in lines that correspond to generally chemo-resistant tumor types.

Few trials have formally tested these concepts in solid tumors. A single-arm phase II study of hydralazine, a weak non-nucleoside DNMT inhibitor, in combination with valproic acid in patients with solid tumors demonstrated responses (4 PR, 8 SD) to chemotherapy on which patients were previously progressing [120]. Recently, two trials have demonstrated the ability of a demethylating agent to sensitize platinum-resistant ovarian cancers to carboplatin. Response rates following azacitidine and decitabine pretreatment were 22% and 35%, respectively [121, 122]. The potential for epigenetic-mediated reversal of resistance to chemotherapy and targeted therapy is exciting given the limited treatment options available for advanced NSCLC, and warrants further testing in both laboratory and clinical settings.

6. Discussion

NSCLC is a disease characterized by both genetic and epigenetic heterogeneity, making traditional histological subtype classifications insufficient for informing treatment decisions. Classification based on mutational profiling of oncogenic drivers has led to substantial advances in the treatment of a subset of patients with advanced NSCLC.

A large fraction of patients, however, have cancers lacking any of the known clinically relevant driver mutations. Cancer-specific epigenetic dysregulation of gene expression may be as important as mutation in driving oncogenesis, and represents an alternative mechanism for modulating key proliferative and survival pathways. The frequent epigenetic silencing of TSG in NSCLC provides interesting "targets" for epigenetic based therapies, and preclinical data continues to support their potential therapeutic value.

Epigenetic regulation of gene expression is multifaceted, involving a host of enzymes modifying both DNA and DNA-associated protein complexes. Many of the critical epigenetic modifications have been defined, and several of the epigenetic modifiers that appear to be dysregulated in cancer can now be inhibited with a variety of targeted agents in preclinical and clinical development. Rational use of these agents has made advances from the early days of high dose administration associated with substantial toxicity and minimal efficacy. Initial studies of single agent epigenetically targeted drugs, including the DNMT inhibitors azacitidine and decitabine, as well as a variety of HDAC inhibitors, have shown minimal clinical activity in lung cancer patients. However, a recent study exploring the combination of the DNMT inhibitor azacitidine with the HDAC inhibitor entinostat, concomitantly targeting two critical facets of epigenetic gene silencing, does appear to have interesting clinical activity. This activity includes objective responses to the therapy itself as well as a possible priming effect, manifest as apparent improvement in tumor responses to subsequent therapies. Important measures of clinical outcome, including overall survival, appear to correlate with target gene demethylation detectable in circulating DNA in patients treated with this therapy.

Still, the clinical utility of epigenetic therapy in NSCLC is only starting to be explored, and many unanswered questions remain. While mounting preclinical evidence suggests that TSG reactivation and associated reestablishment of critical regulatory mechanisms are intimately involved in the anti-tumor effects of epigenetic therapy [86, 109], this has been difficult to convincingly demonstrate, and the underlying mechanisms responsible for clinical response remain controversial [80]. Initial clinical results suggest that select patients derive significant benefit from combination epigenetic therapy, and biomarker driven studies are needed to better identify these patients. The observation that patients who progress on epigenetic therapy may still benefit through improved sensitivity to subsequent therapy [114] presents an exciting avenue for future research, particularly when put into context with existing implications of epigenetic mechanisms in drug resistance [115], and the potential for epigenetic agents to reverse these mechanisms in model systems [116-118].

Future studies will further explore these preliminary observations, including additional evaluation of predictive biomarkers, and formal testing of the priming hypothesis. Improvements in genome wide methylation profiling are defining a key level of the epigenetic landscape, and have the potential, in the future, to provide a means for screening patients to guide treatment decisions, much in the way that mutational screening has done for targeted therapies. This will require determination of specific profiles associated with response to given agents, but large scale efforts such as the TCGA may make this possible.

Given the extensive evidence that epigenetic dysregulation is intimately involved with oncogenesis, targeting this epigenetic dysregulation has become a major clinical

focus. There may, however, be substantial risks as well as benefits in indiscriminately altering the epigenetic landscape. The use of hypomethylating agents in the context of an already hypomethylated tumor epigenome has raised concerns that reactivation of silenced tumor suppressor genes may come at the cost of activating growth and invasion promoting genes, and increasing genomic instability [13-15, 19, 89]. The potential tumor suppressor role of DNMT3a also raises concerns about indiscriminate treatment with demethylating agents [66]. It remains to be seen whether these concerns are warranted, and whether epigenetic therapy will have long term benefit or long term negative consequences in malignant or normal tissues. The current data in NSCLC patients, demonstrating rare but impressively prolonged responses either to epigenetic therapy or to subsequent treatments, suggests that the benefits for these patients may outweigh these risks. Given the lack of effective treatment options for many in this patient population, further exploration of combinatorial epigenetic therapy is warranted.

II. Epigenetic therapy alters proliferative and tumorigenic potential of NSCLC

1. Introduction

In addition to genetic alteration, epigenetic dysregulation is a central contributor to carcinogenesis, and has garnered considerable attention in cancer therapeutic research. Aberrant DNA methylation and histone deacetylation have been shown to contribute to oncogenesis through the silencing of critical tumors suppressor genes [10-12, 27-29]. Like many cancers, NSCLC contains widespread epigenetic alterations, and tumor suppressor gene silencing is an early and critical event in lung cancer development [31-33, 35-37]. Key regulators of these aberrant epigenetic changes include DNA methyltransferases (DNMTs) and histone deacetylases (HDACs), both of which can be targeted pharmacologically.

The nucleoside analogs azacitidine (Aza) and decitabine (DAC) have been extensively studied and shown to covalently inhibit DNMTs and induce their degradation, resulting in loss of DNA methylation [75-81]. DNMT inhibitors were previously explored at or near maximally tolerated doses, levels at which these agents are cytotoxic but have suboptimal effects on DNA methylation. Use of these agents at substantially lower doses has resulted in the successful treatment of hematologic malignancies, including acute myelogenous leukemia (AML) and myelodysplasia (MDS), in select patients [80].

The combination of demethylating agents and HDAC inhibitors (HDIs) has shown considerable promise, both in the laboratory and the clinic. Preclinical studies have demonstrated additive to synergistic effects on re-expression of silenced tumor suppressor genes, induction of apoptosis, inhibition of clonogenicity, and reduction in

tumor burden in various models [105-109]. Combinatorial epigenetic therapy has previously been used with success in the treatment of AML and MDS [110, 111]. Recently, combining Aza with the class I specific HDI, entinostat, resulted in major objective responses in select patients with advanced stage NSCLC [114].

While this activity in advanced stage NSCLC is certainly encouraging, many relevant questions remain. Preclinical and clinical evidence have demonstrated that lower doses of demethylating agents have improved efficacy over high, cytotoxic doses in hematologic malignancies, and in laboratory models of breast cancer [80, 86]. While preclinical studies strongly suggest that the anti-cancer effects of epigenetic agents correlate with alterations in DNA methylation and gene expression, and the associated reestablishment of critical regulatory pathways [86, 109], a causal relationship has been difficult to demonstrate clinically, and the mechanisms responsible for clinical efficacy remain controversial [80, 110, 111].

Using various models of NSCLC encompassing the three most common histological subtypes (adenocarcinoma, squamous cell carcinoma, and large cell carcinoma), we sought to evaluate whether Aza, entinostat, or combination epigenetic therapy alters the tumorigenic capacity of NSCLC, and whether these effects correlate with acute cytotoxicity. We found a lack of correlation between early cytotoxicity and a durable anti-cancer effect in our models, suggesting the involvement of additional mechanisms in the anti-tumor efficacy of these agents.

2. Results

2.1 NSCLC cell lines exhibit differential sensitivity to Aza in cell viability assays

Given the lessons learned in the clinical treatment of AML and MDS regarding the improved efficacy of lower, less toxic doses of Aza [80], we first sought to define doses of Aza that do not result in acute cytotoxicity in NSCLC cell lines. To this end, we assessed sensitivity to Aza in a panel of six NSCLC cell lines, including three adenocarcinoma lines (H358, H838, and A549), one squamous cell carcinoma line. Cells were treated every 24h for 72h with Aza from 10nM-10uM, with five replicates per dose. Immediately following treatment, cell viability was assessed using the CellTiter-Glo luminescence cell viability assay (Promega). Raw data was corrected for background luminescence and the x-axis was log transformed (x=log(x)). Nonlinear regression using the equation log inhibitor vs. response with variable slope was performed to determine IC50 and R^2. Mean values with standard deviation from 2-3 independent experiments are displayed in table 3, and depict varying sensitivity to Aza among the cell lines tested. H460 was the only cell line to exhibit a sub-micromolar IC50 for 72h Aza treatment. Log dose response curves generated from nonlinear regression of transformed data normalized to untreated control cells also highlight the variable sensitivity among cell lines (Figure 2). In addition to having the lowest IC50, H460 cells also exhibited the greatest maximal reduction in cell viability following Aza treatment. Generally, H358 and H1299 viability were unaffected by doses of near 1uM Aza and below. Interestingly, A549 cells appeared to increase in proliferation with increasing doses of Aza up to 1uM, prior to rapidly decreasing in cell viability at higher doses. This effect was extremely reproducible across three independent experiments.

Table 3. IC50 values for NSCLC cell lines treated with azacitidine.

Mean IC50 and R^2 with standard deviation calculated from two (H358, H2170) or three (H460, H358, H1299, A549) independent experiments, each with five replicates per dose tested, from log transformed data analyzed by nonlinear regression in GraphPad Prism 5. The CellTiter-Glo assay was used to assess cell viability following 72h treatment with Aza. A true plateau was not reached for any cell line with up to 10uM Aza. IC50 represent dose at 50% of the maximal inhibition achieved. *Calculated IC50 values for A549 were ambiguous for all three experiments, but data were consistent.

Cell Line	Mean IC50 (+/- SD)	Mean R^2 (+/- SD)
H358	4.111 +/- 0.132	0.9524 +/- 0.0071
H460	0.953 +/- 0.170	0.9881 +/- 0.0048
H838	2.497 +/- 0.270	0.9707 +/- 0.0038
H1299	2.958 +/- 0.307	0.9393 +/- 0.0547
H2170	1.552 +/- 0.063	0.9763 +/- 0.0111
A549*	3.291 +/- 0.059	0.8133 +/- 0.0526

Figure 2. Sensitivity of NSCLC cell lines to azacitidine.

Log dose response curves from representative experiments for NSCLC cell lines treated with Aza every 24h for 72h. Individual curves represent the percentage of viable cells (+/- standard deviation) normalized to untreated control cells within a given cell line, such that the mean luminescence value for untreated controls represents 100%, and 0 = 0%.

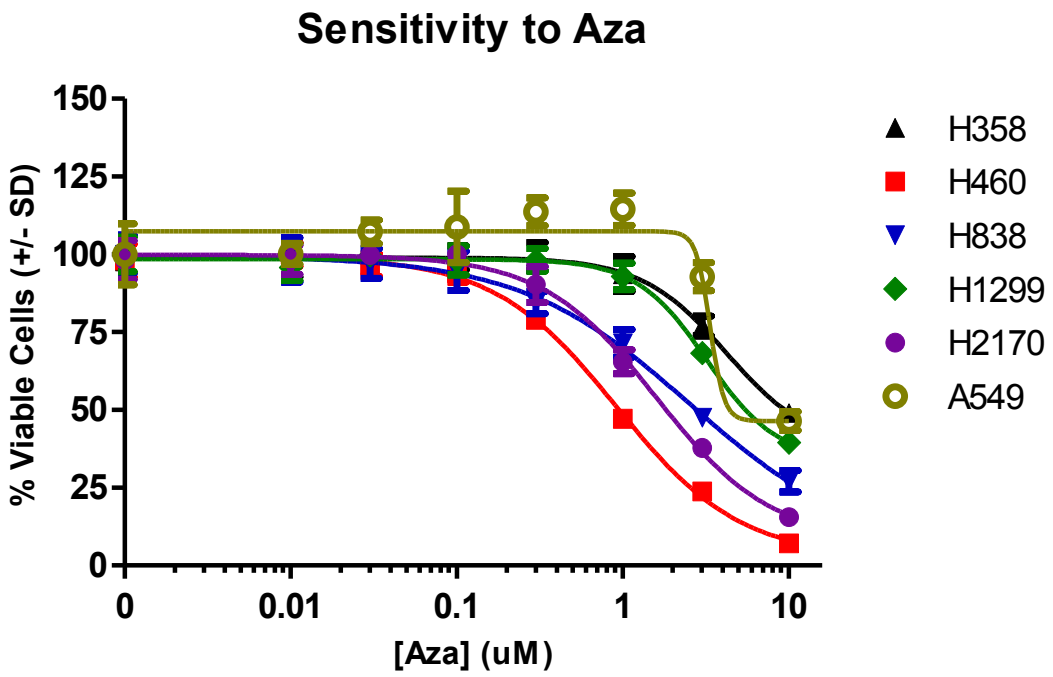

2.2 Dose combinations of Aza and entinostat generally do not synergistically impair cell viability in NSCLC cell lines

Preclinical studies have shown that the combination of a demethylating agent and a HDI can result in additive to synergistic inhibition of DNA synthesis and induction of apoptosis *in vitro*, and inhibition of tumor growth *in vivo* [106-109]. We aimed to determine whether the combination of Aza and entinostat synergistically impairs cell viability in NSCLC cell lines. We employed a previously published method for assessing the potential synergy of drug combinations [123]. We treated NSCLC cell lines in an eight by eight dosing matrix in 96-well plates, with entinostat varied along the y-axis and Aza varied along the x-axis, to provide dose combinations across a broad range of cconcentrations. Inhibition of cell viability or proliferation was assessed immediately

following treatment using the CellTiter-Glo viability assay or CellTiter AQueous One MTS proliferation assay (Promega).

We first assessed whether the combination of Aza and entinostat was synergistic when administered concurrently during the final 24h of the 72h Aza treatment period. Cells were treated with Aza and entinostat increased in 3-fold increments up to 500uM and 5uM, respectively. Response matrices were generated by calculating and plotting inhibition Z at each dose combination relative to the mean of untreated cells (eight replicated). Representative response matrices for H358, H460, and H1299 are shown in Figure 3A (left panel). Entinostat treatment alone was relatively nontoxic until greater than 1uM doses were reached. In H1299 cells, even 5uM entinostat had little to no effect on cell viability. To determine whether the addition of entinostat to Aza treatment produced additive or synergistic inhibition of viability, highest single agent over response (HSA) plots were generated by subtracting from Z for a given dose combination the highest of the two single agent inhibition scores for the corresponding doses. The HSA model, also known as Gaddum's non-interaction, deems synergy as an effect of combination that is greater than the effect of either constituent [124, 125]. HSA plots depicting excess inhibition of viability for a given dose combination are shown in Figure 3A (right panel). Positive values indicate additivity or synergy, while negative values indicate antagonism. The greatest combinatorial effect was noted in H460 cells, with mild effects at moderate dose combinations, and more notable synergy at high dose combinations. In H358 cells, synergistic inhibition only occurred at very high dose combinations. Interestingly, the vast majority of dose combinations in H1299 were antagonistic, particularly at moderate to high doses of entinostat. Results in H838 and

H2170 were similar to H358, while results in A549 were similar to H1299 (data not shown).

Given that Aza must be incorporated into DNA to actively inhibit DNMTs, and that HDAC inhibitor induced G1 arrest through activation of p21 would prevent DNA replication [70, 91], we hypothesized that administration of entinostat after Aza treatment would allow for greater incorporation of Aza into DNA and improve overall inhibition of cell viability. To this end, we performed dose combination matrix studies in which H358 and H460 cells received entinostat for 24h after the 72h Aza treatment period, and proliferation of cells was assessed at 96h using the MTS assay. Lower maximal doses were used in these studies, with Aza increasing in 2-fold increments up to 5uM, and entinostat increasing in 3-fold increments up to 3uM. Dose combinations, administered sequentially, were actually less effective in H358 cells, with no evidence of synergy at even the maximum doses tested (Figure 3B upper). Sequential administration in H460 was also slightly less effective compared to the previous schedule of administration (Figure 3B lower).

Figure 3. The combination of Aza and entinostat does not synergistically inhibit cell viability in NSCLC cell lines. A. Cells were treated with Aza every 24h for 48h, followed by dose combinations of Aza and entinostat for 24h, with each drug concentration increasing in 3-fold increments along a given axis of the dosing matrix. Cell viability was assessed at 72h using the CellTiter-Glo assay, and luminescence values were corrected for background luminescence. **Left** Response matrix depicting inhibition of cell viability for each well (ie. dose combination) of the matrix relative to the average of untreated wells (eight replicates). The red line represents the contour at which 50% inhibition occurs. **Right** Response over highest single agent (HSA) matrix

displaying excess inhibition of viability for a given dose combination after subtraction of the highest of the two single agent inhibition scores for the corresponding doses. Negative values represent antagonistic response resulting from the combination. Independent experiments were repeated at least twice, with 1-2 plates per experiment, to ensure consistent results. Representative data for H358, H460, and H1299 shown. **B.** Cells were treated with Aza every 24h for 72h, followed by entinostat for 24h, with entinostat increasing 3-fold and Aza increasing 2-fold in concentration along the y-axis and x-axis of the dosing matrix, respectively. Proliferation was assessed at 96h using the CellTiter AQueous One MTS proliferation assay and measuring absorbance at 490nm. **Left** Response matrix depicting inhibition of proliferation for each well (ie. dose combination) of the matrix relative to the average of untreated wells (eight replicates). **Right** Response over highest single agent (HSA) matrix displaying excess inhibition of proliferation for a given dose combination after subtraction of the highest of the two single agent inhibition scores for the corresponding doses. Negative values (red) represent antagonistic response resulting from the combination. Independent experiments were repeated at least twice to ensure consistent results. Representative data for H358 and H460 shown.

A.

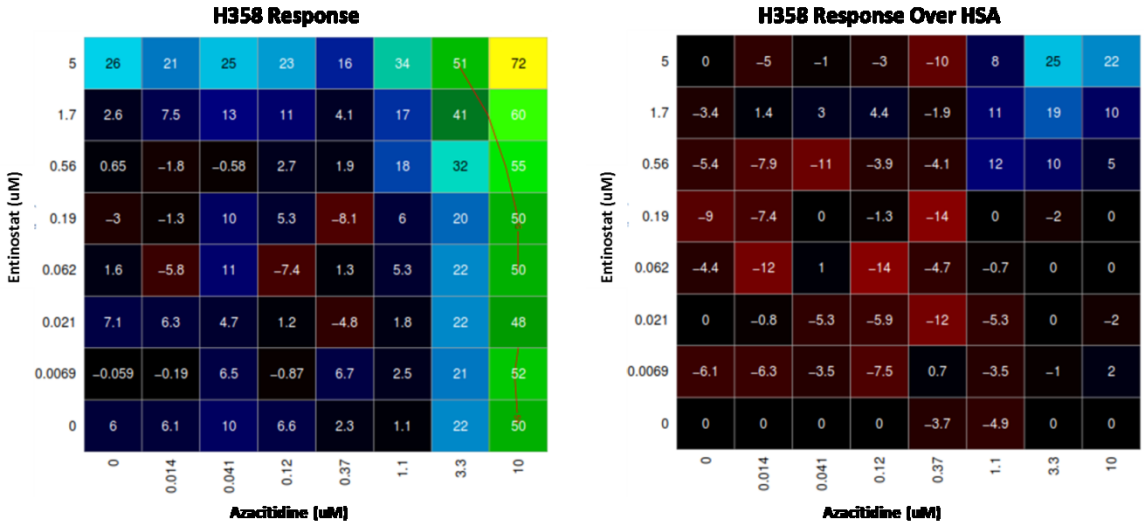

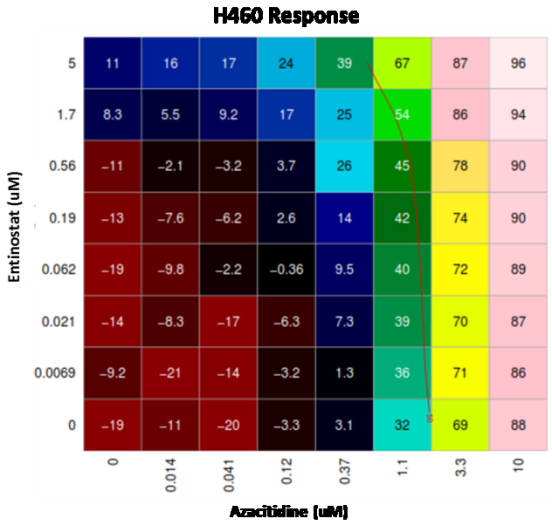
H460 Response
Entinostat (uM)
5 11 16 17 24 39 67 87 96
1.7 8.3 5.5 9.2 17 25 54 86 94
0.56 −11 −2.1 −3.2 3.7 26 45 78 90
0.19 −13 −7.6 −6.2 2.6 14 42 74 90
0.062 −19 −9.8 −2.2 −0.36 9.5 40 72 89
0.021 −14 −8.3 −17 −6.3 7.3 39 70 87
0.0069 −9.2 −21 −14 −3.2 1.3 36 71 86
0 −19 −11 −20 −3.3 3.1 32 69 88
0 0.014 0.041 0.12 0.37 1.1 3.3 10
Azacitidine (uM)

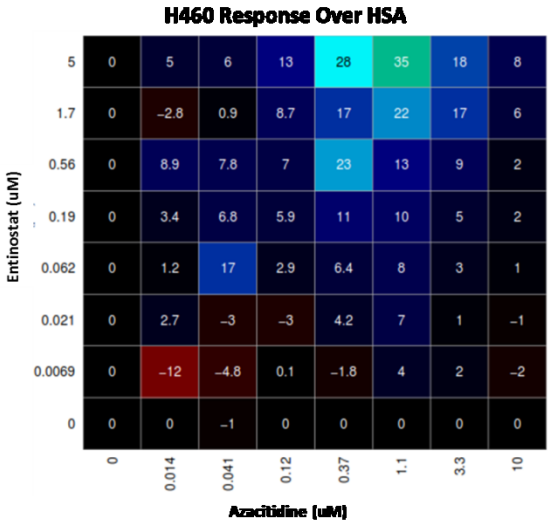
H460 Response Over HSA
Entinostat (uM)
5 0 5 6 13 28 35 18 8
1.7 0 −2.8 0.9 8.7 17 22 17 6
0.56 0 8.9 7.8 7 23 13 9 2
0.19 0 3.4 6.8 5.9 11 10 5 2
0.062 0 1.2 17 2.9 6.4 8 3 1
0.021 0 2.7 −3 −3 4.2 7 1 −1
0.0069 0 −12 −4.8 0.1 −1.8 4 2 −2
0 0 0 −1 0 0 0 0 0
0 0.014 0.041 0.12 0.37 1.1 3.3 10
Azacitidine (uM)

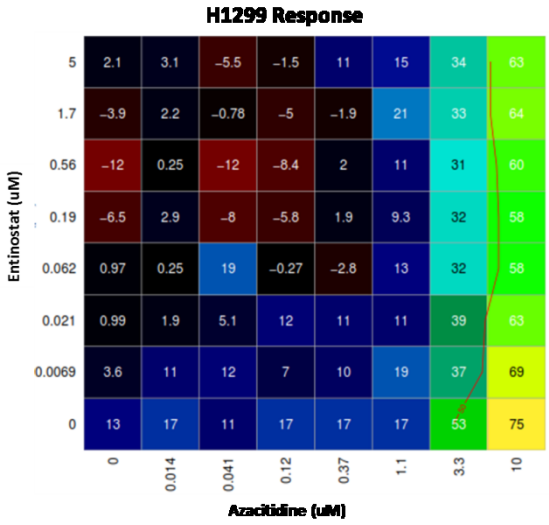
H1299 Response
Entinostat (uM)
5 2.1 3.1 −5.5 −1.5 11 15 34 63
1.7 −3.9 2.2 −0.78 −5 −1.9 21 33 64
0.56 −12 0.25 −12 −8.4 2 11 31 60
0.19 −6.5 2.9 −8 −5.8 1.9 9.3 32 58
0.062 0.97 0.25 19 −0.27 −2.8 13 32 58
0.021 0.99 1.9 5.1 12 11 11 39 63
0.0069 3.6 11 12 7 10 19 37 69
0 13 17 11 17 17 17 53 75
0 0.014 0.041 0.12 0.37 1.1 3.3 10
Azacitidine (uM)

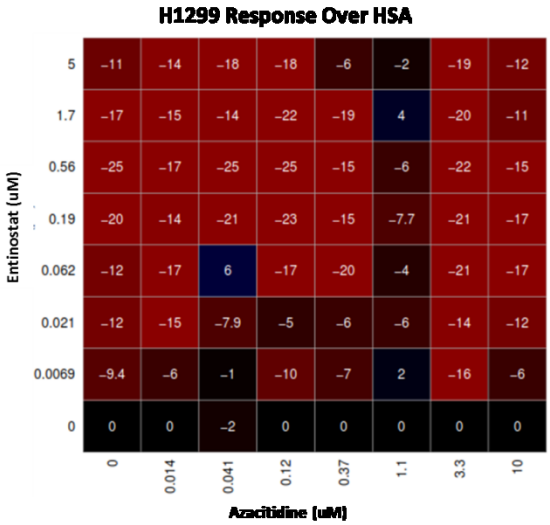
H1299 Response Over HSA
Entinostat (uM)
5 −11 −14 −18 −18 −6 −2 −19 −12
1.7 −17 −15 −14 −22 −19 4 −20 −11
0.56 −25 −17 −25 −25 −15 −6 −22 −15
0.19 −20 −14 −21 −23 −15 −7.7 −21 −17
0.062 −12 −17 6 −17 −20 −4 −21 −17
0.021 −12 −15 −7.9 −5 −6 −6 −14 −12
0.0069 −9.4 −6 −1 −10 −7 2 −16 −6
0 0 0 −2 0 0 0 0 0
0 0.014 0.041 0.12 0.37 1.1 3.3 10
Azacitidine (uM)

B.

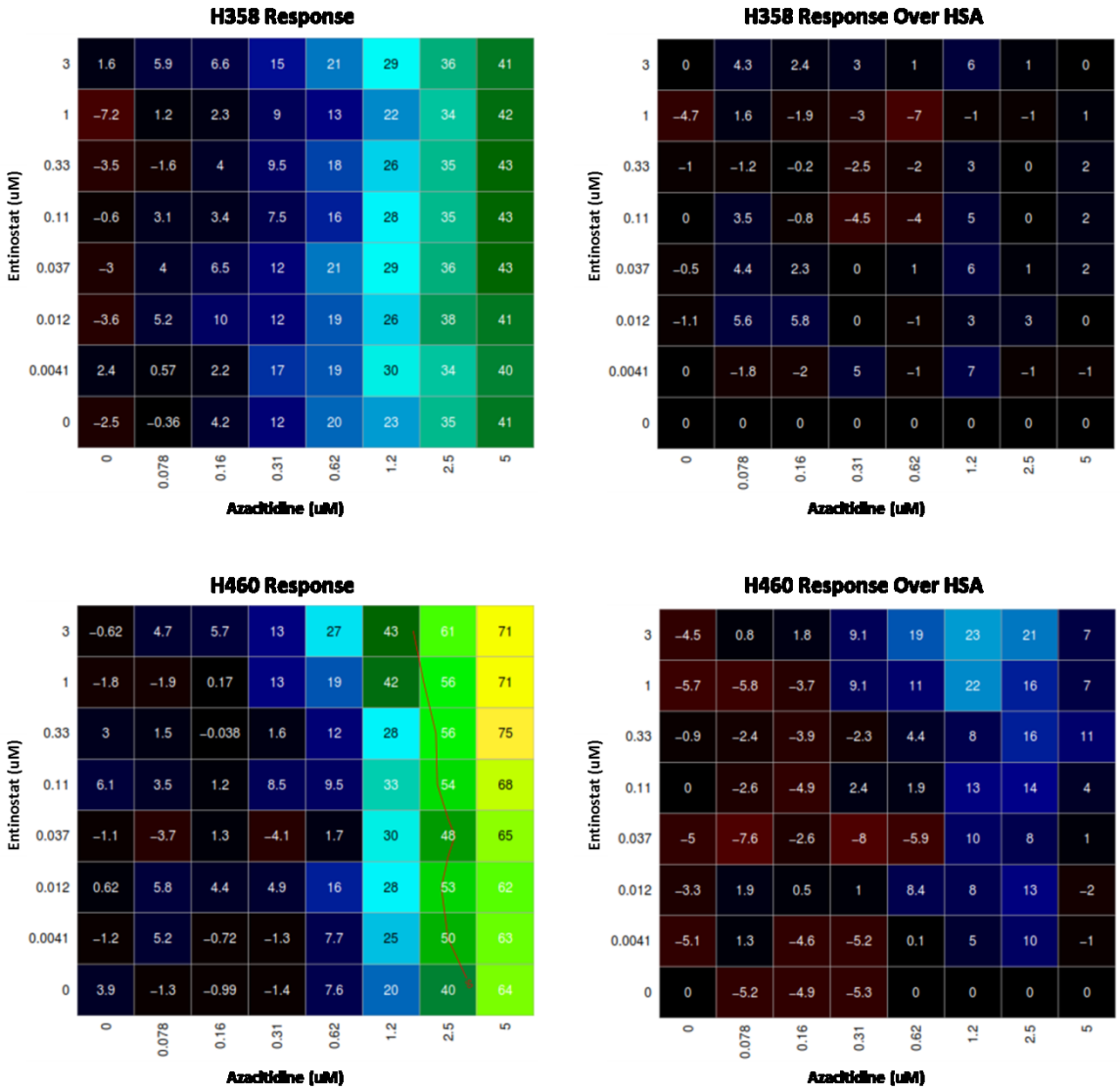

We then questioned whether optimal synergy would occur if both agents were administered concurrently during the first 24h of treatment, followed by Aza only for the reaming 48h. Given that lack of combinatorial benefit in H358, we selected this line for study. Cells were treated with either overlapping or sequential combination, and proliferated was assessed at 96h by MTS assay. Indeed, the overlapping combination resulted in greater inhibition of proliferation at lower doses of either drug compared to

sequential combination treatment (Figure 4A). For the overlapping combination, as doses of either drug increased, single agent inhibition became dominant and combinatorial benefit was lost. However, at moderate doses of Aza, administration of entinostat during the first 24h enhanced inhibition, Z, while administration after Aza treatment resulted in little change in proliferation (Figure 4B).

Figure 4. Overlapping, but not sequential, administration of the combination of Aza and entinostat has combinatorial activity against proliferation of H358 cells. H358 cells were treated with Aza every 24h for 72h, in combination with entinostat for the initial 24h of treatment (overlapping) or the 24h following Aza treatment (sequential), with entinostat increasing 3-fold and Aza increasing 2-fold in concentration along the y-axis and x-axis of the dosing matrix, respectively. Proliferation was assessed at 96h by MTS assay. **A.** Response matrices for overlapping (left) vs. sequential (right) administration depicting inhibition of proliferation for each well (ie. dose combination) of the matrix relative to the average of untreated wells (eight replicates). The red line represents the contour at which 50% inhibition occurs. **B.** Combination curves depicting the increase in inhibition Z resulting from the addition of entinostat (lower) compared to inhibition from Aza alone (upper) for overlapping vs. sequential treatment regimens.

A.

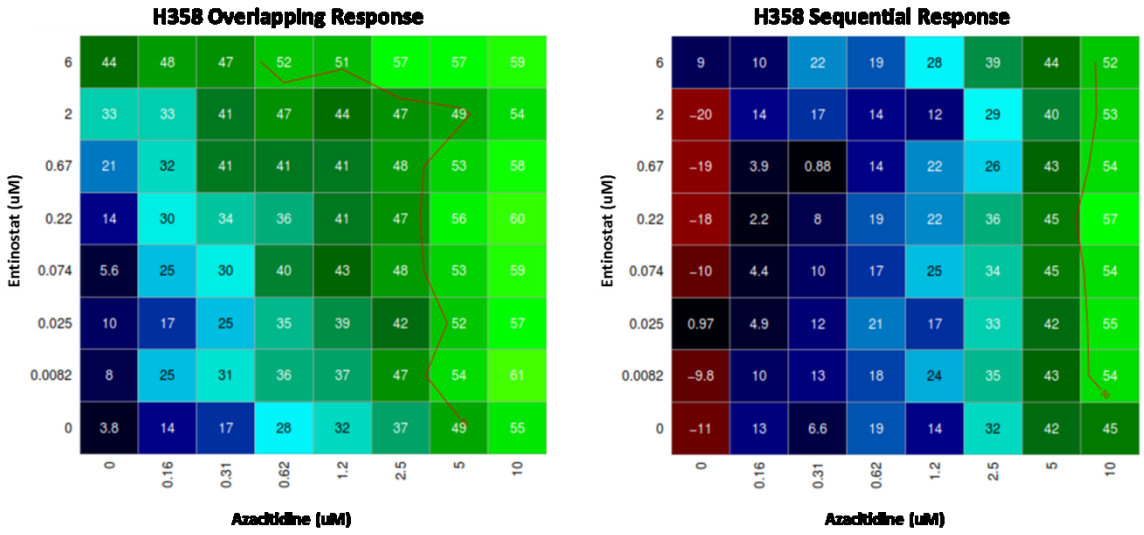
H358 Overlapping Response
Entinostat (uM)
6 44 48 47 52 51 57 57 59
2 33 33 41 47 44 47 49 54
0.67 21 32 41 41 41 48 53 58
0.22 14 30 34 36 41 47 56 60
0.074 5.6 25 30 40 43 48 53 59
0.025 10 17 25 35 39 42 52 57
0.0082 8 25 31 36 37 47 54 61
0 3.8 14 17 28 32 37 49 55
0 0.16 0.31 0.62 1.2 2.5 5 10
Azacitidine (uM)
H358 Sequential Response
Entinostat (uM)
6 9 10 22 19 28 39 44 52
2 −20 14 17 14 12 29 40 53
0.67 −19 3.9 0.88 14 22 26 43 54
0.22 −18 2.2 8 19 22 36 45 57
0.074 −10 4.4 10 17 25 34 45 54
0.025 0.97 4.9 12 21 17 33 42 55
0.0082 −9.8 10 13 18 24 35 43 54
0 −11 13 6.6 19 14 32 42 45
0 0.16 0.31 0.62 1.2 2.5 5 10
Azacitidine (uM)

B.

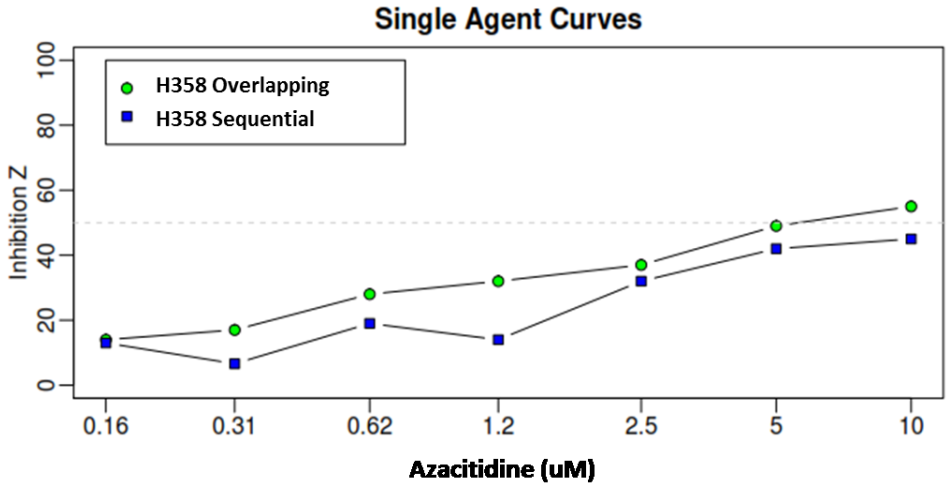
Single Agent Curves
H358 Overlapping
H358 Sequential
Inhibition Z
0 20 40 60 80 100
0.16 0.31 0.62 1.2 2.5 5 10
Azacitidine (uM)

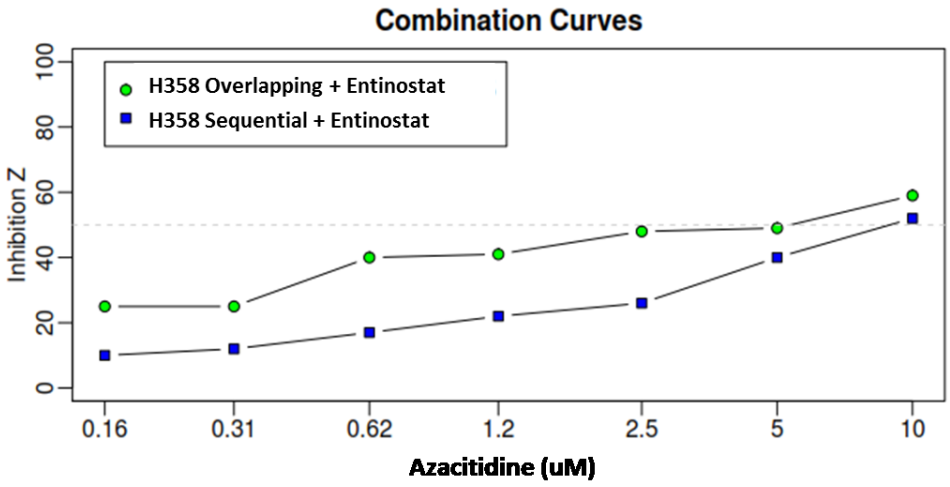

2.3 Epigenetic therapy exerts differential sustained effects on proliferation of NSCLC lines

To determine whether the anti-proliferative effects of epigenetic therapy are sustained after the end of treatment, we first treated cells every 24h with 500nM for 72h, and 50nM entinostat for the final 24h of the treatment period. At the end of treatment, cells were re-seeded, and the CellTiter-Glo viability assay was used to determine the number of viable cells present following growth for 5-7 days without drug. We selected the 500nM Aza since that concentration is sub-IC50 in all six cell lines, and has been shown to alter tumorigenic potential of breast, colon, and lung cancer cell lines without apparent toxicity in the same breast cancer cell line [86]. We chose 50nM entinostat since this represents a clinically achievable concentration [126]. Entinostat was given during the final 24h of the 72h Aza treatment period as a compromise between the overlapping and sequential 96h schedules previously tested in the H358 combination matrix experiments. The effects of Aza treatment on proliferation after treatment were varied among cell lines, with the most significant anti-proliferative effects in H358, H460, and

H2170 (Figure 5A and 5B). Interestingly, while H460 and H2170 represented the two most sensitive cell lines in our 3-day viability assays, H358 was one of the least sensitive cell line in that assay, exhibiting the highest IC50 and lowest maximal inhibition of viability at the end of Aza treatment. A549 cells, which appear to increase in proliferation with Aza treatment in the viability assay, were generally unaffected by epigenetic therapy. Similar to the combination matrix studies, Aza and entinostat inhibited proliferation in an additive manner in H460 cells, while the combination was antagonistic in H1299, and to a lesser extent, H838 cells (Figure 5A and 5B). Entinostat had no effect in the remaining cell lines.

Figure 5. Differential effects on proliferation of NSCLC cell lines following epigenetic therapy. Cells were treated with 500nM Aza every 24h for 72h, 50nM entinostat for 24h from hours 48-72 of the treatment period, combination, or mock. Immediately following treatment, cells were re-seeded at equal number and allowed to proliferate in drug-free media until day 8 (H358, H2170), day 9 (H838, A549), or day 10 (H460, H1299). **A.** Percent viable cells, normalized to Mock, assessed using the CellTiter-Glo luminescence viability assay (Promega). Data shown for H2170, H838, H460, and H1299 are an average of two independent experiments, each with five replicates per condition. Data for H358 and A549 are from representative experiments with five replicates per condition. Statistical significance compared to mock determined by ANOVA with Dunnett's multiple comparison test and denoted as follows: *$p<0.05$, ***$p<0.001$. Otherwise, differences were not significant ($p>0.05$). **B.** Qualitative effects of epigenetic therapy on proliferation of cells visualized by crystal violet staining of cells present on the day noted above for each cell line. Images shown are representative wells of 12-well plates with each condition in triplicate.

A.

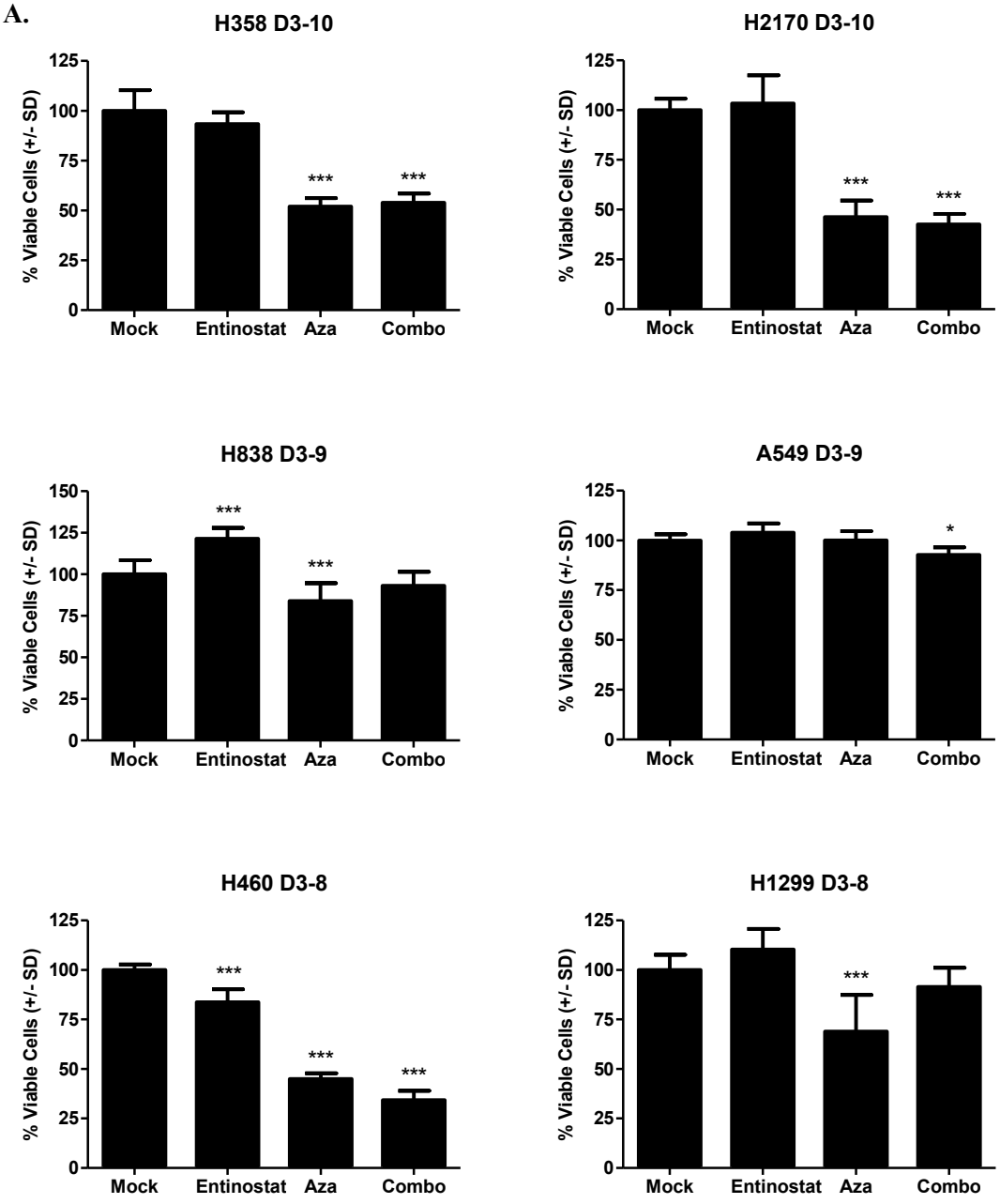
H358 D3-10
% Viable Cells (+/- SD)
125
100
75
50
25
0
***
***
Mock
Entinostat
Aza
Combo
H2170 D3-10
% Viable Cells (+/- SD)
125
100
75
50
25
0
***
***
Mock
Entinostat
Aza
Combo
H838 D3-9
% Viable Cells (+/- SD)
150
125
100
75
50
25
0
***
***
Mock
Entinostat
Aza
Combo
A549 D3-9
% Viable Cells (+/- SD)
125
100
75
50
25
0
*
Mock
Entinostat
Aza
Combo
H460 D3-8
% Viable Cells (+/- SD)
125
100
75
50
25
0
***
***
***
Mock
Entinostat
Aza
Combo
H1299 D3-8
% Viable Cells (+/- SD)
125
100
75
50
25
0
***
Mock
Entinostat
Aza
Combo

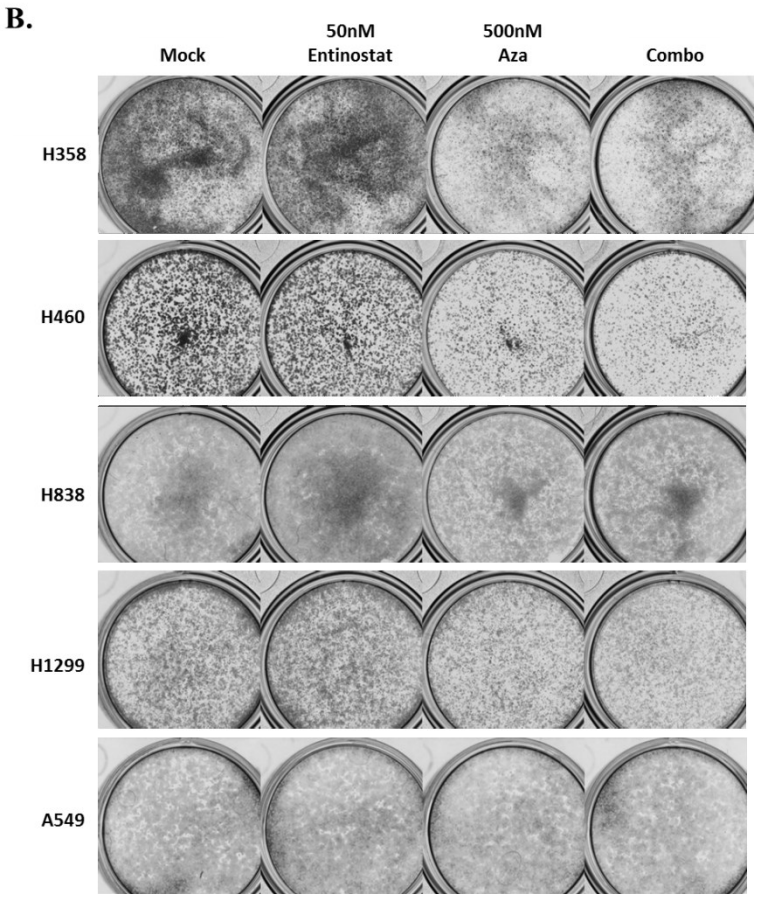

Published data suggests that Aza may deplete self-renewing or clonogenic cell populations in hematologic and breast cancer models [86]. To test whether treatment of cells with epigenetic therapy depletes clonogenic capacity of NSCLC cell lines, we assessed anchorage-dependent growth of colonies on Matrigel^{TM} following epigenetic therapy. We employed the same treatment and similar drug-free recovery regimen as used above in our studies of proliferation after epigenetic therapy. Inhibition of colony formation to a greater extent than the proliferative inhibition we observed in these cells lines may suggest a depletion of clonogenic potential, however we note that to confirm this, assays of anchorage-independent colony growth (ie. methylcellulose) would need conducted. To our surprise, inhibition of colony growth paralleled the trends of above

proliferative inhibition, but the magnitude of effect was generally reduced, suggesting that the effects on colony growth are driven by impaired proliferation of the general cell population, as opposed to depletion of a clonogenic subpopulation (Figure 6A and 6B).

Figure 6. Effects of epigenetic therapy on colony growth parallel effects on proliferation. Cells were treated with 500nM Aza every 24h for 72h, 50nM entinostat for 24h from hours 48-72 of the treatment period, combination, or mock. Immediately following treatment, cells were seeded at equal number with five replicates on a solidified layer of Matrigel™ and allowed to form colonies in the absence of drug. Colonies were stained with MTT reagent and colony number assessed on the day noted for each cell line. **A.** Representative wells depicting qualitative changes in colony growth. **B.** Percent colony formation (mean +/- SD) normalized to mock from representative H358, H460, H2170, and A549 experiments. Experiments were repeated at least twice to ensure consistent results. H838 and H1299 colony number could not be quantified as these cell lines did not form distinct colonies. Statistical significance compared to mock determined by ANOVA with Dunnett's multiple comparison test and denoted as follows: ***$p<0.001$. Otherwise, differences were not significant ($p>0.05$).

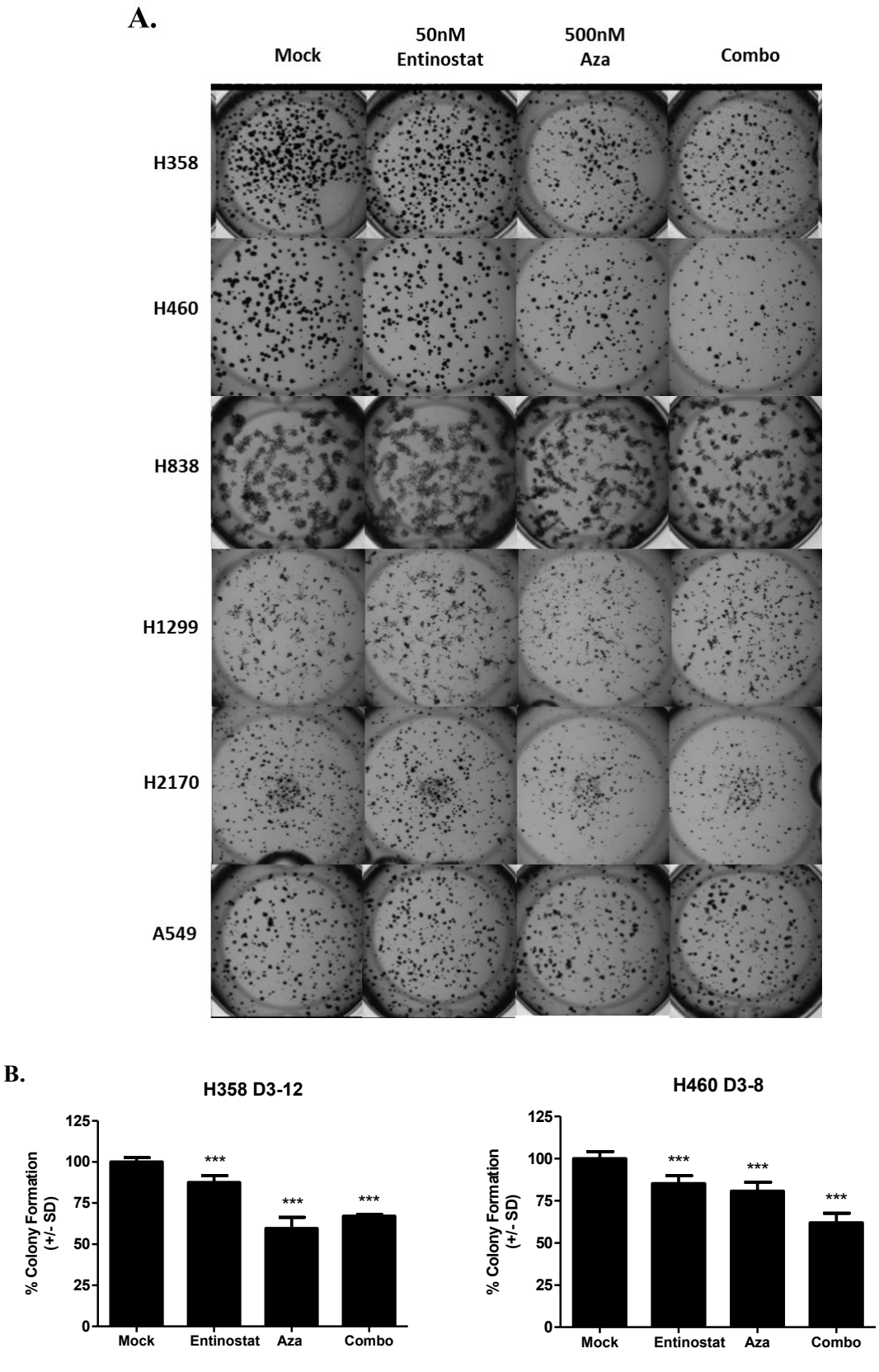
A.
Mock
50nM Entinostat
500nM Aza
Combo
H358
H460
H838
H1299
H2170
A549
B.
H358 D3-12
% Colony Formation (+/- SD)
125
100
75
50
25
0
***
***
***
Mock
Entinostat
Aza
Combo
H460 D3-8
% Colony Formation (+/- SD)
125
100
75
50
25
0
***
***
***
Mock
Entinostat
Aza
Combo

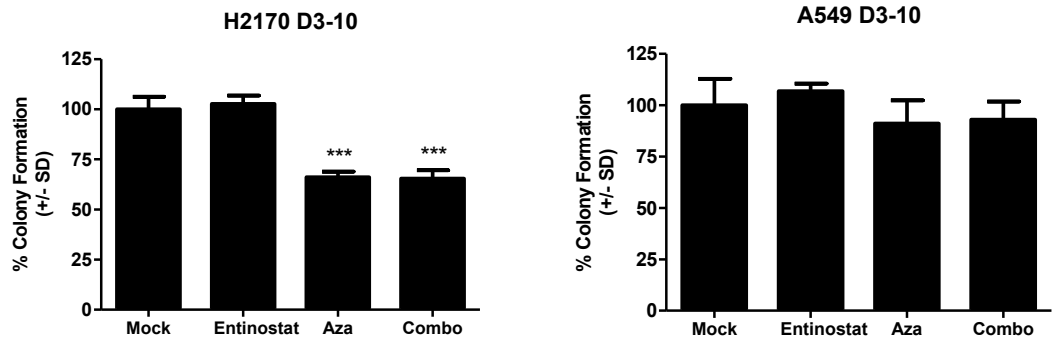

2.4 The cytotoxic effects of overlapping and sequential combination treatment are transient and peak at unique times in H358

The results of our studies of proliferation and colony formation after epigenetic treatment caused us to question whether increased cell death or cell cycle arrest may be responsible for the anti-proliferative effects observed. To address this question, we assessed cell cycle phase and cell death via sub-G1 population at the end of 96h epigenetic treatment, as well as three days and six days after treatment, in H358 cells. H358 cells were selected for several reasons. H358 cells were one of the least sensitive cell lines in our cell viability experiments, yet Aza treatment resulted in a sustained inhibition of H358 proliferation and colony growth after treatment comparable to the much more sensitive (in terms of IC50) H460 and H2170 cell lines. In addition, while 50nM entinostat, administered during the final 24h of Aza treatment, had no effect in H358 cells, moderate dose combinations of Aza and entinostat, administered on the overlapping schedule, more effectively inhibited proliferation of H358 cells than Aza alone in combination matrix studies. Conversely, sequential administration of these same dose combinations did not yield benefit over Aza alone. Given that the effects of Aza on

proliferation do not fully manifest in short term viability studies, the 96h time point may have been too early to assess the combinatorial effects of late administration of entinostat with the sequential schedule. Therefore, we treated H358 cells with overlapping or sequential combination, as well as single agent Aza and entinostat, to not only address whether cytotoxicity or cell cycle arrest are responsible for the anti-proliferative effects of Aza, but also determine how schedule of administration of entinostat affects viability and cell cycle distribution. Cell cycle and sub-G1 analysis was at the end of treatment (96h), on day seven, and on day ten, to determine how long the anti-proliferative effects are sustained. We selected a dose of 500nM for entinostat since 50nM was insufficient to produce any effect in H358, and prior viability and proliferation studies suggested that this does would be relatively non-toxic in H358 cells. Analysis of the sub-G1 population at each time point revealed that cell death resulting from early administration of entinostat was greatest at 96h, while cell death due resulting from sequential administration was greatest at day seven (Figure 7A). In both cases, the magnitude of cell death was indistinguishable from control cells by day ten. Aza induced cell death was slightly higher at day seven, but was also transient. This may explain why inhibition of proliferation by at 96h was slightly more pronounced than inhibition of cell viability at 72h in our MTS and CellTiter-Glo combination assays, respectively. Interestingly, the combinatorial effects were sub-additive regardless of schedule of administration. While cell death was observed following epigenetic treatment, no apparent accumulation in G1, S, or G2/M phases of the cell cycle were noted at days four, seven, or ten (Figure 7B and C, day 10 profiles not shown). Loss of cells in G1 was noted when sub-G1 populations were largest, suggesting that, if cells had temporarily arrested in G1, cell death occurred

relatively quickly. However, mitotic trapping of Aza treated cells with nocodazole also revealed no evidence of G1 or S phase arrest at day four, but instead a loss of G1 cells with concomitant increase in the sub-G1 population (Figure 8).

Figure 7. Overlapping and sequential combination treatment exert transient cytotoxic effects on H358 cells, but do not induce cell cycle arrest. H358 cells were treated in triplicate with 500nM Aza every 24h for 72h, in combination with 500nM entinostat for the initial 24h of treatment (overlapping) or the 24h following Aza treatment (sequential). Cell cycle phase distribution was assessed using flow cytometry to detect propidium iodide staining of DNA content. **A.** Percent of gated cells within the sub-G1 population at days 4 (immediately after treatment), 7, and 10. **B.** Representative cell cycle profiles at end of treatment (day 4). **C.** Representative cell cycle profiles on day 7, following three days in drug-free media.

A.

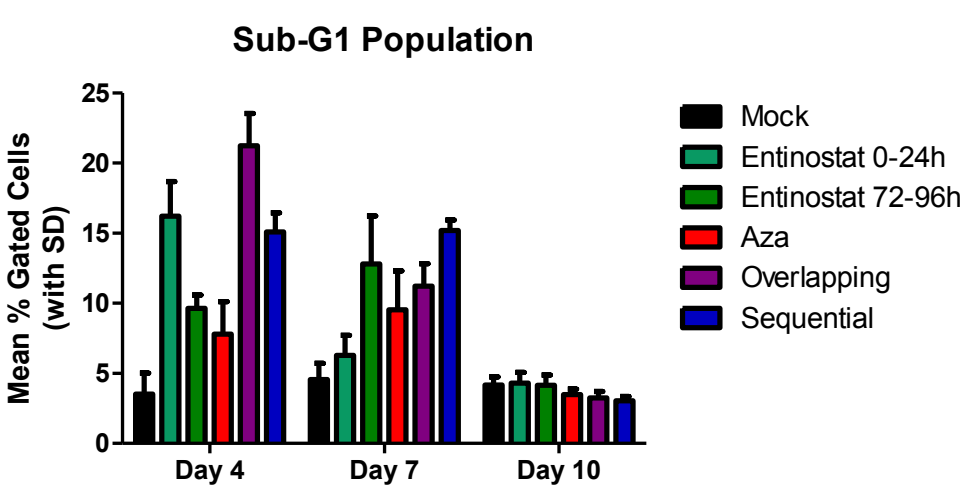

B.

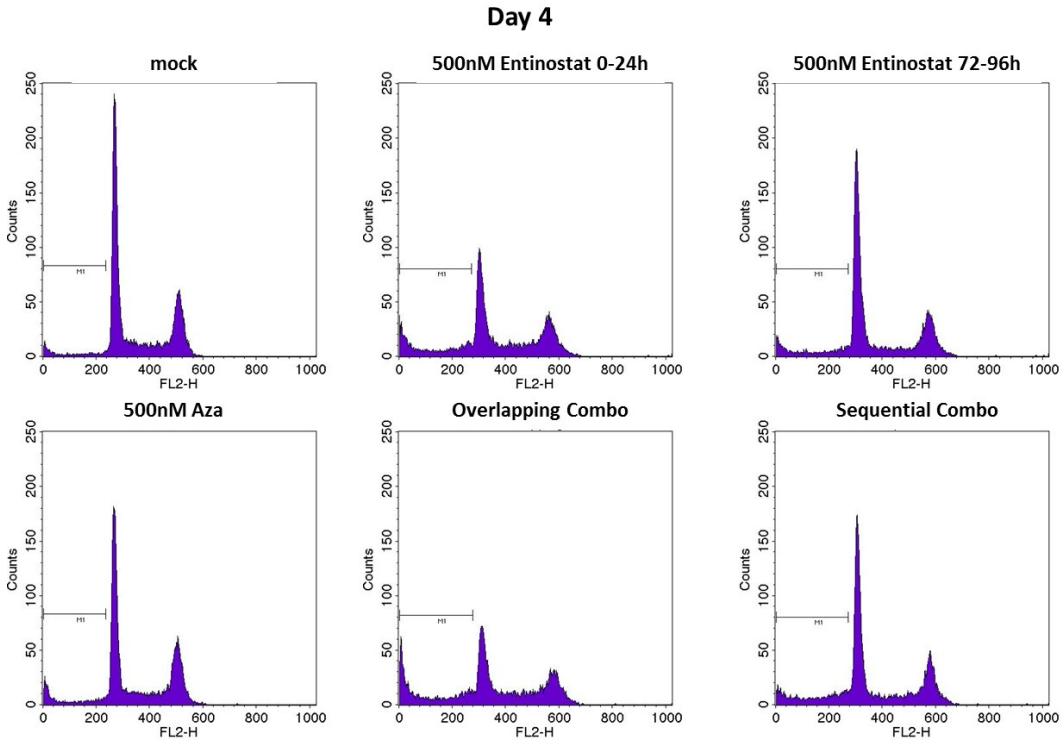
Day 4
mock
500nM Entinostat 0-24h
500nM Entinostat 72-96h
500nM Aza
Overlapping Combo
Sequential Combo
Counts
FL2-H
M1
0
50
100
150
200
250
0
200
400
600
800
1000

C.

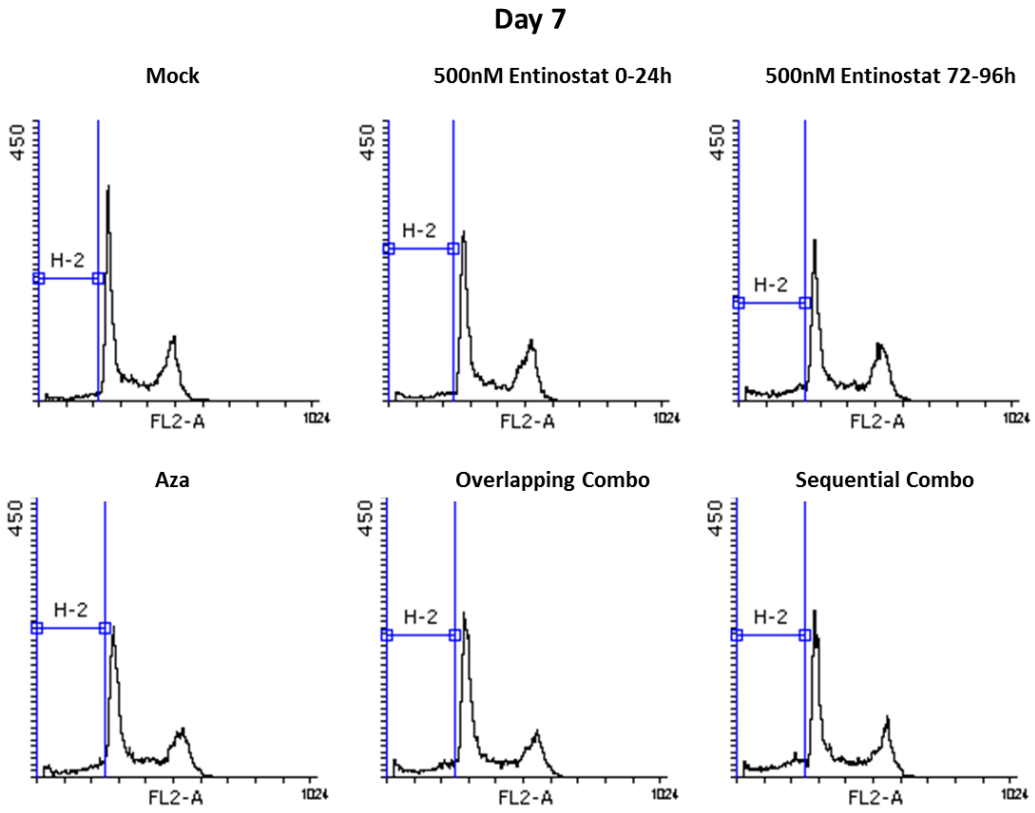

Figure 8. Azacitidine does not induce G1 arrest in H358 cells. Cells were treated in triplicate with 500nM Aza every 24h for 72h. Cells were then cultured an additional 24 h in drug-free media, or treated with nocodazole (100 ng/mL) for 24h to trap cells in G2/M. Cells were then immediately ethanol fixed and cell cycle phase distribution was assessed using flow cytometry to detect propidium iodide staining of DNA content. Representative cell cycle profiles shown.

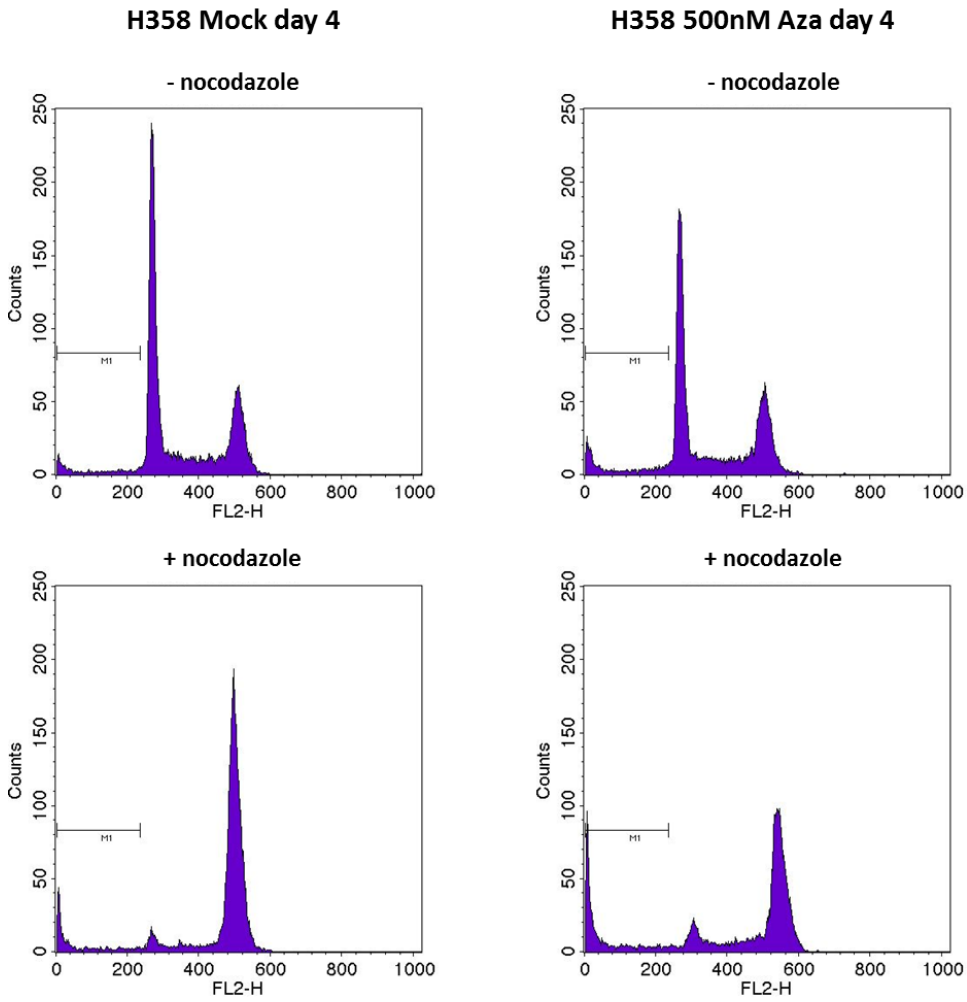

2.5 Epigenetic therapy *in vitro* reactivated the key tumor suppressor gene, *p16*, and produced durable effects on tumorigenicity *in vivo*

Our results from the cell cycle experiments suggested that the cytotoxic effects of Aza and entinostat are transient, with cells exhibiting normal cell cycle profiles and viability within six days of the end of treatment. Our colleagues reported that *in vitro* treatment of breast, colon, and lung cancer cell lines 500nM Aza produced durable anti-tumor effects *in vivo*, and demonstrated that this dose had minimal effects on viability and cell cycle phase in the same breast cancer cell line [86]. We employed a similar

experimental design to determine whether the Aza and combination treatment, while only transiently effecting cell viability, could produce durable impairment of tumorigenicity of H358 xenografts. To this end, we treated H358 cells every 24h for 72h with 500nM Aza, and administered 500nM entinostat for the final 12h of the treatment period. The 72h treatment schedule was chosen because overlapping versus sequential combination treated cells were indistinguishable in terms of viability and cell cycle profile by day ten. In addition, we reduced duration of entinostat treatment to decrease the early toxicity of combination treatment, since prior work has shown that HDI treatment for as short as 6-12 hours, in combination DAC for 72h was sufficient to induce synergistic re-expression of silenced tumors suppressor genes [105]. After treatment, cells were rested in drug free media for four days prior to injection of treated cells into NOD/SCID mice on day seven to assess tumorigenicity. In parallel with assessment of H358 xenograft growth, we examined changes in methylation and expression of *p16*, which is epigenetically silenced by promoter hypermethylation in H358, to ensure our treatment regimen produces changes at the epigenetic level. Figure 9A shows demethylation of the *p16* promoter with Aza treatment at days three and seven, with increased gene expression by day seven. Interestingly, the addition of entinostat did not augment *p16* re-expression. Despite this, combination treatment resulted in greater inhibition (approximately 50% vs. 30%) of H358 xenograft growth than did Aza treatment (Figure 9B).

To assess durability of the effects of epigenetic therapy on tumorigenicity of H358, we harvested and pooled tumors within each group, and generated single cells suspensions for injection into a secondary group of NOD/SCID mice. Animals were injected with 10^4 viable cells each to assess both tumor take rate and tumor growth.

Tumor take rated was unaffected by epigenetic therapy, with 1/9 mock, 1/8 combination, and 2/10 Aza injections not producing tumors. Conversely, Aza and combination tumor growth remained significantly inhibited compared to mock tumor growth by week nine after injection (Figure 9C). The durability of these effects is particularly striking given the short duration of *in vitro* epigenetic treatment and the length of time that lapsed (>4 weeks) prior to secondary transplant.

Figure 9. Epigenetic therapy *in vitro* reactivates the tumor suppressor gene p16 and exerts durable anti-tumor effects against H358 xenografts *in vivo*. H358 cells were treated 500nM Aza every 24h for 72h, with or without 500nM entinostat for the final 12h of the 72h treatment period. Cells were harvested at the end of treatment on day 3, reseeded at equal number for each condition, and cultured in drug-free media for four days. **A. Upper** Methylation specific PCR (MSP) depicting complete methylation of the *p16* promoter at days 3 and 7, as evidence by the absence of unmethylated (U) PCR product. Treatment with 500nM Aza results in appearance of unmethylated product and reduction in methylated (M) product, indicating demethylation of *p16* at days 3 and 7. **Lower** Quantitative RT-PCR from triplicate reactions depicting reactivation of p16 expression following Aza and combination (Aza and entinostat) treatment, with peak expression occurring on day 7. **B.** On day 7, cells at equal number per condition were injected subcutaneously into the hind flank of NOD/SCID mice ($2x10^6$ viable cells/mouse). Growth of H358 xenografts following transient *in vitro* exposure to Aza, with or without entinostat, shown as mean tumor volume +/- SEM. Statistical significance compared to mock determined by two-way ANOVA with Bonferroni posttests. **C.** Tumors within each group were harvested and pooled. Single cells suspensions were generated and cells at equal number per condition were injected into a second group of NOD/SCID mice (10^4 viable cells/mouse). Points represent

individual tumor volumes nine weeks post injection. Statistical significance determined by ANOVA with Dunnett's multiple comparison test.

A.

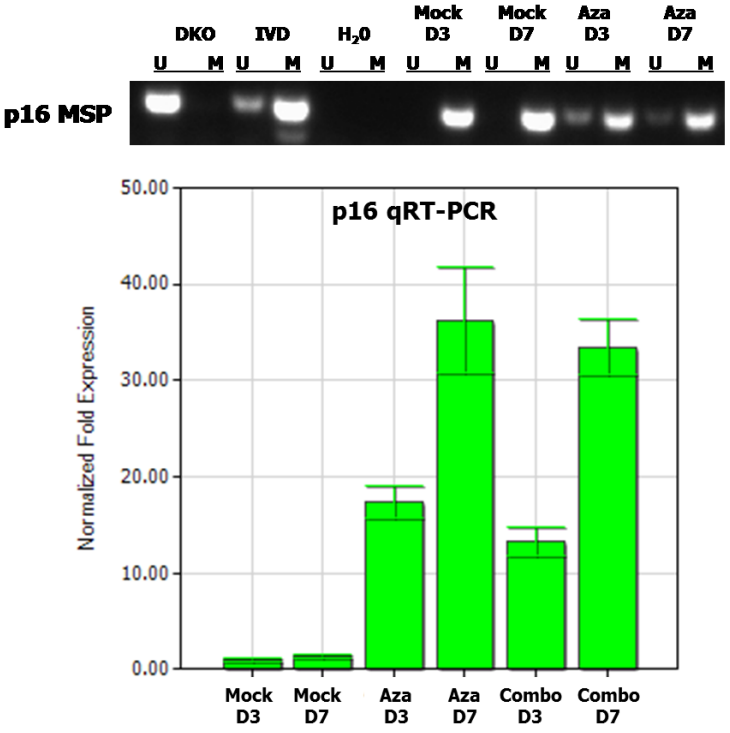

B.

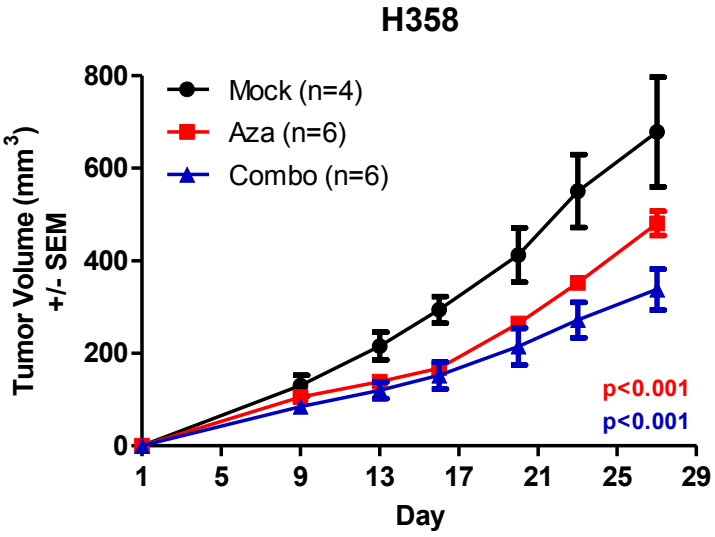

C.

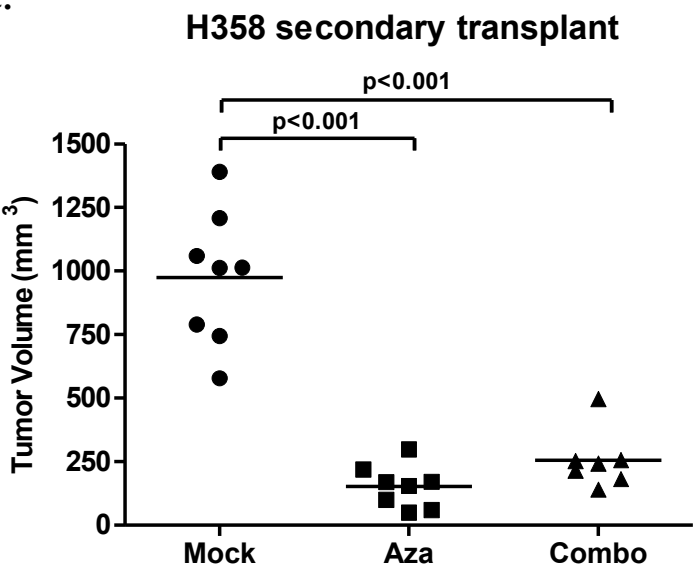

2.6 Reactivation of *p16* is not critical for anti-tumor efficacy of epigenetic therapy in H358 xenografts

There is considerable evidence that methylation and silencing of *p16* is a critical step in the development of NSCLC, particularly the high incidence and early occurrence of *p16* silencing, as well as the critical role for p16 in the regulation of cell cycle progression [31-33, 35, 36]. Since *p16* is densely hypermethylated and transcriptionally silenced in H358 cells, and our work demonstrated that treatment with Aza alone or in combination with entinostat resulted in both *p16* gene re-expression and anti-tumor efficacy, we hypothesized that, if *p16* reactivation plays a key role important in anti-tumor response, knockdown of p16 with shRNA would both prevent gene reactivation after Aza treatment and abrogate anti-tumor efficacy. To test this, we first screened six shRNAs directed at p16 in H596 cells, which overexpress p16 protein as a result of a mutation in *Rb*, to select the optimal shRNA. Oligo 82 results in complete knockdown of

p16 in H596 cells, as shown by Western blot (Figure 10A). We then generated H358 cell lines expressing shRNA oligo 82 (p16_82) or scramble control (scram), and treated cells with mock, Aza, or the combination of Aza and 50nM entinostat, with entinostat administered to cells during the final 24h of Aza treatment. We returned to 50nM entinostat given its clinical relevance over higher doses. We assessed p16 transcript levels on day 7, and found that Aza and combination treatment reactivated p16 expression in scram cells, but not p16 knockdown cells, although a minor increase in expression was noted in p16_82 cells treated with combination (Figure 10B, upper). We then examined protein levels of p16 on day 7. Despite reactivation of p16 transcript in scram cells, protein was undetectable by Western blot (Figure 10B, lower). Given that H358 cells normally completely silence p16, we considered the possibility that the level of p16 protein tolerable by H358 cells may be below the limit of detection, and proceeded to assess whether knockdown of p16 transcript reactivation abrogated inhibition of colony formation or tumorigenicity of H358. Colony formation on Matrigel^{TM} was inhibited equally by Aza and combination in both scram and p16_82 cells (Figure 10C). Moreover, tumorigenicity of both scram and p16_82 H358 xenografts was impaired to a similar degree (Figure 10D). These data suggest that p16 re-expression is not important for Aza induced anti-tumor response in H358 xenografts, either because the protein itself is not expressed following upregulation of transcript, or the undetectable amount of protein that is expressed in scram cells does not contribute to anti-tumor response.

Figure 10. Reactivation of p16 is not critical for anti-tumor efficacy of epigenetic therapy in H358. A. Short hairpin RNA (shRNA) oligos directed at p16 transcript were screened in H596 cells, which overexpress p16 as a result of a mutation in *Rb*. Cells expressing p16 or scrambled

control (scram) shRNA were generated by lentiviral infection and selection with puromycin. Western blots show knockdown of p16 protein by oligo 82. **B.** H358 cells expressing p16_82 or scram shRNA were treated with mock, 500nM Aza every 24h for 72h, or the combination of Aza with 50nM entinostat for the final 24h. **Upper** Quantitative RT-PCR from triplicate reactions depicting reactivation of p16 expression on day 7 in scram cells treated with Aza or combo, but prevention of gene reactivation in p16_82 knockdown H358 cells. **Lower** Western blots depicting a lack of detectable p16 protein in scram cells despite reactivation of transcript. **C.** Epigenetic treated H358 scram and p16_82 knockdown cells were seeded at equal number on solidified Matrigel™ on day 10 to assess colony formation, with four replicates per condition. Data shown as percent colony formation with standard deviation. No differences in inhibition of colony growth by Aza and combo treatment were observed between scram and p16_82 cells. **D.** Mock and Aza treated H358 scram and p16_82 knockdown cells were injected subcutaneously into the right hind flank of NOD/SCID mice on day 10 to assess growth of xenografts tumors (mock, n=7; Aza, n=8). No significant difference in inhibition of tumor growth by Aza pretreatment was observed between scram and p16_82 cells.

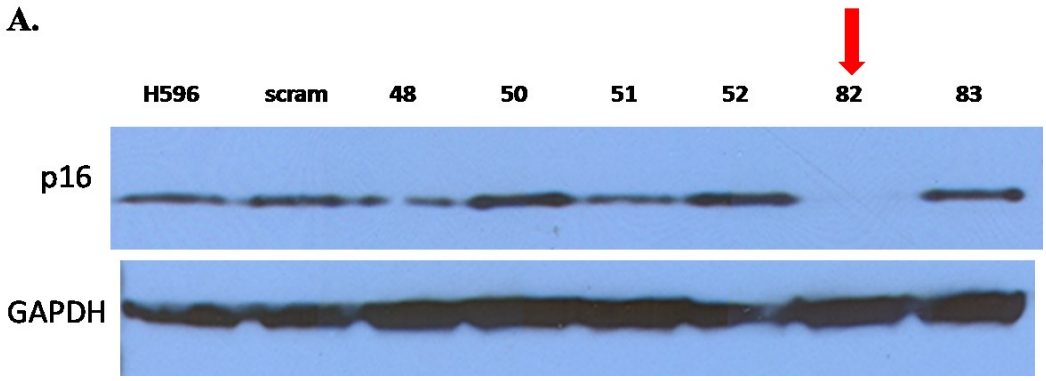

B.

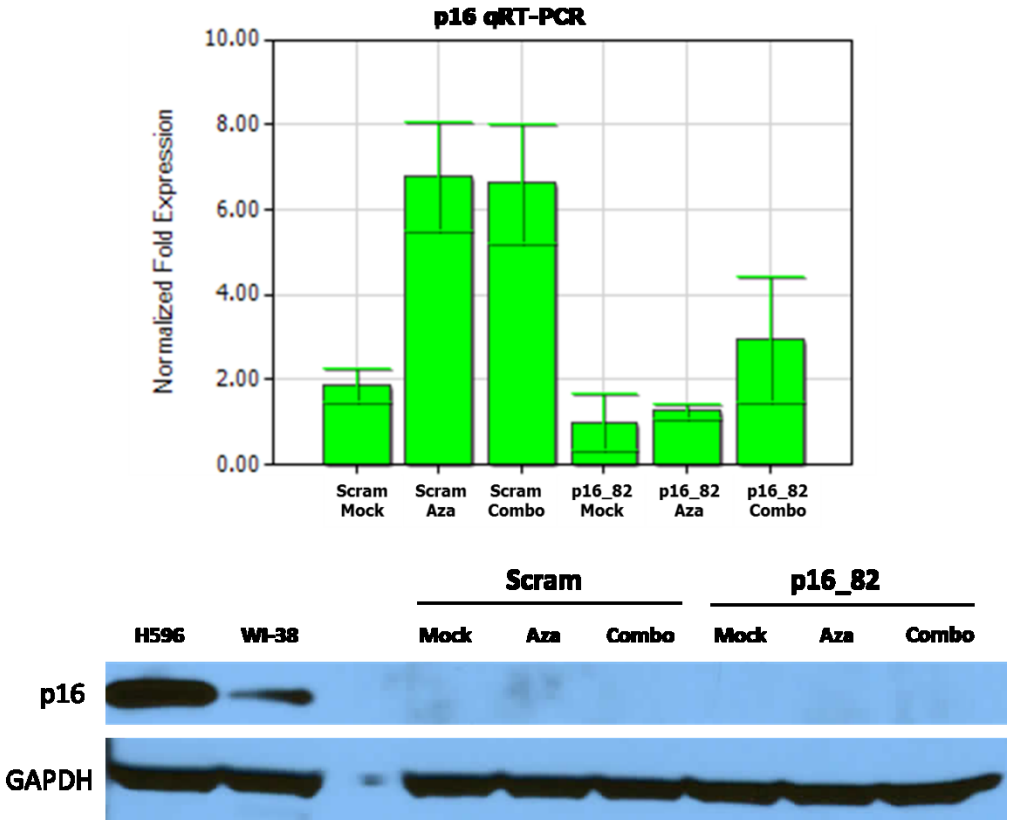
p16 qRT-PCR
Normalized Fold Expression
10.00
8.00
6.00
4.00
2.00
0.00
Scram Mock
Scram Aza
Scram Combo
p16_82 Mock
p16_82 Aza
p16_82 Combo
Scram
p16_82
H596
WI-38
Mock
Aza
Combo
Mock
Aza
Combo
p16
GAPDH

C.

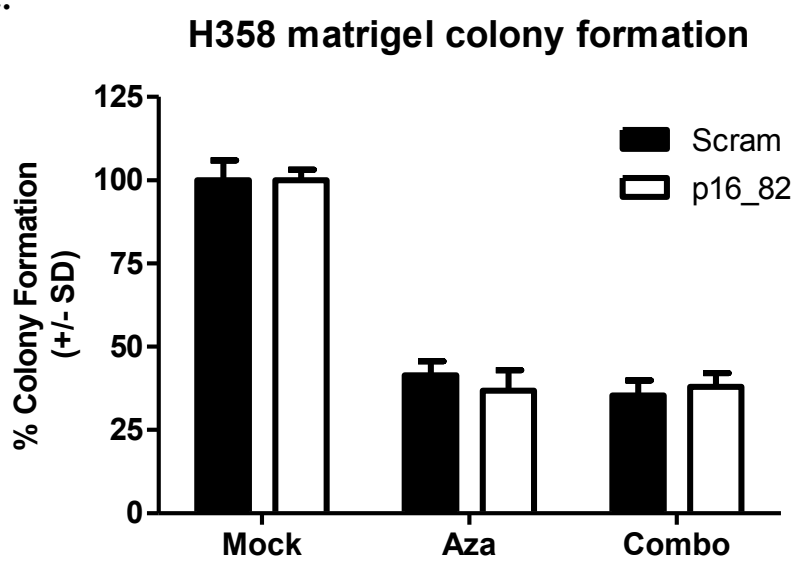
H358 matrigel colony formation
% Colony Formation (+/- SD)
125
100
75
50
25
0
Scram
p16_82
Mock
Aza
Combo

D.

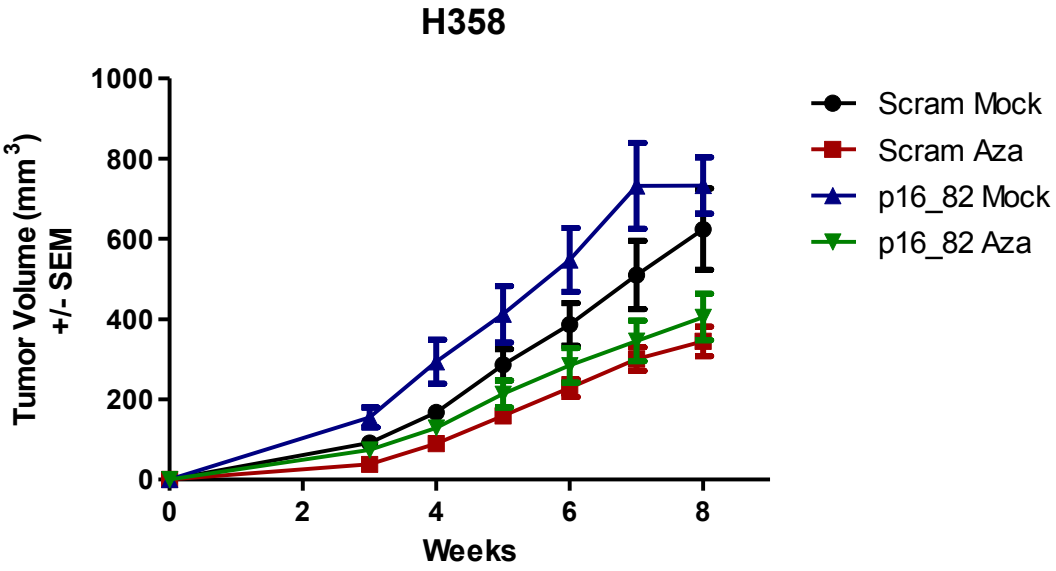

2.7 Epigenetic therapy exerts differential effects on tumorigenicity of NSCLC xenografts

The finding that in short, 3-day *in vitro* treatment with epigenetic therapy reduced tumorigenicity of H358 xenografts prompted us to expand the tumorigenicity studies to our entire panel of cell lines. Again, cells were treated every 24h for 72h with 500nM Aza or mock, and given 50nM entinostat or mock for the final 24h. Cells were rested in drug free media for seven days and then injected into both flanks of NOD/SCID mice, with five mice per arm for a total of n = ten tumors. Interestingly, the epigenetic therapy exerts differential effects on tumorigenicity of these cell lines (Figure 11), and the results of our *in vitro* studies are not directly predictive of these effects. H358 is one of the least sensitive cell lines to Aza in 72h viability experiments, yet exhibit pronounced proliferative inhibition after Aza treatment. Here, a statistically significant reduction in tumorigenicity by Aza, with or without entinostat ($p<0.001$ for both), mirrors the sustained effects of Aza on proliferation after treatment. Similarly, modest combinatorial

benefit was observed in H460 xenografts, following the trend observed in combination matrix, post treatment proliferation, and colony formation studies, however the effects of Aza and combination therapy on tumorigenicity were less pronounced than effects achieved *in vitro*. More interesting are the results in H2170 and H1299 xenografts. Based on cell viability experiments, H2170 is the second most sensitive line to Aza. In addition, H2170 proliferation and colony growth were significantly impaired post Aza treatment. Conversely, the effects of Aza or combination therapy on H2170 tumor growth were minimal, and statistically insignificant. H1299 xenograft growth was moderately inhibited by Aza alone ($p<0.001$), but substantially inhibited by combination epigenetic therapy ($p<0.001$). This is particularly interesting given that H1299 cells are relatively insensitive to Aza treatment in viability assays, and that combination treatment was antagonistic in H1299 *in vitro*. In tumorigenicity studies, in addition to all *in vitro* studies, A549 is unaffected by epigenetic treatment. We were unable to assess the effects of epigenetic therapy on tumorigenic potential of H838 as we were unable to efficiently establish H838 xenografts, even from mock cells, despite multiple attempts.

Figure 11. Effects of *in vitro* epigenetic therapy on tumorigenicity of NSCLC xenografts. Cells were treated with 500nM Aza every 24h for 72h, 50nM entinostat for 24h from hours 48-72 of the treatment period, combination, or mock. Immediately following treatment on day 3, cells were re-seeded at equal number and cultured in the absence of drug for seven days. On day 10, cells at equal number were injected subcutaneously into left and right hind flanks of five female NOD/SCID mice per condition (n=10 tumors). Curves represent mean tumor volume +/- SEM for each epigenetic pretreatment condition. Statistical significance compared to mock determined by

two-way ANOVA with Bonferroni posttests. Otherwise, differences were not significant ($p>0.05$).

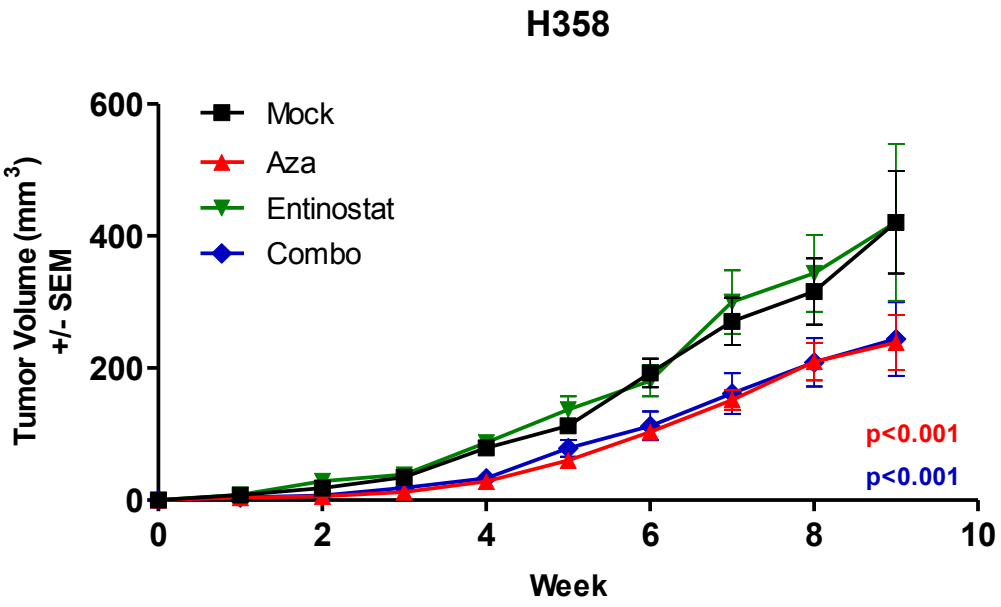

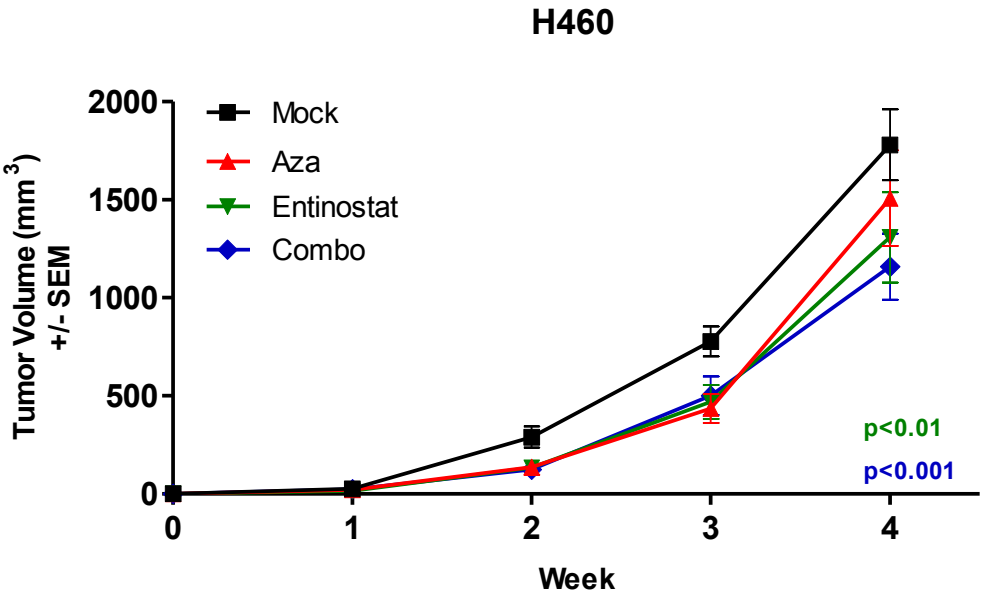

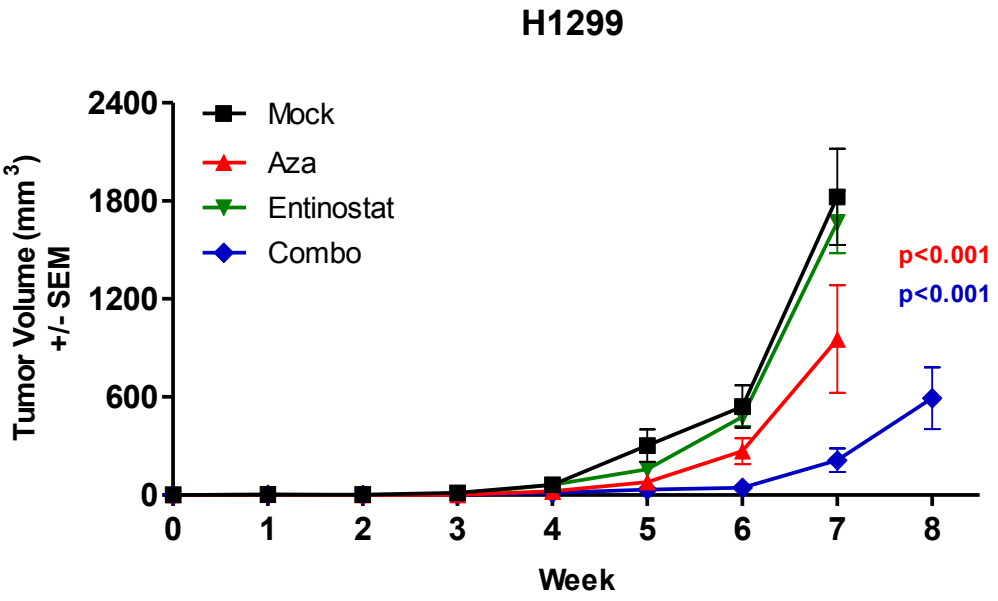
H1299
Mock
Aza
Entinostat
Combo
Tumor Volume (mm3)
+/- SEM
2400
1800
1200
600
0
0
1
2
3
4
5
6
7
8
Week
p<0.001
p<0.001

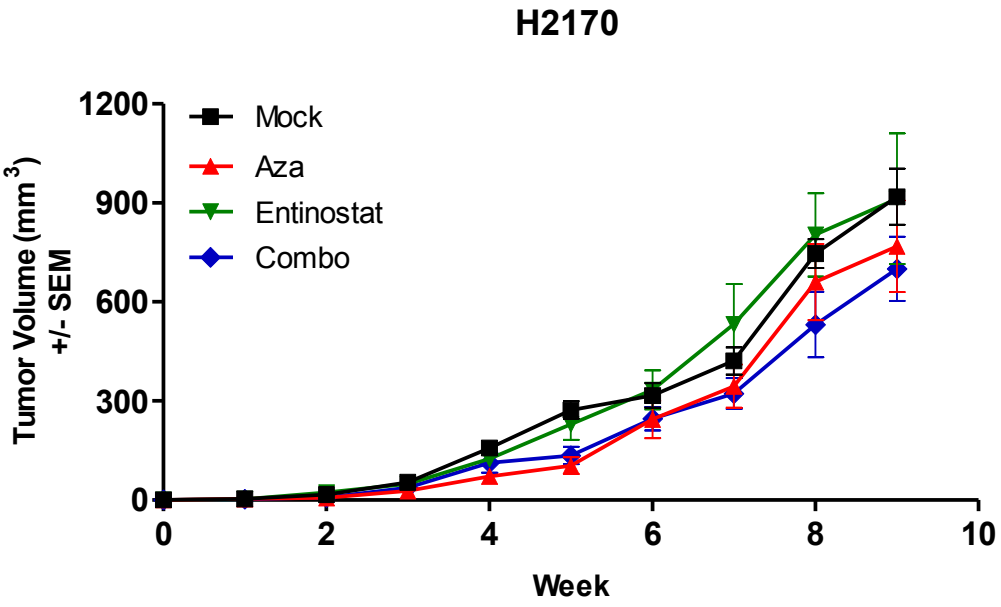
H2170
Mock
Aza
Entinostat
Combo
Tumor Volume (mm3)
+/- SEM
1200
900
600
300
0
0
2
4
6
8
10
Week

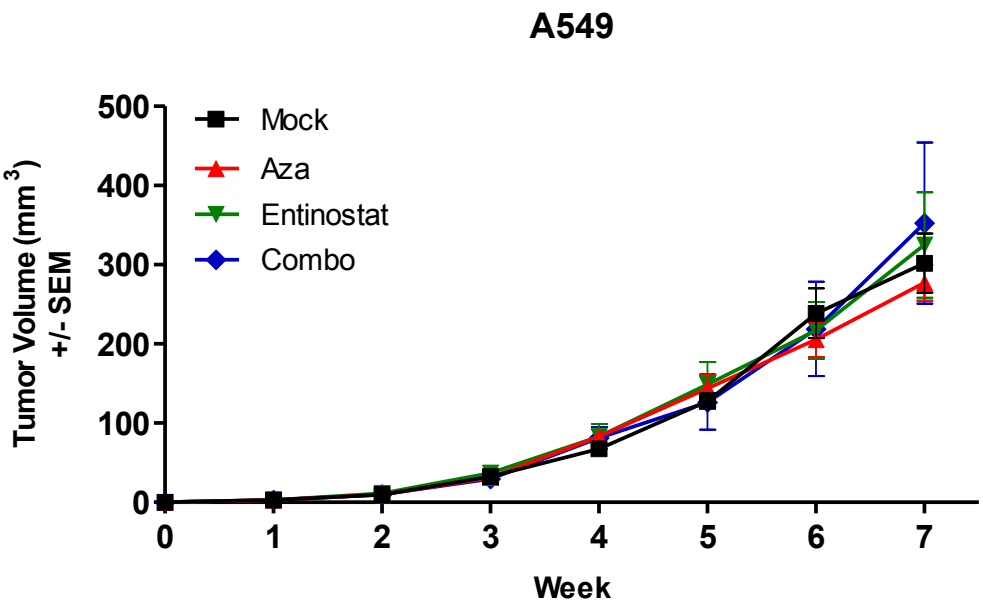

3. Discussion

Using a sub-IC50 dose of Aza, and a low, but clinically achievable, 50nM concentration of entinostat, we demonstrated differential effects on long term tumorigenic potential of xenografts established from *in vitro* treated NSCLC cell lines, without clear association with acute cytotoxic response to Aza or combination treatment. In addition, results of short term viability assays and longer term studies of proliferation and colony growth *in vitro* did not correlate in several cell lines. Interestingly, in two cell lines exhibiting some of the lowest "sensitivity" to Aza in standard cell viability assays, H358 and H1299, *in vitro* treatment with Aza produced significant anti-tumor effects *in vivo*. In contrast, H460 and H2170 xenografts were only modestly affected by Aza, despite these cell lines representing the two most "sensitive" lines in 72h viability assays. Perhaps most striking were the results of combination therapy in H1299. While the combination of Aza and entinostat was antagonistic in H1299 cells in our combination

matrix viability studies and in studies of post treatment proliferation, tumorigenic potential of H1299 xenografts was dramatically reduced by combination therapy.

We also demonstrated combinatorial activity in H358 xenografts established from cells treated *in vitro* with Aza and the higher (but shorter duration), 500nM dose of entinostat. Tumor growth was inhibited by approximately 50%, compared to approximately 30% for Aza alone. Sub-G1 analysis of H358 cells at day seven revealed increased cell death in cells that received 500nM entinostat after treatment with Aza (sequential administration) compared to Aza only treated cells. In addition, cell death resulting from Aza treatment was increased at day seven compared to day four. While in this study, duration of entinostat treatment was reduced to 12hr (vs. 24h), and administration was moved to the final 12h of the 72 Aza treatment period, it is possible that, similar to the results of sub-G1 analysis, tumors grown from combination treated cells exhibited increased cytotoxicity at the time of injection (day seven), and as a result, greater tumor growth inhibition was observed, compared to Aza treatment alone. However, we noted that the growth of tumors in both groups tracked closely for the first two weeks after injection. Then, the growth rate of Aza tumors increased relative to combination treated tumors. Since our cell cycle data also demonstrated a return to normal viability by day ten, it is unlikely that cytotoxicity alone accounts for the anti-tumor effects of both groups, or for the greater effects of combination treatment. In addition, serial transplant of these tumor cells showed the effects on tumor growth were extremely durable. Lastly, Aza still elicited a strong anti-tumor effect in H358 cells that were injected into mice seven days after treatment, the time point by which H358 cells exhibited viability similar to control cells.

Combinatorial epigenetic therapy has already shown promising clinical activity, eliciting major objective responses in a small subset of patients [114]. While the mechanisms that drive clinical efficacy of epigenetic therapy in lung cancer remain unknown, and controversial, insight into these mechanisms is slowly being gleaned from preclinical work, such as studies that demonstrated that relatively low doses of demethylating agents could impair the clonogenic and tumorigenic capacity of leukemia and breast cancer cell lines, while simultaneously reactivating tumor suppressor genes and restoring critical regulatory pathways [86]. While epigenomic studies have not yet been completed, our results strongly suggest the efficacy in our xenografts models is being mediated through non-cytotoxic mechanisms.

4. Materials and Methods

Cell lines and Reagents

NCI-H358, NCI-H460, NCI-H838, NCI-H1299, NCI-H2170, A549, and NCI-H596 were obtained from the American Type Culture Collection (ATCC) and cultured in RPMI-1640 supplemented with 10% FBS, penicillin/streptomycin, 2 mmol/L l-glutamine, 1 mmol/L sodium pyruvate, 10 mmol/L HEPES buffer, and 1.5 g/L sodium bicarbonate. Cells were cultured in a humidified incubator at 37ºC with 5% CO_2.

Drugs and Reagents

5-azacitidine (Aza) was purchased from Tocris Bioscience, dissolved in 1x PBS as a 4mM stock, and stored at -80ºC in aliquots. Fresh aliquots of Aza were thawed immediately prior to use. Entinostat was provided by Syndax Pharmaceuticals and stored

at -20ºC in a desiccator. A 20mM stock solution and serial dilutions to 200uM in DMSO were made and stored at -20ºC. Drug was thawed immediately prior to use and diluted 1:4000 in culture media to provide the desired concentration of entinostat and 0.025% DMSO in media.

Cell viability assays

Cells were seeded in opaque walled 96-well plates as follows: H358 = 4200 cells/well, H460 = 1000 cells/well, H838 = 1700 cells/well, H1299 = 1000 cells/well, H2170 = 4200 cells/well, A549 = 1700 cells/well. Approximately 24h later, cells were treated with the following concentrations of Aza with five replicates per each: 0nM, 10nM, 30nM, 100nM, 300nM, 1uM, 3uM, and 10uM. Cells were retreated every 24h for 72h. Following treatment, ATP content was measured as an indicator of cell viability using the CellTiter-Glo Luminescent Cell Viability Assay (Promega). Cells were incubated with prepared CellTiter-Glo reagent for 10 min at room temperature, and luminescence was read on a SpectraMax M2e plate reader (Molecular Devices). Raw data were corrected for background luminescence, transformed (x=log(x)), and analyzed by nonlinear regression using the equation, log(inhibitor) vs. response with variable slope in GraphPad Prism 5 to obtain IC50 values and R^2. Experiments were repeated at least twice, and mean IC50 and R^2 with standard deviation are provided. Log dose response curves were generated by normalizing transformed data to 0nM control wells and analyzing normalized data by nonlinear regression using the equation, log(inhibitor) vs. response with variable slope. Curves from representative experiments are shown.

Synergy matrix assays

For 72h treatment experiments, cells were seeded in opaque walled 96-well plates in a nine well by eight well matrix as follows: H358 = 4200 cells/well, H460 = 1000 cells/well, H838 = 1700 cells/well, H1299 = 1000 cells/well, H2170 = 4200 cells/well, A549 = 1700 cells/well. Approximately 24h after plating, cells were treated with Aza every 24h for 48h, followed by dose combinations of Aza and entinostat for 24h, with each drug concentration increased in 3-fold increments along a given axis of the dosing matrix. Cell viability was assessed at 72h using the CellTiter-Glo assay (Promega). Raw data were corrected for background luminescence and inhibition, Z, was calculated for each well using the equation, $Z = (1-T/C)*100$, where T equals the background corrected luminescence for a given well (ie. dose combination) and C equals the mean background corrected luminescence of eight untreated control wells. Inhibition scores were plotted in a response matrix. Next, a response over highest single agent (HSA) matrix was generated by subtracting the highest Z for each single agent in the corresponding row and column from Z for a given dose combination. Independent experiments were repeated at least twice, with 1-2 plates per experiment, to ensure consistent results, and representative data shown. For 96h treatment experiments, H358 and H460 cells were seeded at 3200 cells/well and 1000 cells/well, respectively, in a nine well by eight well matrix in 96-well plates. Cells were treated with Aza every 24h for 72h, with the concentration of Aza increased in 2-fold increments along the x-axis of the matrix. Cells were treated with entinostat either during the first 24h (overlapping) or for 24h following Aza treatment (sequential), with the concentration of entinostat increased in 3-fold increments along the y-axis of the matrix. Proliferation was assessed at 96h using the

CellTiter AQueous One MTS proliferation assay (Promega) and absorbance at 490nm measured on a SpectraMax M2e plate reader (Molecular Devices). Response and HSA matrix plots were generated as described above. Experiments were repeated at least twice to ensure consistent results, and representative data shown.

Cell cycle assay following epigenetic therapy

H358 cells were seeded at 9.6 x 10^4 cells/well in 6-well plates and allowed to adhere for approximately 24h. Cells then were treated in triplicate with 500nM Aza or mock (1x PBS) in fresh media every 24h for 72h. Cells received 500nM entinostat during the first 24h of treatment (overlapping) or for 24h following treatment with Aza (sequential). Cells that did not receive entinostat were mock treated with 0.025% DMSO. All media was saved in separate 6-well plates after removal from cells. At the end of treatment, cells were washed and harvested. Saved media, washes, and cells for each replicate were pooled and centrifuged 5 min at 300 x g. Cells were washed in 2mL 1% FBS/1x PBS and centrifuged again. Cells were resuspended in 1mL cold 1x PBS, and fixed in 9mL cold 70% ethanol for at least 24h at 4°C. Fixed cells were centrifuged at 300 x g for 5 min, resuspended in 1.5mL of a 2:1 mix of 1% FBS/1x PBS and phosphate citric acid buffer (pH 7.8), and incubated for 5 min at RT. After centrifugation and removal of supernatant, cells were resuspended in 300uL of PI staining solution (10ug/mL propidium iodide and 3 K.U. of RNase A in 1% FBS/1x PSB) and incubated at 37°C for 30 min. Flow cytometry was performed to detect propidium iodide staining of DNA. Ten thousand PI positive gated events were collected for each sample. Similarly, cells that received

epigenetic therapy and were cultured in drug free media until day 7 and day 10 time points were also harvested, fixed, and analyzed as described.

H358 tumorigenicity and serial transplant

H358 cells were seeded at 3 x 10^6 cells per T75cm^2 flask. Approximately 18h later, cells were treated with 500nM Aza or mock (1x PBS) in fresh media every 24h for 72h. During the final 12h of the 72h treatment period, Aza treated cells received either 500nM entinostat or 0.05% DMSO, and mock treated cells received 0.05% DMSO. Cells were harvested at the end of treatment on day 3, reseeded at equal number, and cultured for four days in drug free. On day 7, cells were harvested, counted, and suspended in a 50:50 mix of 1x PBS and Matrigel^{TM}. Female NOD/SCID mice, 5-7 weeks old, were then injected subcutaneously in the right hind flank with a 100uL volume containing 2 x 10^6 viable cells. Tumor volume measurements were calculated as (L x W^2)/2. Statistical significance compared to mock was determined by repeated measures two-way ANOVA with Bonferroni posttests in GraphPad Prism 5. On day 29 post injection, tumors within each group were pooled and mechanically disrupted to generate single cell suspensions. Cells were injected into a second cohort of NOD/SCID mice at 10^4 viable cells per injection. Statistical significance at week 9 post injection was determined by ANOVA with Dunnett's multiple comparison test in GraphPad Prism 5. Protocols for these experiments were approved by the John Hopkins University Animal Care and Use Committee and were strictly followed.

Methylation specific PCR (MSP) to detect *p16* methylation

DNA was isolated from H358 cells at 72h and at day seven using the Qiagen DNA Mini kit. Quantity and purity were assessed by measuring absorbance at 260nm and 280nm on the NanoDrop spectrophotometer (Thermo Scientific). Bisulfite conversion of 1ug of DNA per sample was performed using the Zymo EZ DNA methylation kit. MSP was performed on the IQ5 thermal cycler (Bio-Rad) using *p16* primers and conditions as previously described [127]. PCR products were visualized on a 2% agarose gel with GelStar™ Nucleic Acid Gel Stain (Lonza).

Quantitative RT-PCR to detect *p16* gene expression

RNA was isolated using TRIzol® and provided protocol (Life Technologies). Quantity and purity were assessed by measuring absorbance at 260nm and 280nm on the NanoDrop spectrophotometer (Thermo Scientific). cDNA was synthesized from 1ug of RNA using the Quantitect Reverse Transcription Kit and provided protocol (Qiagen). PCR using template cDNA, iQ SYBR Green Supermix, and standard thermocycling conditions was performed on the IQ5 thermal cycler and real-time detection system (Bio-Rad). Primers for p16 and GAPDH were previously published [21, 128]. p16 expression was normalized to GAPDH for each sample.

shRNA knockdown of p16

Lentiviral particles were generated in 293T cells (2.5 x 10^6 cells per T25 flask) and H596 and H358 cells were infected according to The RNAi Consortium (TRC) Library Production and Performance Protocols (Broad Institute) [129]. p16 shRNA constructs were obtained from TRC. The pLKO.1-scramble control vector (Addgene plasmid 1864)

was kindly provided by Dr. Timothy F. Burns. Selection with 0.5ug/mL puromycin began 24h after infection.

Western blot for p16

Protein was isolated from H358 cell pellets rinsed with 1x PSB and lysed in 1x RIPA buffer containing protease and phosphatase inhibitors (Sigma). Protein was quantified using the BCA Protein Assay (Thermo Scientific Pierce) and measuring absorbance at 562nm on the SpectraMax M2e plate reader (Molecular Devices). Proteins were resolved by electrophoresis on 12% NuPAGE® Bis-Tris Gels (Life Technologies). Proteins were transferred to a PVDF membrane, and blots were blocked for 1h at RT in 5% milk/0.2% TBST. Blots were probed with p16 and GAPDH primary antibodies (Cell Signaling Technologies) at 1:1000 in 5% milk/0.2% TBST, overnight at 4°C. Blots were then washed 4 x 5min at RT with 0.1% TBST (GAPDH) or 0.2% TBST (p16). Blots were probed with anti-Rabbit HRP secondary antibody for 90 min at RT, then washed again as described. Proteins were detected using Amersham^{TM} ECL^{TM} Plus (GAPDH) or Amersham^{TM} ECL^{TM} Prime (p16) (GE Healthcare).

Treatment of cell lines with epigenetic therapy for proliferation, colony formation, and tumorigenicity studies

H358, H460, H838, H1299, H2170, and A549 cells were seeded at 1 x 10^6, 2 x 10^5, 3.5x10^5, 2 x 10^5, 1 x 10^6, and 3.5 x 10^5 cells per 75cm^2, respectively, and allowed to adhere approximately 20-24h. Cells were then treated with 500nM Aza or mock (1x PBS) in fresh media every 24h for 48h, then treated with 500nM Aza, 50nM entinostat,

combination, or mock (1x PBS) for the final 24h of treatment. All treatments contained a final of 0.025% DMSO for the final 24h treatment.

Assessment of proliferation following epigenetic therapy

Following 72h epigenetic treatment, cells were seeded in opaque walled 96-well plates with five replicates per condition, as follows: H358 = 1000 cells/well, H460 = 500 cells/well, H838 = 1000 cells/well, H1299 = 500 cells/well, H2170 = 1500 cells/well, A549 = 1000 cells/well. Cells were cultured 5-7 days in the absence of drug. The number of viable cells present was then determined using the CellTiter-Glo assay (Promega). Data were corrected for background absorbance and normalized to mock to determine the percent of viable cells present. Data for H460, H838, H1299, and H2170 represent an average of normalized data from two independent experiments. Data for H358 and A549 are from a single experiment, as prior experiments for H358 and A549 using the CellTiter AQueous One MTS assay produced similar results. Statistical significance for each condition compared to mock was determined in GraphPad Prism 5 using ANOVA with Dunnett's multiple comparison test.

Crystal violet staining of proliferating cells after epigenetic therapy

Following 72h epigenetic treatment, cells were seeded in 12-well plates in triplicate, as follows: H358 = 2 x 10^4 cells/well, H460 = 5000 cells/well, H838 = 10^4 cells/well, H1299 = 5000 cells/well, A549 = 10^4 cells/well. Cells were cultured 5-7 days in the absence of drug, then stained with crystal violet (0.5% in 95% ethanol).

Matrigel™ colony formation assay

Following 72h epigenetic treatment, cells were seeded on a 40uL layer of solidified Matrigel™, with five replicates per condition, as follows: H358 = 2000 cells/well, H460 = 500 cells/well, H838 = 1000 cells/well, H1299 = 500 cells/well, H2170 = 1500 cells/well, A549 = 1000 cells/well. Colonies were grown 5-9 days, stained with MTT reagent, and imaged and counted on the GelCount™ colony counter (Oxord Optronix). Colony number was normalized to mock to determine % colony formation. Experiments were repeated at least twice, with the exception of H838 and H1299 which did not form distinct colonies and could not be quantified. Statistical significance for each condition compared to mock was determined in GraphPad Prism 5 using ANOVA with Dunnett's multiple comparison test.

Xenograft tumorigenicity experiments

Following epigenetic treatment, cells were cultured for seven days in drug free media. On day 10, cells were harvested, counted, and injected subcutaneously into the left and right hind flank of 5-7 week old female mice, in a total volume of 100uL, consisting of a 50:50 mix of 1x PBS and Matrigel™. Cell numbers per injection were as follows: H358 = 3.5 x 10^5, H460 = 2 x 10^5, H1299 = 2 x10^5, H2170 = 3.35 x 10^5, and A549 = 1.5 x 10^5. Tumor volume measurements were calculated as (L x W x H). Statistical significance compared to mock was determine by repeated measures two-way ANOVA with Bonferroni posttests in GraphPad Prism 5. Protocols for all animal experiments were approved by the John Hopkins University Animal Care and Use Committee and were strictly followed.

III. Epigenetic therapy as a primer for subsequent chemotherapy

1. Introduction

Lung cancer remains a dominant public health burden as the leading cause of cancer-related mortality worldwide [1]. Non-small cell lung cancer (NSCLC) accounts for approximately 80% of all lung cancer cases, and comprises several histological subtypes, including adenocarcinoma, squamous cell carcinoma, and less commonly, large cell carcinoma. The high incidence of NSCLC cases and poor prognosis necessitate research to define novel and more effective treatment options. Treatment of adenocarcinoma has advanced in recent years with mutational characterization and the development of targeted therapies against EGFR and ALK [3-5]. However, many NSCLC patients do not harbor *EGFR* mutations or *ALK* fusions, and are unlikely to benefit from these agents. In addition, acquired resistance and disease recurrence also limit their utility [7-9]. As a result, NSCLC is still frequently treated with conventional cytotoxic chemotherapy, which is often hampered by limited efficacy, high toxicity, and again, resistance and recurrence of disease.

There is a wealth of evidence (reviewed elsewhere, and outlined in the introductory chapter of this thesis) that epigenetic dysregulation, including silencing of tumors suppressor genes, is intimately involved in lung carcinogenesis [33, 130]. Recently, epigenetic therapy has garnered considerable interest as a promising therapeutic option for NSCLC following the results of a phase I/II trial of the combination of the demethylating agent, azacitidine (Aza), and the class I specific histone deacetylase inhibitor (HDI), entinostat (MS275), in advanced stage disease [114]. While only a small number of patients (2/34) exhibited objective responses to combination

epigenetic therapy alone, some of these responses were surprisingly durable, with two patients experiencing disease stabilization for 14 and 18 months. Also intriguing was the observation that several patients, including some who progressed quickly on epigenetic therapy, responded surprisingly well to subsequent chemotherapy (Figure 12), despite a median of three prior therapies for this patient population. Two patients survived 44 and 52 months after epigenetic therapy while receiving only one subsequent treatment regimen [114].

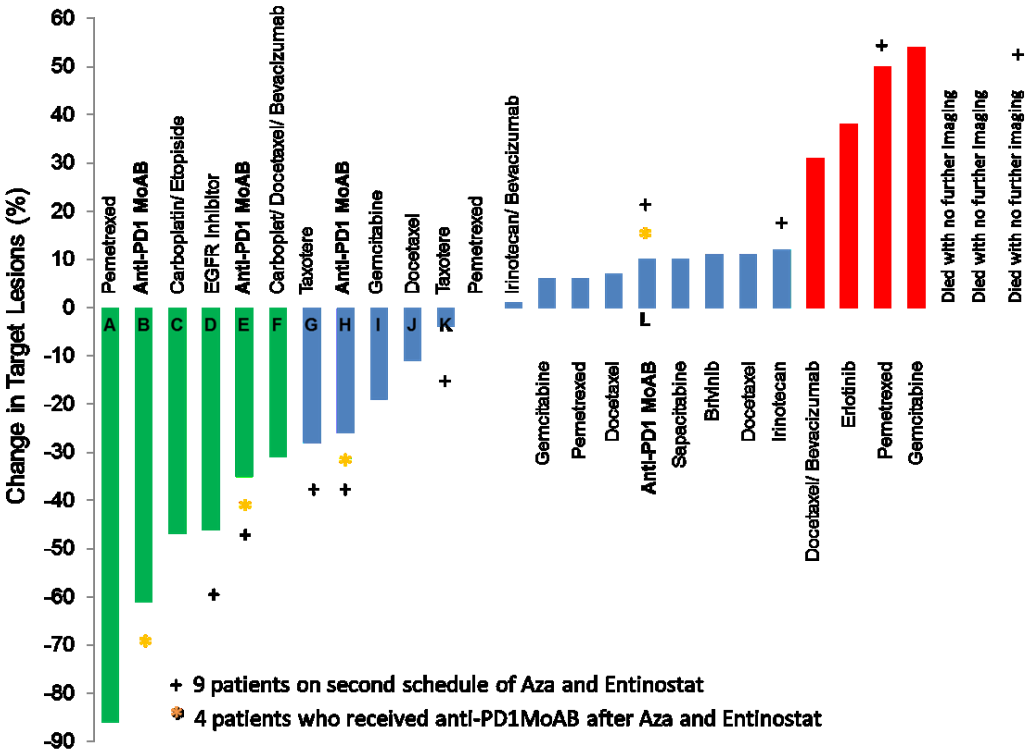

Figure 12. Maximal change in tumor size in response to subsequent chemotherapy following combinatorial epigenetic therapy. Green bars represent objective responses by RECIST criteria to specified subsequent treatment regimen as measured by the % change in

maximal diameters of target lesions. Blue bars represent disease stabilization, while red bars indicate disease progression. Graphs updated from Juergens et al., 2011.

Interestingly, a similar scenario was previously observed in a pilot phase I/II study of decitabine in stage IV NSCLC patients, with one patient receiving chemotherapy roughly six months after treatment with the demethylating agent, decitabine (DAC), and surviving 81 months [87]. Although comprising only a small number of patients, these observations suggest the potential for epigenetic therapy to sensitize NSCLC to subsequent chemotherapy. While not yet formally tested in NSCLC, supporting clinical evidence for a priming effect does exist for solids tumors. Two recent trials demonstrated that treatment with a demethylating agent (Aza or DAC) sensitizes resistant and refractory ovarian tumors to platinum chemotherapy [121, 122].

Preclinical evidence is also mounting describing the involvement of epigenetic mechanisms in drug resistance in cancer [115, 116, 118, 131, 132], and several studies have demonstrated sensitization of solid cancers to chemotherapy following treatment with epigenetic based therapies, in association with reactivation of silenced tumor suppressor genes or restoration of tumor suppressor protein expression [116, 117, 131]. Interestingly, one of these studies found that the combination of DAC and the pan-HDI, belinostat, was more effective than decitabine alone at reactivating the silenced tumor suppressor, *hMLH1*, and sensitizing a cisplatin resistant ovarian cancer cell line to cisplatin, both *in vitro* and *in vivo* [131]. Another recent paper directly implicated an epigenetic mechanism involving increased expression of the histone demethylase, JARID1A/KDM5A, and loss of H3K4me2/me3 histone marks, in tolerance of a mutant *EGFR* NSCLC line to EGFR targeted therapy, and demonstrated the ability to prevent or

suppress the phenotype through treatment with HDIs [118]. These latter two studies highlight a distinct role for histone deacetylase (HDAC) inhibition, in addition to DNA demethylation, in reversal of epigenetically mediated resistance mechanisms.

Here we test, using several preclinical models encompassing the three most common histological subtypes, whether priming with single agent or combination epigenetic therapy sensitizes NSCLC to various subsequent chemotherapeutic agents. We find that the combination of azacitidine and entinostat enhances sensitivity of select NSCLC tumors to irinotecan *in vivo*, while sensitivity to other chemotherapeutic agents remains largely unaffected both *in vitro* and *in vivo*.

2. Results

2.1 Epigenetic therapy does not sensitize NSCLC cell lines to subsequent chemotherapy in acute cytotoxicity assays

We aimed to determine whether epigenetic therapy sensitizes NSCLC cell lines to subsequent chemotherapy *in vitro*. We selected H1299 (large cell carcinoma), H358, H838, and A549 (all adenocarcinoma) for study. We first treated cell lines with 500nM Aza every 24 hours for 72 hours (days 0-3), 50nM entinostat for 24 hours (days 2-3), combination, or mock treatment. At the end of treatment on day 3, cells were harvested, reseeded, and rested in drug free media for one week prior to exposure to various chemotherapeutic agents on day 10. Cisplatin, docetaxel, gemcitabine, and vinorelbine were selected as they are FDA approved for the treatment of NSCLC. Two additional agents, the hsp90 inhibitor, 17-AAG, and the proteasome inhibitor, bortezomib, were also included. It has been shown in breast cancer that HDAC1 maintains the chaperone,

hsp90, in a deacetylated state, allowing its association with and preventing proteasomal degradation of DNA methyltransferase 1 (DNMT1). HDAC1 inhibition induces hsp90 hyperacetylation, disrupts association of hsp90 with DNMT1, and promotes ubiquitination and degradation of DNMT1 via the proteasome [58]. Since HDAC1 is a target of entinostat, we hypothesized that pretreatment with entinostat may augment sensitivity to 17-AAG.

Pretreated cells were seeded at equal number in 96-well plates on day 9, and treated with chemotherapy for 72h beginning on day 10. Following treatment, cell viability was immediately assessed using the CellTiter-Glo luminescence viability assay, with three replicates per dose tested. Raw data values were corrected for background luminescence to represent the total number of viable cells present. The chemotherapy dose range was then transformed to a log scale (x=log(x)). Nonlinear regression of corrected, transformed data was performed using the equation, log(inhibitor) vs. response with variable slope, to obtain IC50 values, 95% confidence intervals, and R^2 for each epigenetic pretreatment condition and chemotherapy tested (Table 4). In cases where a maximal inhibition plateau was not reached and the calculated IC50 was ambiguous (H358 and H838 cisplatin), IC50 was considered not determined (ND). Experiments were repeated at least twice, with the exception of vinorelbine for H358 and H1299, where no notable differences were observed. Statistical analysis of logIC50 and standard error of logIC50 via ANOVA with Tukey's multiple comparison test revealed no statistically significant differences in IC50 among pretreatment conditions for any evaluable chemotherapy tested.

Table 4. Calculated IC50 values for chemotherapy following epigenetic priming.

IC50, 95%CI, and R^2 calculated from representative experiments with three replicates per dose tested. No statistically significant differences in IC50 by ANOVA with Tukey's Multiple Comparison Test were observed. ND denotes IC50 values were not determined.

Cell Line	Condition	IC50	95% CI	R^2
		17AAG		
H1299	Mock	99.29nM	92.06 to 107.1	0.9951
	Entinostat	94.44nM	86.83 to 102.7	0.9961
	Aza	93.99nM	82.25 to 107.4	0.9907
	Combination	102.0nM	91.60 to 113.6	0.9898
H358	Mock	42.19nM	29.45 to 60.43	0.9213
	Entinostat	31.56nM	28.13 to 35.41	0.9848
	Aza	41.49nM	33.84 to 50.88	0.9709
	Combination	37.57nM	33.71 to 41.87	0.9902
A549	Mock	46.38nM	37.55 to 57.29	0.9828
	Entinostat	44.42nM	35.82 to 55.08	0.9814
	Aza	34.28nM	28.15 to 41.74	0.9710
	Combination	37.62nM	31.07 to 45.56	0.9901
		Bortezomib		
H1299	Mock	5.616nM	5.057 to 6.238	0.9966
	Entinostat	6.000nM	5.252 to 6.855	0.9960
	Aza	5.996nM	5.714 to 6.292	0.9993
	Combination	5.862nM	5.267 to 6.524	0.9959
H358	Mock	4.648nM	3.882 to 5.564	0.9831
	Entinostat	4.342nM	3.880 to 4.860	0.9931
	Aza	4.623nM	4.312 to 4.956	0.9977
	Combination	4.331nM	3.979 to 4.714	0.9961
H838	Mock	8.075nM	6.887 to 9.467	0.9938
	Entinostat	7.581nM	6.844 to 8.397	0.9989

	Aza	6.797nM	6.175 to 7.481	0.9972
	Combination	6.492nM	5.303 to 7.947	0.9847
A549	Mock	6.402nM	5.539 to 7.399	0.9929
	Entinostat	6.414nM	5.668 to 7.258	0.9938
	Aza	6.377nM	5.063 to 8.033	0.9780
	Combination	6.621nM	5.403 to 8.115	0.9871
		Cisplatin		
H1299	Mock	1.777μM	1.400 to 2.256	0.9714
	Entinostat	1.717μM	1.209 to 2.437	0.9637
	Aza	1.398μM	1.104 to 1.771	0.9801
	Combination	1.526μM	0.926 to 2.511	0.9401
H358	Mock	ND	-	-
	Entinostat	ND	-	-
	Aza	ND	-	-
	Combination	ND	-	-
H838	Mock	ND	-	-
	Entinostat	ND	-	-
	Aza	ND	-	-
	Combination	ND	-	-
A549	Mock	2.981uM	2.338 to 3.800	0.9720
	Entinostat	3.352uM	1.834 to 6.127	0.9620
	Aza	3.599uM	1.641 to 7.891	0.8781
	Combination	4.211uM	0.916 to 19.36	0.9108
		Docetaxel		
H1299	Mock	2.345nM	1.903 to 2.889	0.9855
	Entinostat	2.301nM	1.906 to 2.778	0.9856
	Aza	2.162nM	1.809 to 2.585	0.9894
	Combination	2.397nM	2.111 to 2.722	0.9923
H838	Mock	1.380nM	1.153 to 1.651	0.9862

	Entinostat	1.115nM	1.006 to 1.236	0.9949
	Aza	1.259nM	1.099 to 1.441	0.9920
	Combination	1.074nM	0.773 to 1.491	0.9615
A549	Mock	1.121nM	0.742 to 1.693	0.9701
	Entinostat	0.986nM	0.739 to 1.315	0.9816
	Aza	1.499nM	1.086 to 2.069	0.9811
	Combination	1.076nM	0.686 to 1.686	0.9673
		Gemcitabine		
H1299	Mock	7.736nM	6.695 to 8.938	0.9887
	Entinostat	6.939nM	5.892 to 8.173	0.9888
	Aza	5.876nM	4.375 to 7.870	0.9656
	Combination	6.075nM	5.024 to 7.344	0.9854
H838	Mock	38.55nM	26.08 to 56.98	0.9265
	Entinostat	42.75nM	31.31 to 58.38	0.9576
	Aza	38.94nM	27.84 to 54.45	0.9457
	Combination	44.80nM	31.63 to 63.45	0.9511
		Vinorelbine		
H1299	Mock	2.841nM	2.547 to 3.168	0.9942
	Entinostat	2.782nM	2.482 to 3.118	0.9944
	Aza	2.727nM	2.398 to 3.100	0.9934
	Combination	2.386nM	2.066 to 2.755	0.9901
H358	Mock	2.844nM	2.274 to 3.557	0.9854
	Entinostat	2.351nM	1.873 to 2.952	0.9867
	Aza	2.029nM	1.537 to 2.679	0.9739
	Combination	2.075nM	1.550 to 2.778	0.9719
H838	Mock	2.479nM	2.207 to 2.784	0.9899
	Entinostat	2.422nM	2.143 to 2.738	0.9901
	Aza	2.172nM	1.928 to 2.446	0.9916
	Combination	2.034nM	1.732 to 2.387	0.9865

A549	Mock	0.736nM	0.640 to 0.845	0.9890
	Entinostat	0.730nM	0.641 to 0.832	0.9904
	Aza	0.866nM	0.368 to 2.037	0.9810
	Combination	0.751nM	0.6210to 0.909	0.9794

Transformed data were then normalized to untreated controls within each pretreatment group for a given chemotherapy. Log dose response curves generated from normalized data demonstrate minimal differences in response to chemotherapy across cell lines, pretreatment conditions, and chemotherapy tested (Figure 13).

Figure 13. Epigenetic priming does not alter chemosensitivity of NSCLC cell lines. Log dose response curves for NSCLC cell lines treated with chemotherapy for 72h one week after treatment with epigenetic therapy (50nM entinostat for 24h, 500nM Aza for 72h, combination, or mock). Individual curves represent the percentage of viable cells (+/- standard deviation) for each epigenetic pretreatment condition normalized to its own untreated control cells, such that the highest values for each pretreatment condition represent 100%, and 0 = 0%.

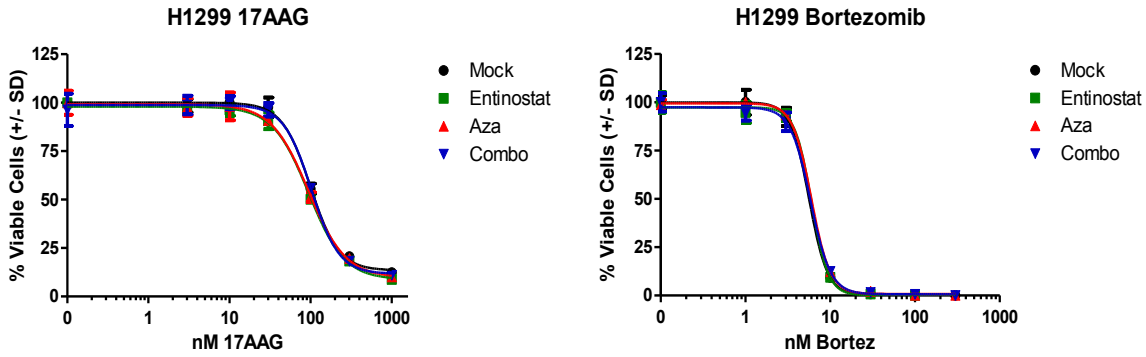

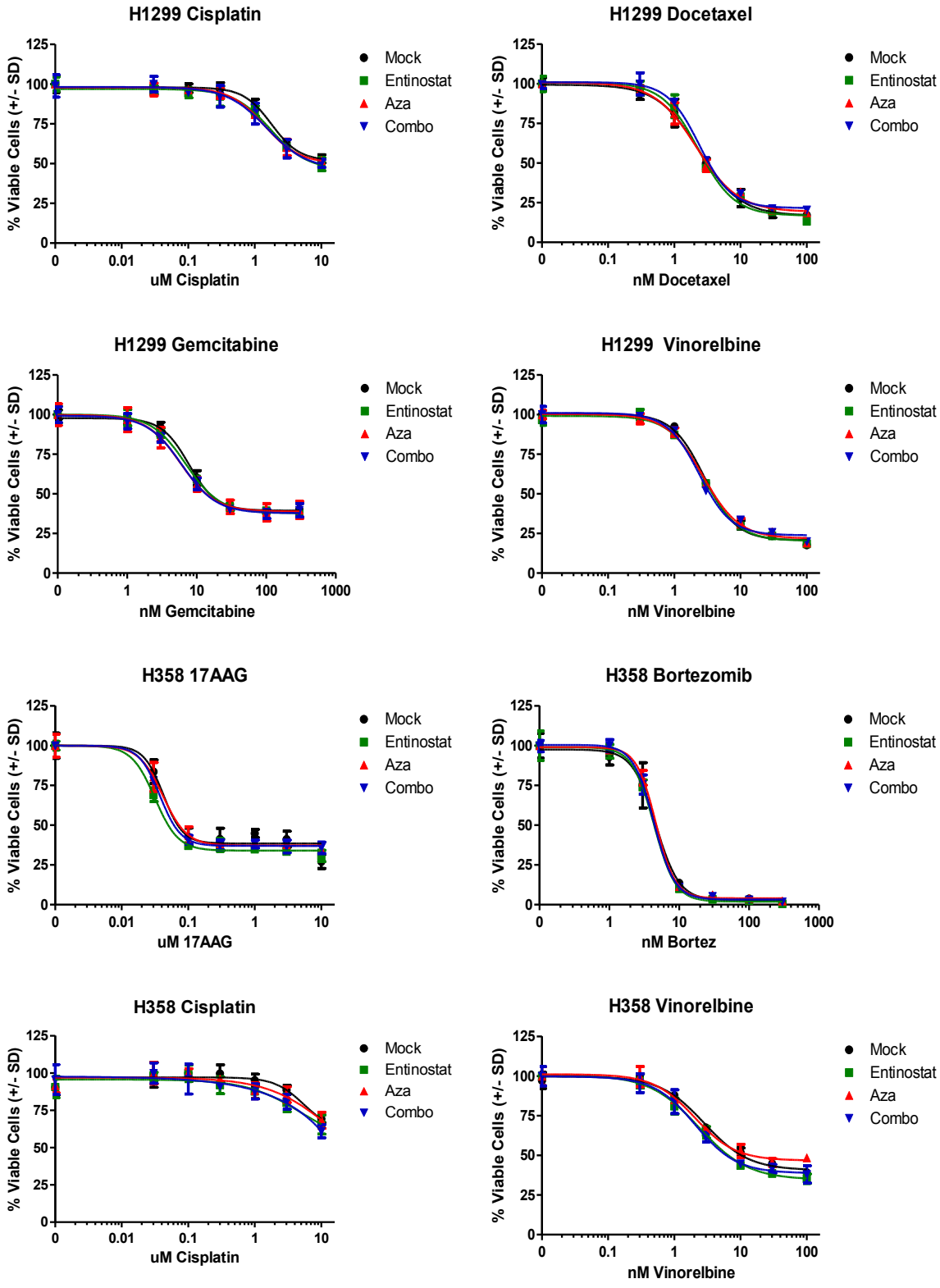
H1299 Cisplatin
% Viable Cells (+/- SD)
uM Cisplatin
H1299 Docetaxel
nM Docetaxel
H1299 Gemcitabine
nM Gemcitabine
H1299 Vinorelbine
nM Vinorelbine
H358 17AAG
uM 17AAG
H358 Bortezomib
nM Bortez
H358 Cisplatin
uM Cisplatin
H358 Vinorelbine
nM Vinorelbine
Mock
Entinostat
Aza
Combo

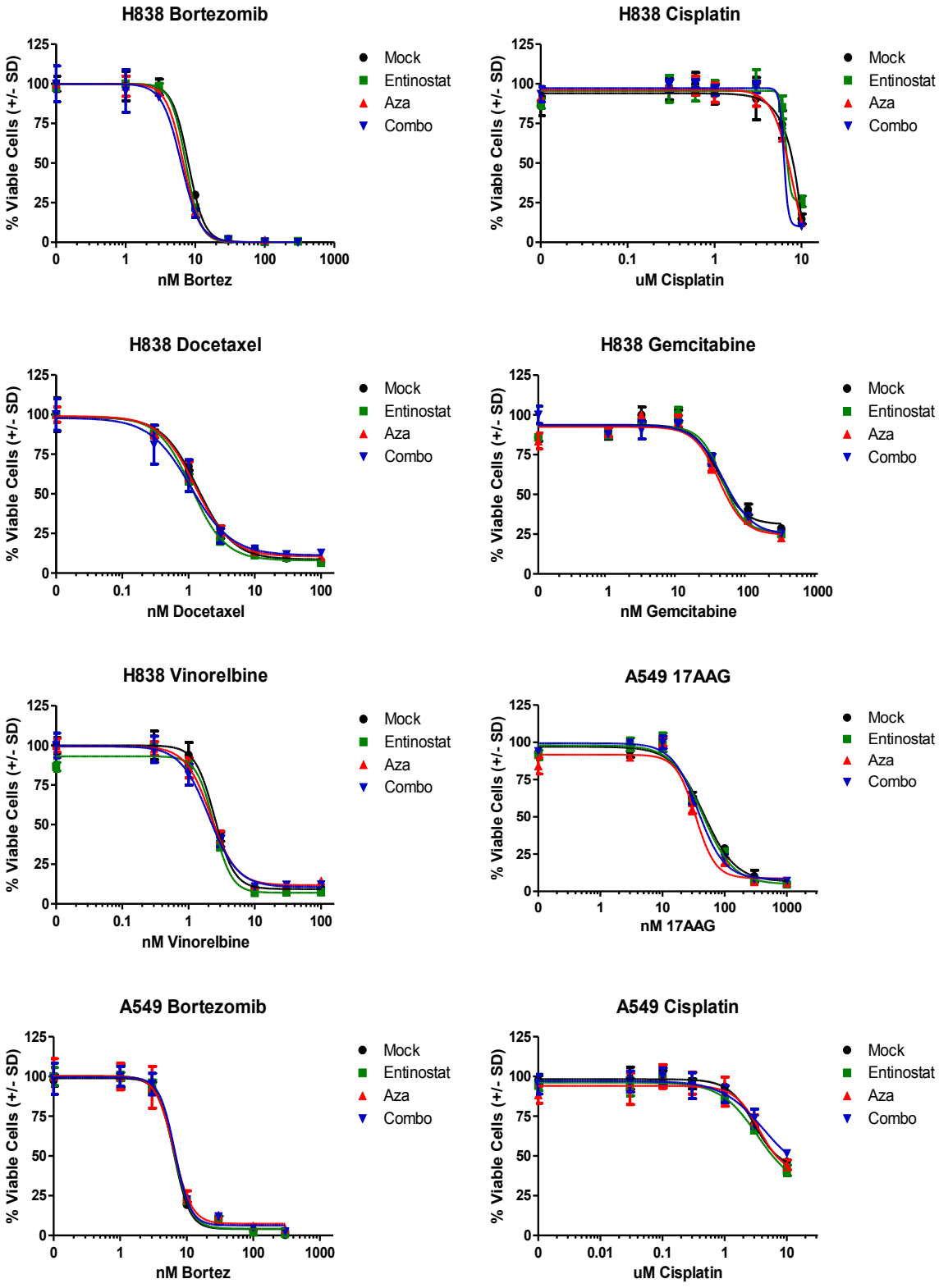
H838 Bortezomib
% Viable Cells (+/- SD)
nM Bortez
H838 Cisplatin
uM Cisplatin
H838 Docetaxel
nM Docetaxel
H838 Gemcitabine
nM Gemcitabine
H838 Vinorelbine
nM Vinorelbine
A549 17AAG
nM 17AAG
A549 Bortezomib
nM Bortez
A549 Cisplatin
uM Cisplatin
Mock
Entinostat
Aza
Combo

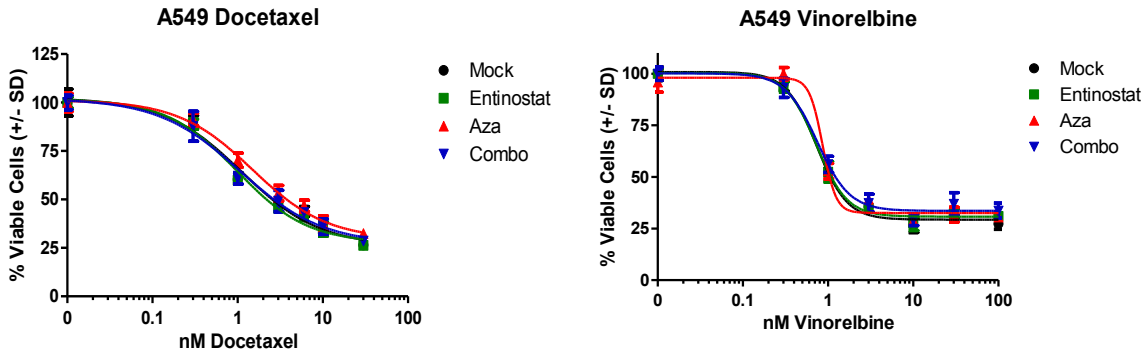

2.2 Epigenetic therapy does not augment inhibition of colony growth by subsequent chemotherapy in NSCLC cell lines

To further test whether epigenetic therapy sensitizes NSCLC to the effects of chemotherapy *in vitro*, we selected sub- or near-IC50 doses of select chemotherapeutic agents and assessed the effects of these agents on colony growth with or without pretreatment with epigenetic therapy, using the treatment paradigm previously described. H358 and A549 cell lines were initially selected for their ability to form distinct colonies on a reconstituted basement membrane matrix. Pretreated cells were seeded on Matrigel^{TM} one day prior to 72h treatment with chemotherapy. Colonies were grown an additional 2-4 days after treatment, imaged (Figure 14A), and quantified. After normalization to untreated controls within each epigenetic pretreatment group, we found that prior epigenetic treatment did not alter inhibition of H358 colonies by gemcitabine, or 17-AAG (Figure 14B). For A549 cells, pretreatment with azacitidine slightly reduced efficacy of 600nM cisplatin ($p<0.05$), while combination pretreatment resulted a minor attenuation of colony inhibition by 1nM docetaxel ($p<0.01$) (Figure 14C and D). No significant differences were noted among pretreatment groups in response to 6nM bortezomib, 10nM 17-AAG (data not shown), and 30nM 17-AAG.

Figure 14. Epigenetic therapy does not enhance the effects of chemotherapy on colony growth on Matrigel™. H358 and A549 cells were seeded on a solidified Matrigel™ layer six days after 72h treatment with epigenetic therapy. Beginning the following day, cells were treated with chemotherapy for 72h. Drug was then removed and colonies were permitted to grow 2-4 additional days until stained with MTT reagent and counted. Colony number was then normalized to untreated controls (PBS or DMSO) for each epigenetic pretreatment condition. **A.** Representative H358 colonies following treatment with 10nM gemcitabine, 10nM 17-AAG, or 20nM 17-AAG. **B.** H358 percent colony formation relative to untreated control calculated from one experiment with 5 replicates. **C.** Representative A549 colonies following treatment with 6nM bortezomib, 10nM 17-AAG, 30nM 17-AAG, 600nM cisplatin, or 1nM docetaxel. **D.** A549 percent colony formation relative to untreated control, averaged from two independent experiments (total 9 replicates). Statistical significance by ANOVA with Tukey's multiple comparison test denoted as follows: * $p<0.05$, ** $p<0.01$.

A.

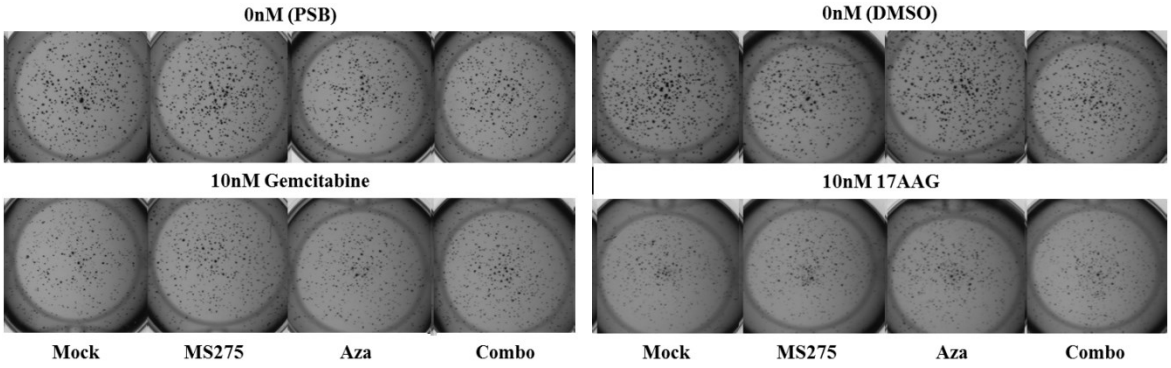

B.

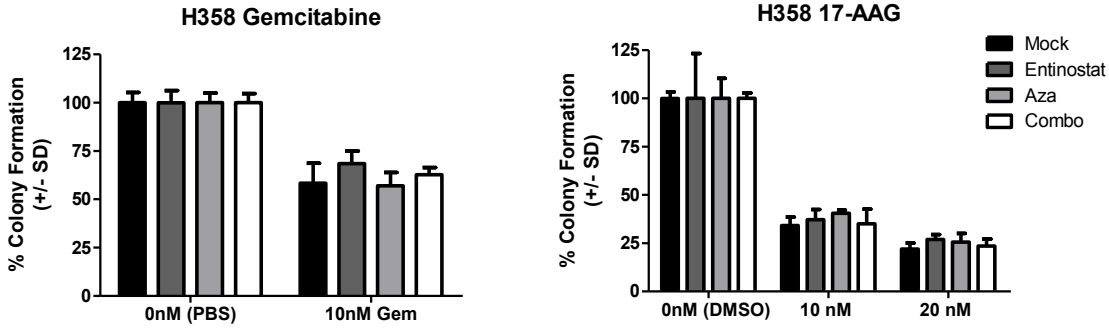
H358 Gemcitabine
% Colony Formation (+/- SD)
125
100
75
50
25
0
0nM (PBS)
10nM Gem
H358 17-AAG
% Colony Formation (+/- SD)
125
100
75
50
25
0
0nM (DMSO)
10 nM
20 nM
Mock
Entinostat
Aza
Combo

C.

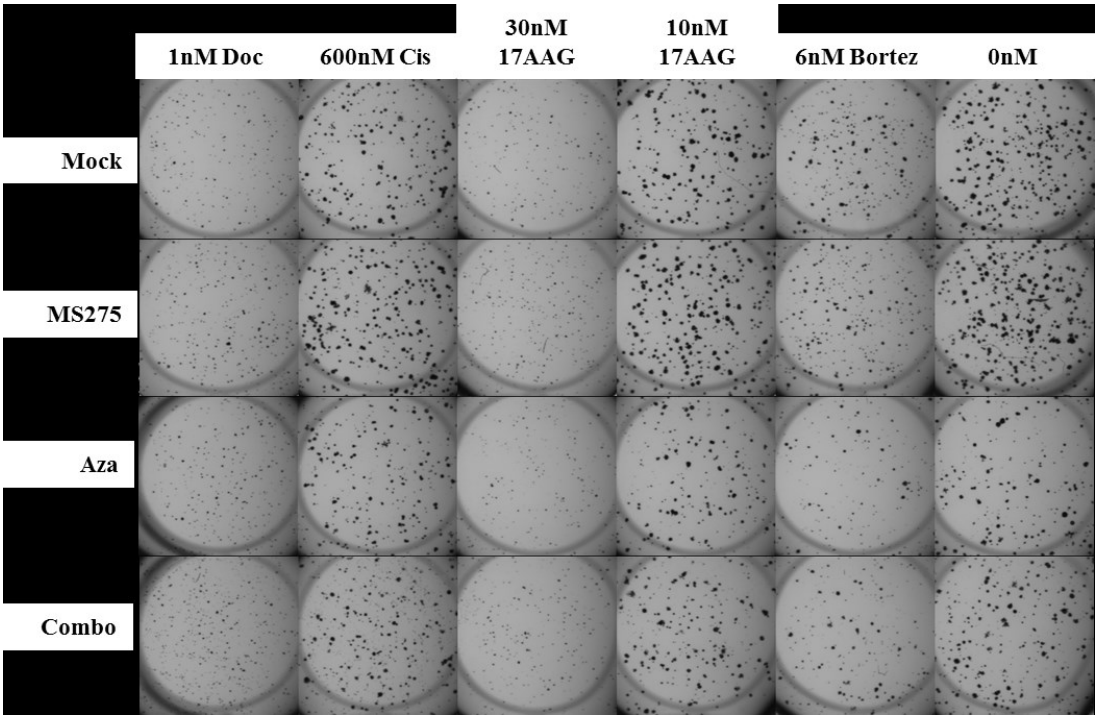
1nM Doc
600nM Cis
30nM 17AAG
10nM 17AAG
6nM Bortez
0nM
Mock
MS275
Aza
Combo

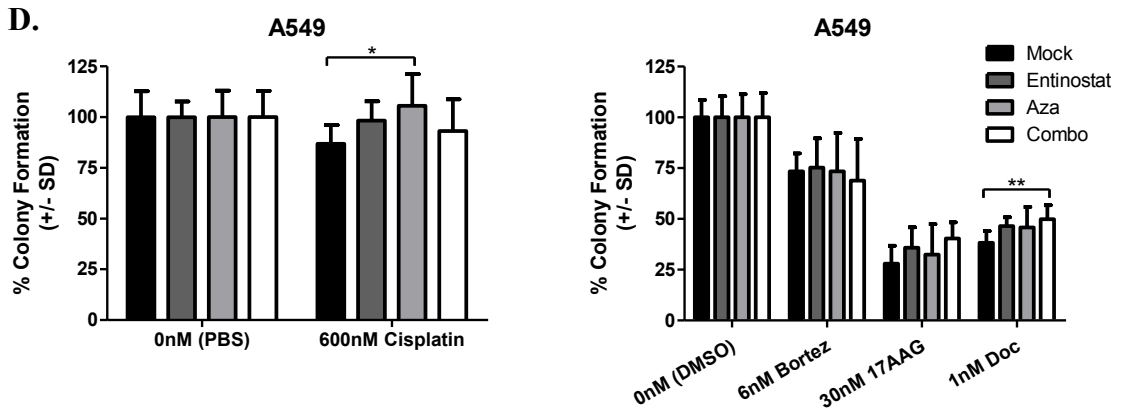

We also questioned whether prior epigenetic therapy would affect anchorage independent colony growth, a measure of clonogenic potential, of NSCLC following treatment with chemotherapy. Prior work has shown that relatively low, non-toxic doses of demethylating agents (DAC and Aza) alone can blunt clonogenic and tumorigenic potential of leukemia and breast cancer, suggesting depletion of progenitor or tumor initiating cell populations [86]. We hypothesized that pretreatment with epigenetic agents would also attenuate clonogenic capacity of NSCLC. In addition, if epigenetic pretreatment sensitizes NSCLC to chemotherapeutics, we would predict a greater attenuation of clonogenic capacity following chemotherapy than achieved with epigenetic therapy alone. To test this, we utilized a methylcellulose colony formation assay. H1299 cells were treated with combination epigenetic therapy or mock as described above. Pretreated cells were then treated with 300nM or 600nM cisplatin, or 3nM bortezomib for 72h, beginning on day 10. At the end of chemotherapy treatment, cells were seeded in methylcellulose (10^3 viable cells per dish in triplicate) and allowed to grow colonies for two weeks prior to counting colony number. Pretreatment with the combination of Aza and entinostat attenuated colony growth across all chemotherapy doses tested, relative to

mock pretreatment (Figure 15A), with the exception of 600nM cisplatin, which abrogated colony formation entirely. However, when normalized to untreated control (0nM PBS or 0nM DMSO) within a given pretreatment group, there were no significant differences in colony inhibition resulting from treatment with 300nM cisplatin or 3nM bortezomib ($p>0.05$) (Figure 15B).

Figure 15. Methylcellulose colony formation following chemotherapy is not altered by epigenetic priming. H1299 cells were treated 72h with combination epigenetic therapy, rested seven days in drug free media, then treated for 72h with 300nM cisplatin, 3nM bortezomib. Following chemotherapy treatment, 10^3 viable cells were seeded in methylcellulose (in triplicate), allowed to grow as colonies for two weeks prior, and counted. **A.** Percent colony formation of combination pretreatment relative to mock pretreatment (+/- standard deviation). **B.** Percent colony formation relative to untreated control within each pretreatment condition (+/- standard deviation). p-value determined by unpaired t test.

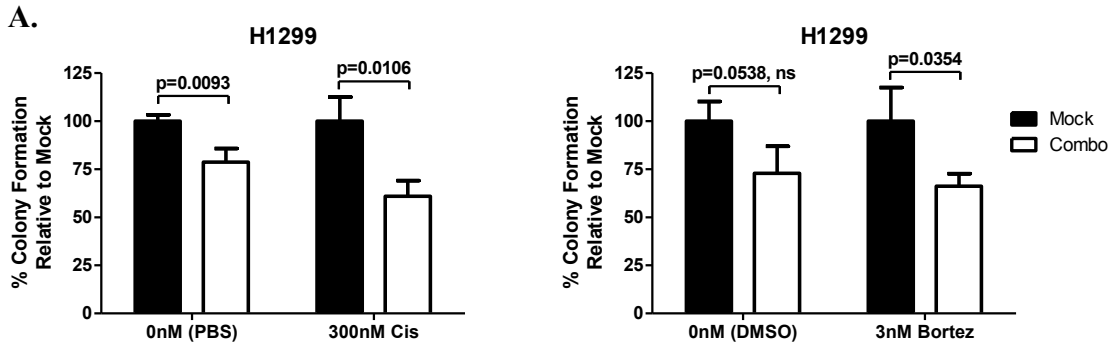

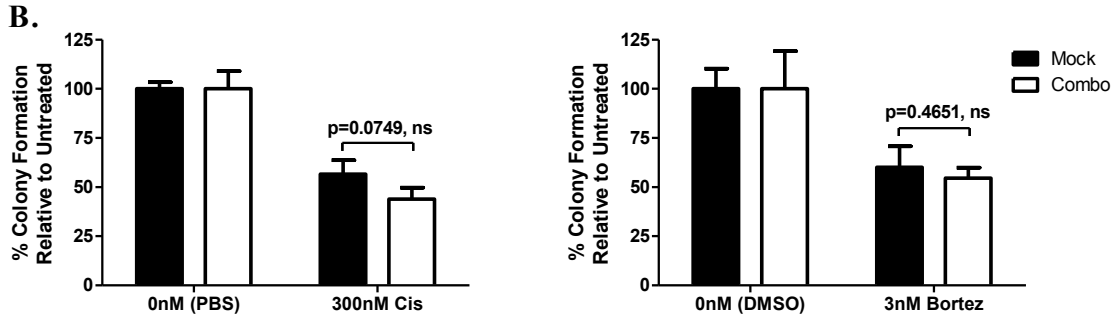

2.3. *in vitro* combinatorial epigenetic therapy exerts differential effects on *in vivo* chemosensitivity of NSCLC cell line xenografts

Given the limitations of *in vitro* model systems, we aimed to determine whether *in vitro* pretreatment with the combination of azacitidine and entinostat, following our treatment paradigm previously described, alters sensitivity of NSCLC cell line xenografts to subsequent chemotherapy *in vivo*. This model allows for controlled exposure to epigenetic therapy prior to establishment of xenografts. Two cell lines, A549 and H460, were selected for these studies since their tumor growth rate *in vivo* is unaffected (A549) or only moderately impaired (H460) by epigenetic treatment *in vivo*. After pretreatment and a seven day, drug-free recovery period, cells were injected on day 10 into the flank of NOD/SCID mice to establish tumors.

Tumors established from mock and combination epigenetic pretreated A549 cells were allowed to reach approximately 250mm^3 (+/- 20%) prior to randomization on day 1 to one of three chemotherapy treatment arms: vehicle (saline) twice weekly, 2mg/kg cisplatin weekly, or 10mg/kg irinotecan twice weekly. Chemotherapy treatment was initiated on day 2 and lasted for three weeks. All drugs were administered intraperitoneally. We observed no difference in growth between mock and combination

pretreated tumors that received vehicle or cisplatin (Figure 16A). However, epigenetic pretreatment appeared to selectively augment response to irinotecan compared to mock pretreatment (Figure 16B). Using a linear mixed effects model, we determined that irinotecan treatment decreased the rate of growth of mock pretreated and epigenetic pretreated tumors by 5.8mm^3/day and 16.8mm^3/day, respectively, compared to vehicle treatment, and that this difference was statistically significant (p=0.00013 by restricted maximum likelihood estimation). Therefore, *in vitro* pretreatment with combination epigenetic therapy sensitizes A549 xenografts to irinotecan treatment *in vivo*.

Figure 16. Response of A549 xenografts to irinotecan, but not cisplatin, is augmented by epigenetic therapy. Subcutaneous hind flank tumors were established in NOD/SCID mice from A549 cells treated *in vitro* with mock or the combination of Aza and entinostat. Once tumors reached approximately 250mm^3, they were randomized to receive 2mg/kg cisplatin (days 2,9,16), 10mg/kg irinotecan (days 2,5,9,12,16,19), or saline vehicle (days 2,5,9,12,16,19), all by intraperitoneal administration. **A.** Mean tumor volume (+/- SEM) of mock and combination epigenetic pretreated tumors that received vehicle or cisplatin. Pretreatment with epigenetic therapy did not alter response to cisplatin. **B.** Mean tumor volume (+/- SEM) of mock and combination epigenetic pretreated tumors that received vehicle or irinotecan. Using a mixed-effects model we determined that combination epigenetic pretreatment augmented response to irinotecan (p=0.00013).

A.

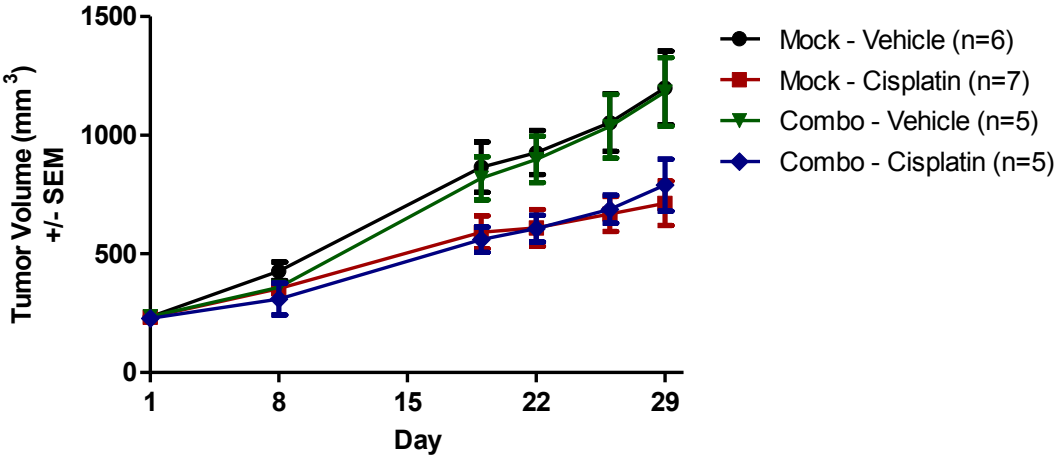

B.

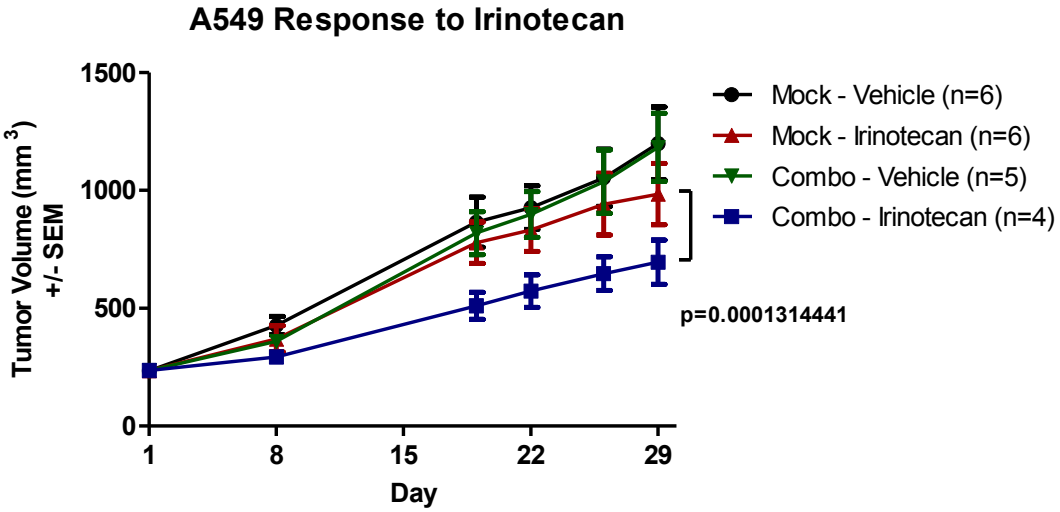

Similar to A549, H460 tumors established from mock and combination epigenetic pretreated cells were allowed to reach approximately 250mm^3 (+/- 20%) and then randomized to one of three chemotherapy treatment arms: vehicle (saline), 2.5mg/kg docetaxel escalated to 5mg/kg docetaxel, or 10mg/kg irinotecan. Each treatment consisted of four intraperitoneal injections beginning on day 1 immediately after

randomization. Docetaxel was escalated to 5mg/kg for the final two injections. Epigenetic pretreated tumors exhibited a modestly increased rate of growth compared to vehicle control in response to docetaxel, while mock pretreated tumors were unaffected by docetaxel treatment (Figure 17A). Once tumors volumes for each pretreatment were normalized to the corresponding vehicle controls (Figure 17B), we found that the differences in response to docetaxel were not significant ($p>0.05$ by 2-way ANOVA). Mock pretreated tumors were modestly inhibited by irinotecan (approximately 40% by end of study, compared to vehicle control), while combination epigenetic pretreated tumors did not respond to irinotecan treatment (Figure 17C). Comparison of normalized tumor volumes revealed a significant difference ($p<0.05$ by 2-way ANOVA) in response to irinotecan between pretreatment groups (Figure 17D).

Figure 17. Epigenetic therapy desensitizes H460 xenografts to subsequent chemotherapy. Hind flank tumors were established in NOD/SCID mice from H460 cells treated *in vitro* with mock or the combination epigenetic therapy. Tumors of approximately $250mm^3$ were randomized to receive 2.5mg/kg docetaxel (ip, q4d x 2) escalated to 5mg/kg docetaxel (q4d x 2), 10mg/kg irinotecan (ip, q4d x 4), or saline vehicle (ip, q4d x 4). **A.** Mean tumor volume (+/- SEM) of mock and combination epigenetic pretreated tumors that received vehicle or docetaxel. Epigenetic pretreatment let to a modest increase in growth in response to docetaxel. **B.** Response to docetaxel for each pretreatment group normalized to its own vehicle control across measurements days. Error bars represent 95% CI. Differences in response to docetaxel between pretreatment groups were not significant by two-way ANOVA ($p>0.05$). **C.** Mean tumor volume (+/- SEM) of mock and combination epigenetic pretreated tumors that received vehicle or irinotecan. Combination epigenetic pretreatment attenuated response to irinotecan treatment. **D.** Normalized

response to irinotecan (relative to vehicle control) for each pretreatment. Error bars represent 95% CI. Significance determined by two-way ANOVA.

A.

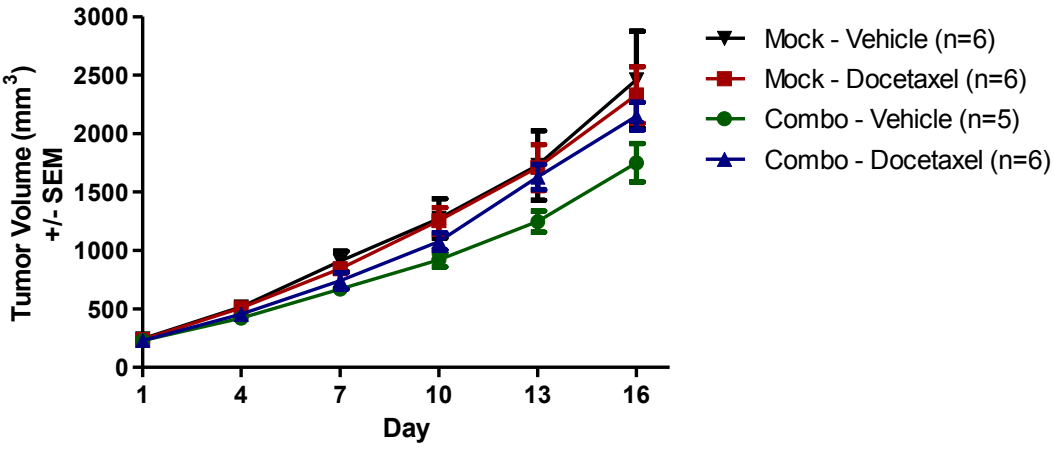

B.

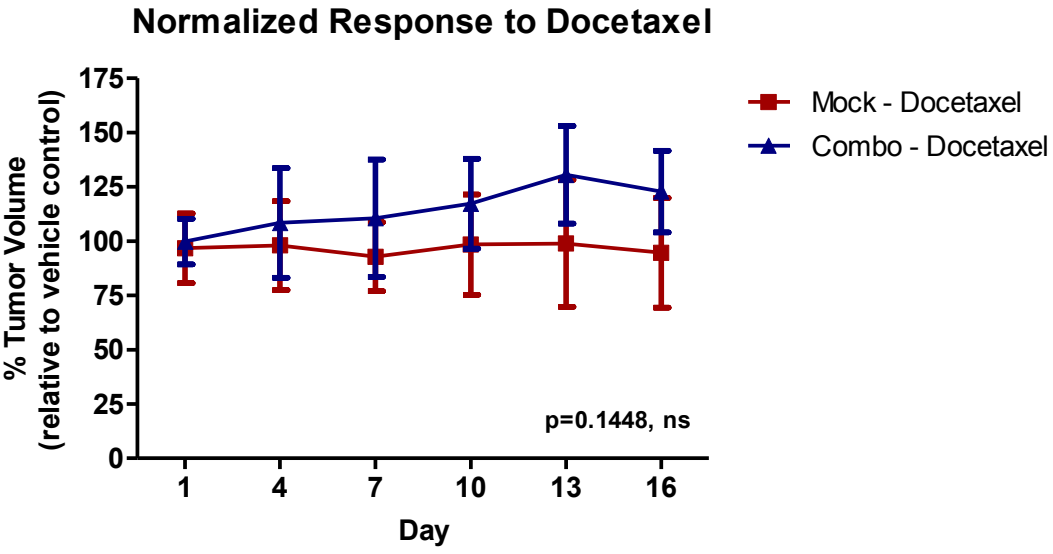

C.

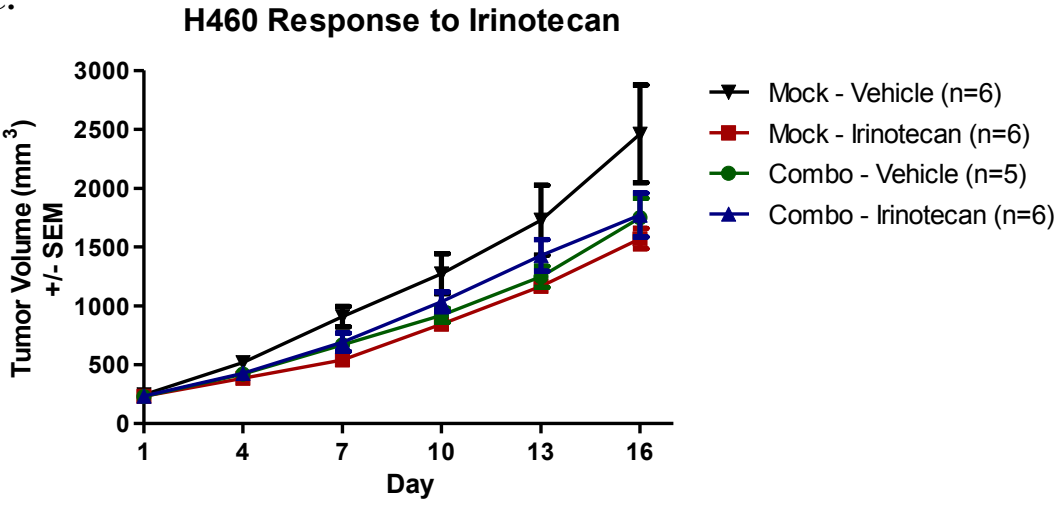

D.

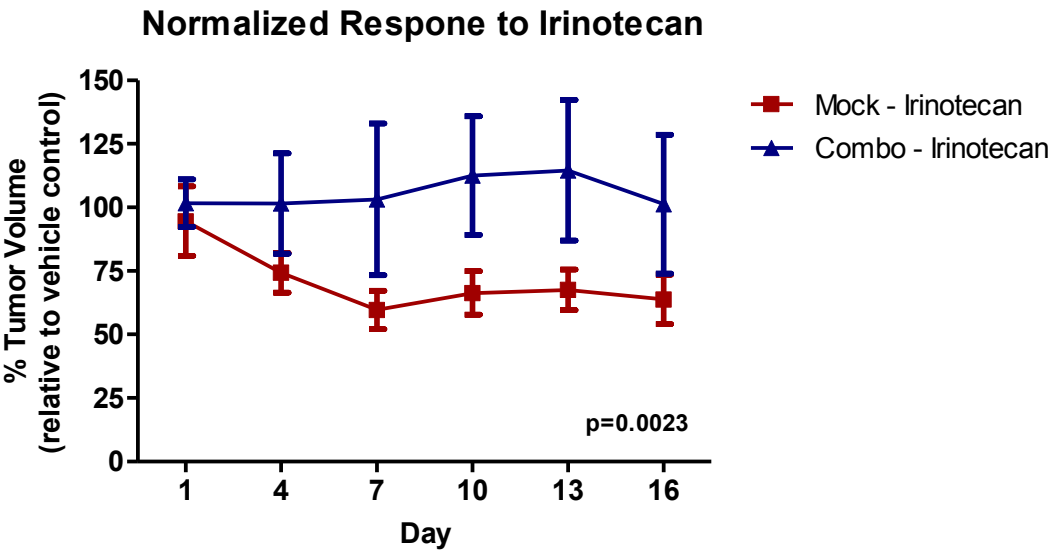

2.4 *in vivo* combinatorial epigenetic therapy does not sensitize H358 xenografts to cisplatin or irinotecan

We next assessed whether *in vivo* epigenetic therapy sensitizes NSCLC tumors to immediate subsequent chemotherapy. H358 xenografts were selected due to the slower

rate of tumor growth *in vivo*, permitting for repeated cycles of epigenetic therapy prior to chemotherapy. Tumor bearing, nu/nu mice were treated each week with 0.5mg/kg Aza subcutaneously on days 1-5 and 1mg/kg entinostat intraperitoneally on day 5, or vehicle, for four one-week cycles, and then randomized to chemotherapy arms at the beginning of week five (day 29). A similar schedule and dose of entinostat has been used successfully in orthotopic models of NSCLC in rats [109]. The dose of Aza was chosen since it is well tolerated based on prior laboratory work, and has been shown to be more efficacious in certain breast cancer xenografts than higher doses [86]. Following epigenetic therapy, mice were treated by with either saline vehicle twice weekly, 2mg/kg cisplatin weekly, or 10mg/kg irinotecan twice weekly, for four weeks beginning the day after randomization. Drugs were administered by intraperitoneal injection. Figure 18A shows that epigenetic therapy has a modest effect on tumor growth, and growth inhibition reached significance by day 29 ($p<0.05$ by two-way ANOVA with Bonferroni posttests). H358 xenografts did not respond to subsequent cisplatin or irinotecan treatment, regardless of pretreatment (Figure 18B).

Figure 18. Epigenetic therapy *in vivo* does not sensitize H358 xenografts to immediate subsequent chemotherapy. A. Nude mice bearing H358 xenografts were treated with 0.5mgkg Aza (sc, days 1-5) and 1mg/kg entinostat (ip, day 5), or vehicle, for four one-week cycles. Epigenetic therapy causes a modest tumor growth inhibition that reached significance by day 29 ($p<0.05$ by two-way ANOVA with Bonferroni posttests). **B.** Pretreated mice were randomized to one of three chemotherapy arms on day 29: vehicle (ip saline, days 2 & 5), 2mg/kg cisplatin (ip, day 2), or 10mg/kg irinotecan (ip, days 2 & 5,). Mice were treated for four one-week cycles. No responses to chemotherapy were observed for either pretreatment. **Upper** Vehicle pretreated

mice: Vehicle n=8, Cisplatin n=7, Irinotecan n=6. **Lower** Epigenetic pretreated mice: Vehicle n=6, Cisplatin n=7, Irinotecan n=7.

A.

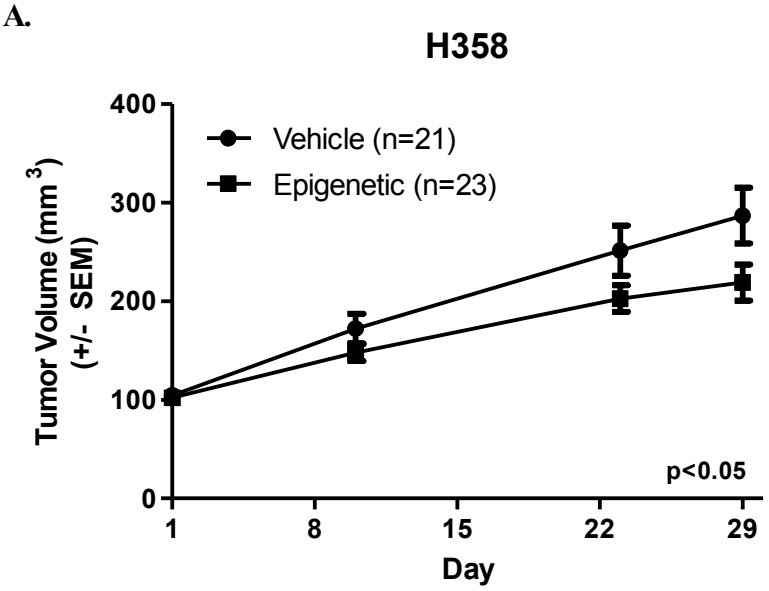

B.

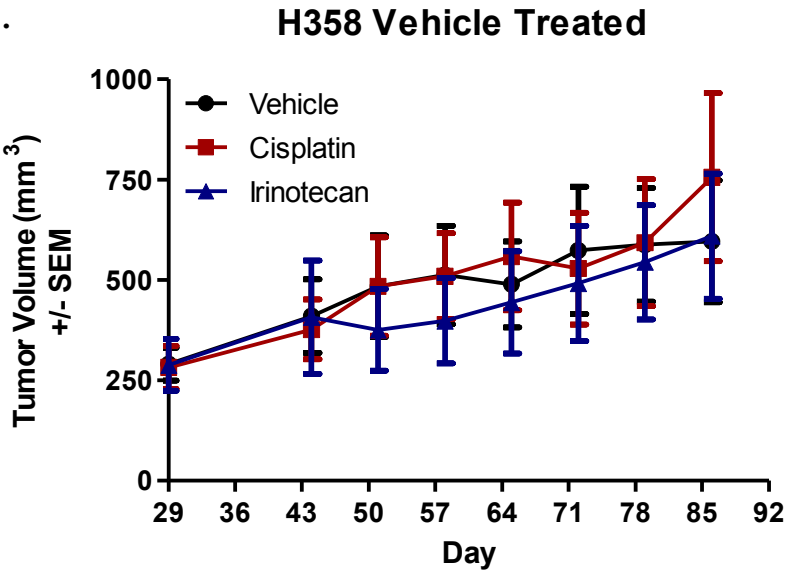

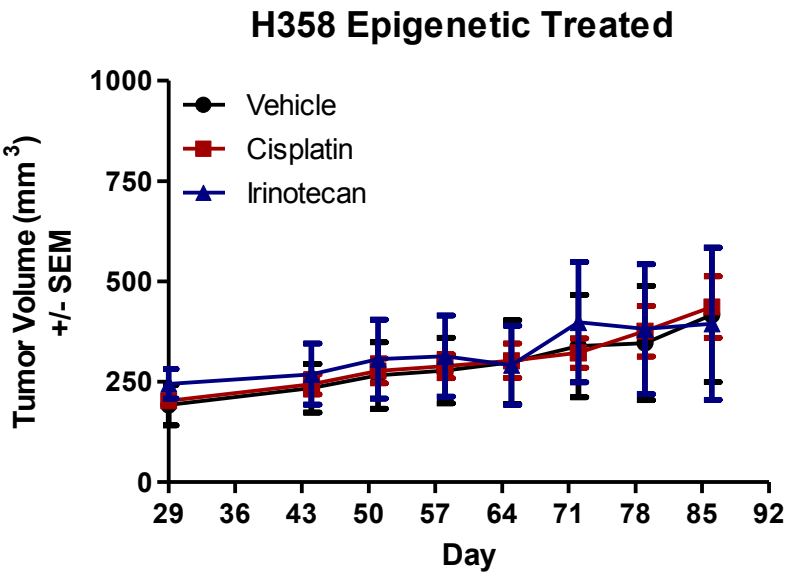

2.5 Combination epigenetic therapy has utility as a priming therapy in a patient-derived NSCLC xenograft model

We extended our study of epigenetic priming to two of our patient-derived NSCLC xenograft (PDX) models, LX7 (adenocarcinoma) and LX14 (squamous cell carcinoma). These xenografts were previously established in immunocompromised mice immediately following collection of cells from NSCLC patients, and serially passaged such that they have never been cultured in medium. Similarly derived small cell lung cancer PDXs have previously been shown to exhibit gene expression patterns more closely related to primary patient tumors than to cell lines derived from the PDXs [133]. Therefore, we believe our NSCLC PDXs may better represent patient tumors than standard cell line xenograft models.

To assess the effects of epigenetic priming on response of LX14 to subsequent gemcitabine therapy, tumors were established in NOD/SCID mice from LX14 cell

suspensions harvested from freshly grown tumors. Treatment began when tumors reached approximately 115mm^3 (+/- 30%). Mice received epigenetic therapy (n=7) or vehicle (n=7) for three weeks as follows: 0.5mg/kg Aza (or vehicle) subcutaneously on days 1-5 and 1mg/kg entinostat (or vehicle) intraperitoneally on day 5. Epigenetic therapy resulted in minor, but not statistically significant (p=0.14 by two-way ANOVA), tumor growth inhibition (Figure 19A). All mice within the vehicle treatment arm were euthanized and tumors harvested on day 20, while mice in the epigenetic arm remained on study until day 22. Representative tumors from the vehicle arm were pooled and mechanically disrupted to form a single cell suspension. All tumors from the epigenetic treatment arm were pooled due to the larger variation in tumor size at the time of harvest. Viable cells were then immediately injected into the hind flank of new NOD/SCID mice (vehicle: 7.5x10^5 cells/mouse, epigenetic: 5x10^5 cells/mouse). Mice bearing tumors that reached approximately 250mm^3 (+/- 20%) were randomized to receive 30mg/kg gemcitabine or vehicle every third day for five intraperitoneal injections. LX14 tumors were highly sensitive to gemcitabine, remaining relatively cytostatic for the duration of treatment. Epigenetic therapy did not improve duration of response, as tumors rapidly increased in size upon cessation of gemcitabine treatment, comparable to vehicle pretreated tumors (Figure 19B).

Figure 19. Epigenetic therapy does not extend duration response to gemcitabine in a patient derived xenograft model of squamous cell carcinoma. A. LX14 bearing NOD/SCID mice received sc Aza on days 1-5 and ip entinostat on day 5, or vehicle, weekly for three weeks (n=7 per arm). Differences in tumor growth between vehicle and epigenetic arms were not significant by two-way ANOVA with Bonferroni posttests. **B.** NOD/SCID mice bearing LX14

tumors established from pooled vehicle or epigenetic pretreated tumors were treated with 30mg/kg gemcitabine (ip, q3d x5) or vehicle. Both pretreatment arms responded strongly to gemcitabine, and prior epigenetic therapy did not delay rapid growth of tumors following cessation of gemcitabine treatment.

A.

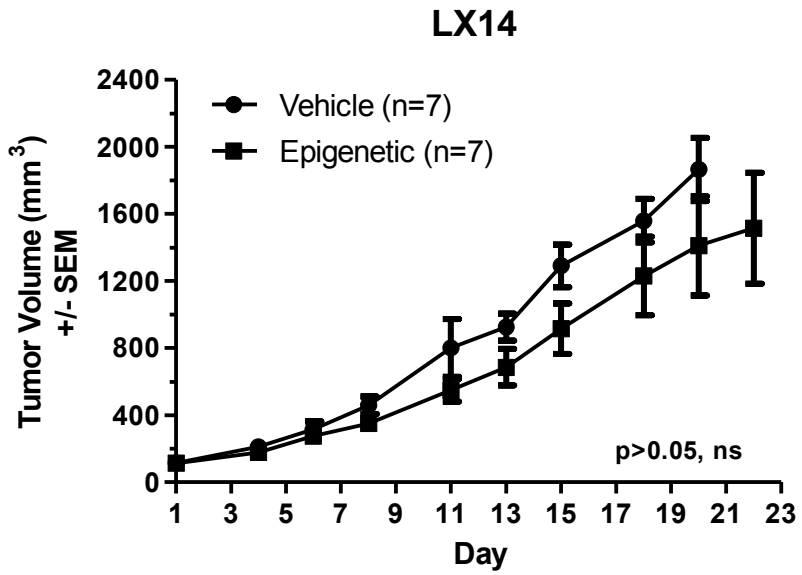

B.

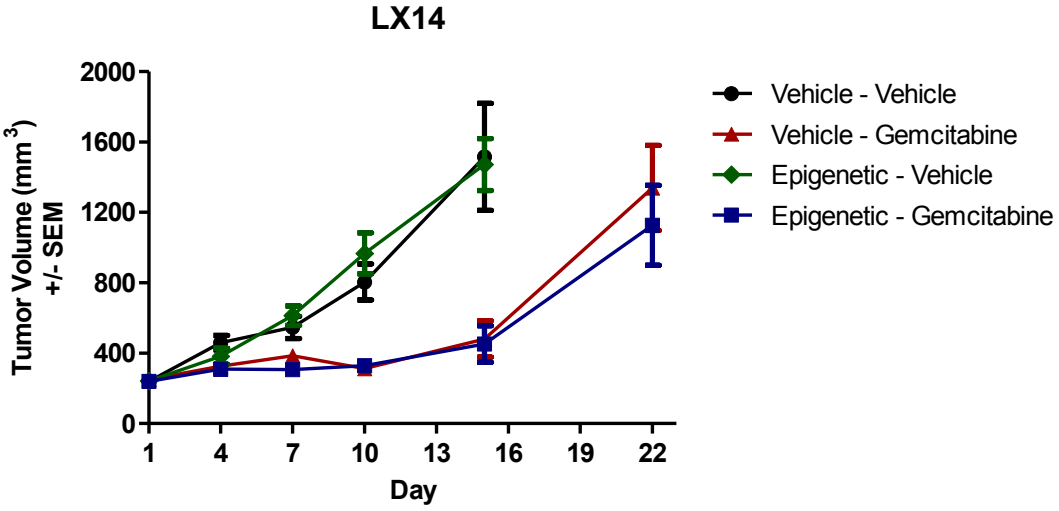

We employed a similar study design with our second PDX model, LX7. Once tumors reached approximately 160mm^3 (+/- 25%), LX7 bearing NOD/SCID mice were randomized to receive vehicle (n=9) or epigenetic therapy (n=9), with the same doses and route of administration as used for LX14. Mice were treated with Aza on days 1-3, 6-10, 13-17, and entinostat on days 3, 10, 17. Combination epigenetic therapy resulted in a modest, but statistically significant ($p=0.0055$ by linear mixed effects model and restricted maximum likelihood estimation) inhibition of LX7 growth (Figure 20A). Representative tumors from the vehicle and epigenetic arms were harvested days 16 and 17, respectively. Tumors within a given treatment arm were pooled, mechanically processed into a single cell suspension, and frozen for later use. Pretreated cells were later thawed, counted, and injected into the hind flank NOD/SCID mice ($1.3x10^6$ viable cells/mouse) to establish subcutaneous tumors for treatment with chemotherapy. Mice bearing tumors of approximately 140mm^3 (+/- 15%) were randomized to receive 2mg/kg cisplatin weekly, 10mg/kg irinotecan every fourth day, or vehicle every fourth day. Treatment consisted of two cisplatin, three vehicle, or three irinotecan intraperitoneal injections. No significant difference in response to cisplatin or irinotecan was observed between vehicle and epigenetic pretreated tumors, with minimal response to cisplatin and slight tumor regression in response to irinotecan for both pretreatment conditions (Figure 20B). However, the growth rate of irinotecan treated tumors in both pretreatment arms increased within three days of cessation of irinotecan treatment. Vehicle and cisplatin treated mice were euthanized on day 22 due to large tumor burden, while irinotecan treated tumors were allowed to grow. By day 32, we noted a small difference in mean tumor volume (+/- SEM) between pretreatment arms (1345 ± 136 mm^3 for vehicle

pretreated vs. 1072 ± 131 for epigenetic pretreated), however this difference was not significant (p=0.19 by t test). Beginning on day 32, mice were subjected to a repeat cycle of irinotecan therapy (10mg/kg days 32, 36, 40) to determine whether response to irinotecan following tumor regrowth was altered by prior epigenetic therapy. Two of eight mice within the vehicle pretreatment arm were euthanized early due to excessive body weight loss (day 42, final tumor volume = 1576mm^3) and a large ulcerated tumor (day 45, final tumor volume = 2789mm^3). Interestingly, epigenetic pretreated LX7 tumors exhibited increased sensitivity to irinotecan upon repeat exposure, with regression of mean tumor volume to slightly below baseline (day 32), compared to vehicle pretreated tumors, exhibited only a brief, mean cytostatic response (Figure 20C and D). Using a linear mixed effects model, and adjusting for the difference in tumors sizes between arms at the initiation of repeat treatment on day 32, we determined that mean tumor volume increases 33.5mm^3/day in vehicle-pretreated mice, whereas in epigenetic pretreated mice, volume increases by 23.9mm^3/day (p=0.013 by restricted maximum likelihood estimation). In both arms, tumor growth rapidly increased roughly one week after the final dose of irinotecan, indicating that the degree of response, but not duration, was altered by epigenetic priming.

Figure 20. Epigenetic therapy sensitizes a patient derived model of adenocarcinoma to repeat treatment with irinotecan, but does not sensitize to cisplatin. A. LX7 bearing NOD/SCID mice were treated with 0.5mg/kg Aza (sc) on days 1-3, 6-10, 13-17, and 1mg/kg (ip) entinostat on days 3, 10, 17, or vehicle (n=9 per arm). Epigenetic therapy inhibited LX7 tumor growth by approximately 23% by day 15. Significance determined using a linear mixed effects model and restricted maximum likelihood estimation. **B.** NOD/SCID mice bearing LX7 tumors

established from pooled vehicle or epigenetic pretreated tumors were treated with 10mg/kg irinotecan (ip, q4d x 3), 2mg/kg cisplatin (ip, q7d x 2), or vehicle. Both pretreatment arms responded strongly to irinotecan, but exhibited minimal response to cisplatin. **C-D.** Irinotecan tumors were allowed to grow following cessation of treatment. On day 32, mice were re-challenged with 10mg/kg irinotecan on days 32, 36, and 40 (same dose and schedule as first cycle). Epigenetic pretreated LX7 tumors exhibited greater response to repeat irinotecan therapy (p=0.013 by linear mixed effects model and restricted maximum likelihood estimation). *Two mice in the Vehicle – Irinotecan arm were euthanized early (day 42 and 45 after final measurements) for n=6 after day 45.

A.

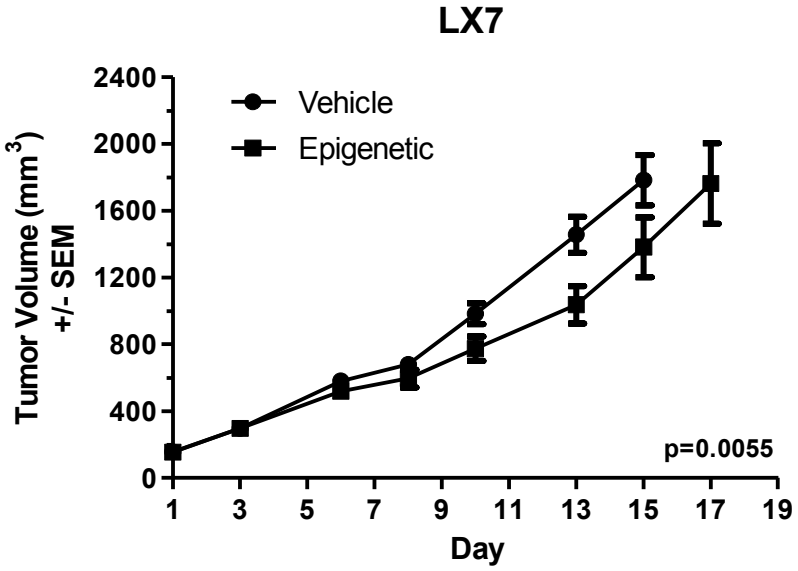

B.

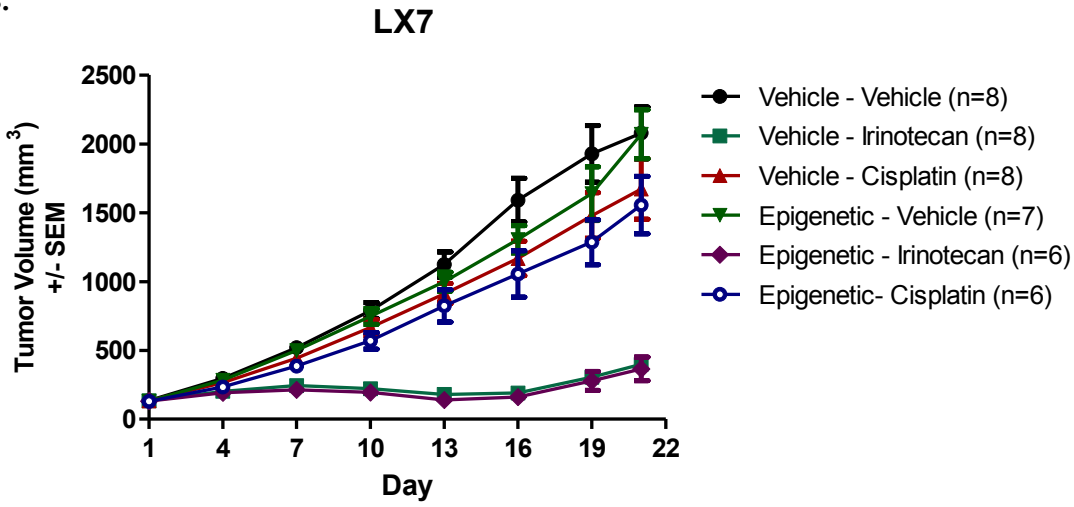
LX7
Tumor Volume (mm3) +/- SEM
2500
2000
1500
1000
500
0
1
4
7
10
13
16
19
22
Day
Vehicle - Vehicle (n=8)
Vehicle - Irinotecan (n=8)
Vehicle - Cisplatin (n=8)
Epigenetic - Vehicle (n=7)
Epigenetic - Irinotecan (n=6)
Epigenetic- Cisplatin (n=6)

C.

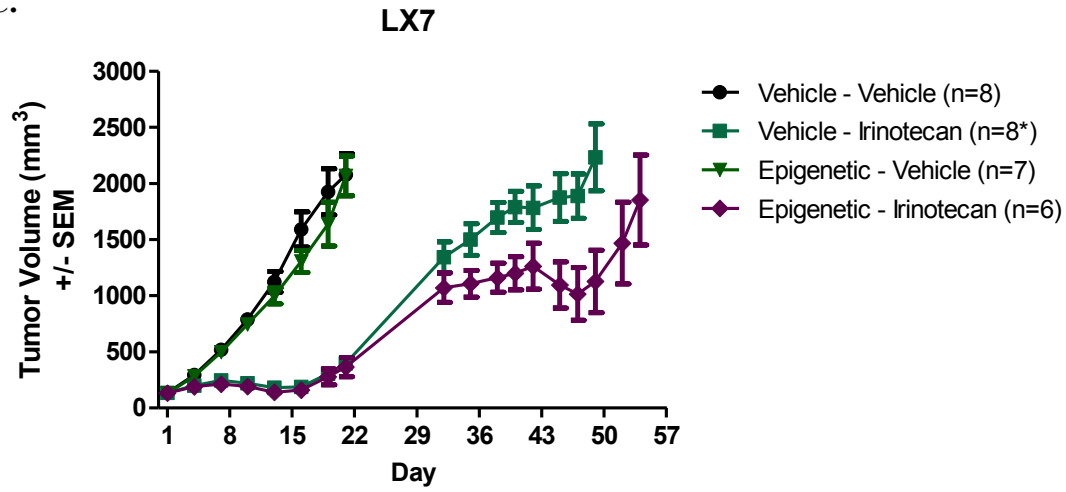
LX7
Tumor Volume (mm3) +/- SEM
3000
2500
2000
1500
1000
500
0
1
8
15
22
29
36
43
50
57
Day
Vehicle - Vehicle (n=8)
Vehicle - Irinotecan (n=8*)
Epigenetic - Vehicle (n=7)
Epigenetic - Irinotecan (n=6)

D.

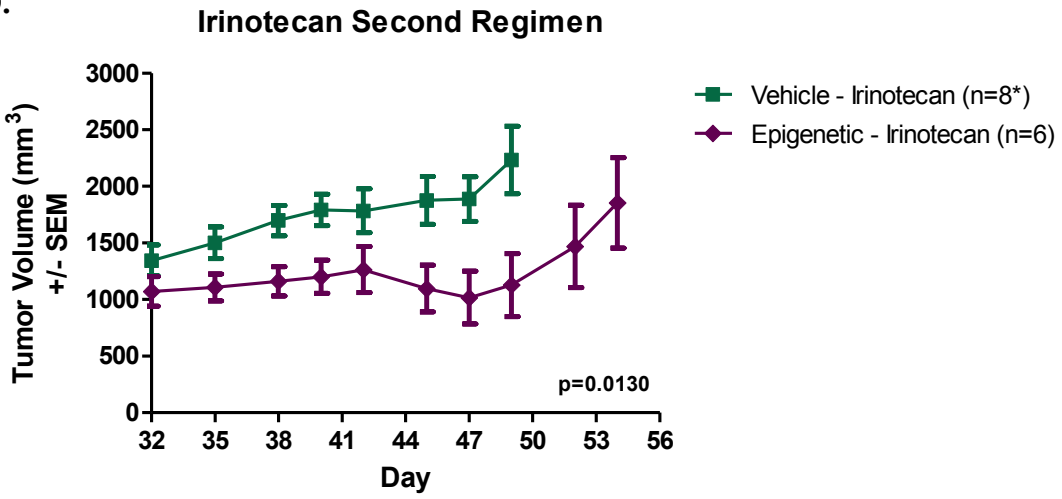

3. Discussion

Our *in vitro* assays generally showed no evidence in support of the epigenetic priming hypothesis. It is plausible that an important component necessary for effective epigenetic priming in NSCLC is interaction of epigenetic pretreated cells with the host tumor microenvironment, something that is absent in these models. In our results from the Matrigel™ colony formation assays, pretreatment of A549 with Aza and combination appears to slightly attenuate the effects of cisplatin and docetaxel, respectively. These results suggest that the effects of epigenetic pretreatment of NSCLC on response to subsequent chemotherapy may vary with a given epigenetic or chemotherapeutic agent. However, it is important to note that, while statistically significant, the differences are minor. In addition, these negative effects were not observed in our cell viability experiments, or in the more relevant xenograft model. Response of A549 xenografts to cisplatin therapy following *in vitro* pretreatment with combination epigenetic therapy was unaltered. Response of H358 and LX7 xenografts to cisplatin therapy was also

unchanged. We did, however, note that epigenetic priming had a negative impact on response of H460 xenografts to irinotecan, and resulted in a slightly increased rate of growth of docetaxel treated tumors compared to vehicle treated.

These results are contrary to the sensitization observed in A549 and LX7 xenografts. Xenografts established from mock pretreated A549 cells were minimally responsive to irinotecan, whereas tumors grown from epigenetic pretreated cells exhibited increased sensitivity to the same irinotecan therapy. The data are striking given that transient (72h) *in vitro* treatment with epigenetic therapy did not affect the growth of A549 xenografts, yet altered the response of established xenografts to a chemotherapeutic agent weeks later. This is of interest in light of the clinical observations of several patients whose disease progressed on epigenetic therapy but who experienced better than expected responses to subsequent chemotherapy. Both our data and the clinical trial observations suggest that the effects of epigenetic therapy, even if not sufficient to provide an anti-tumor response, can be durable, and that immediate response may not be necessary for patients to derive benefit from this approach. LX7 PDXs established from vehicle and epigenetic pretreated LX7 tumors both responded strongly to initial, short duration (three injections) irinotecan therapy, but recovered relatively quickly following cessation of treatment. Upon treatment with a second regimen of irinotecan, epigenetic pretreated LX7 tumors exhibited increased response to therapy, characterized by a slowed growth rate followed by regression of mean tumor volume to slightly below baseline (day 32). In comparison, vehicle pretreated tumors exhibited an increased rate of growth, followed by a very brief period of cytostatic behavior, but not tumor regression. The LX7 data are particularly intriguing for two reasons. First, LX7 is a patient-derived

adenocarcinoma model maintained in mice and may better reflect the biology of disease than ex vivo cell line models, as suggested by earlier data from our group [133]. Second, LX7 tumors responded well to initial therapy, but grew quickly after treatment ended, which is reminiscent of the short-lived response to chemotherapy seen in many NSCLC patients. In addition, tumors that had no prior exposure to epigenetic therapy did not respond as well to the second cycle of irinotecan therapy, which is often the case for recurrent NSCLC, while tumors previously exposed to epigenetic therapy again exhibited a small degree of tumor regression prior to regrowth roughly one week after the end of irinotecan therapy. Since H460 comprises a different histology than A549 and LX7 (large cell carcinoma vs. adenocarcinoma, respectively), it is possible that the utility of epigenetic priming may vary with disease.

Using two models of human lung adenocarcinoma, the cell line, A549, and the patient-derived primary xenograft, LX7, we demonstrated sensitization of established xenografts to irinotecan chemotherapy following prior exposure to combinatorial epigenetic therapy *in vitro* and *in vivo*, respectively. These data suggest the potential for epigenetic therapy to sensitize NSCLC to a given subsequent chemotherapy, and support our clinical observations in which advanced stage, NSCLC patients with a median of three prior therapies achieved better than expected responses to subsequent chemotherapy following treatment with the combination of azacitidine and entinostat.

Nonetheless, it must be acknowledged that in the majority of models and with the majority of cytotoxic chemotherapy agents tested, we were not able to demonstrate that combinatorial epigenetic therapy with azacitidine and entinostat enhanced tumor sensitivity to subsequent chemotherapy. Taken together, these data call into question

whether in fact azacitidine and entinostat exposure could augment chemotherapeutic efficacy in a substantial fraction of lung cancer patients. There are many potentially relevant differences between efficacy in preclinical models and clinical outcome in patients, notably differences in drug pharmacokinetics. A randomized phase II clinical trial to specifically address this question in patients with advanced lung cancer has been initiated at Johns Hopkins, with plans to expand this study to a number of other collaborating centers. This study offers the opportunity to address this hypothesis directly. Comparative data from the clinical trial in progress and the preclinical work presented here will be of interest in defining the extent to which these preclinical models can reflect treatment paradigms of relevance to the human disease.

4. Materials and Methods

Cell lines and Reagents

NCI-H1299, NCI-H358, NCI-H838, NCI-H460, and A549 were obtained from the American Type Culture Collection (ATCC) and cultured in RPMI-1640 supplemented with 10% FBS, penicillin/streptomycin, 2 mmol/L l-glutamine, 1 mmol/L sodium pyruvate, 10 mmol/L HEPES buffer, and 1.5 g/L sodium bicarbonate. Cells were cultured in a humidified incubator at 37ºC with 5% CO_2.

Drugs and Reagents

5-azacitidine (Aza) was purchased from Tocris Bioscience. For *in vitro* use, Aza was dissolved in 1x PBS as a 4mM stock and stored at -80ºC in aliquots. Fresh aliquots of Aza were thawed immediately prior to use. For *in vivo* studies, Aza was dissolved in

saline (0.9% sodium chloride) at 1mg/mL and stored at -80ºC in aliquots. Fresh aliquots were thawed and diluted 1:10 in saline immediately prior to injection. Entinostat was provided by Syndax Pharmaceuticals. For *in vitro* experiments, entinostat was dissolved in DMSO as a 200uM solution stored at -20ºC. Drug was thawed immediately prior to use and diluted 1:4000 in culture medium to provide a final concentration of 50nM entinostat and 0.025% DMSO in medium. For *in vivo* use, entinostat was dissolved at 2mg/ml in DMSO and stored at -20ºC. Immediately prior to injection, entinostat was thawed and diluted 1:10 in saline for a final of 10% DMSO per injection. 17-AAG and bortezomib were purchased from LC Labs. Docetaxel and vinorelbine were obtained from Selleck Chemicals. Each was dissolved in DMSO, and appropriate dilutions in DMSO were made for *in vitro* studies to provide a final of 0.025% DMSO in medium. Cisplatin (APP Pharmaceuticals) and Gemcitabine (Sagent Pharmaceuticals) were obtained from the Johns Hopkins Hospital pharmacy. Gemcitabine was dissolved in saline. For *in vitro* use, cisplatin and gemcitabine were diluted with 1x PBS. For *in vivo* experiments, both drugs were diluted in saline. Docetaxel (Hospira) and Camptosar (Pfizer) were obtained from the Johns Hopkins Hospital pharmacy for *in vivo* use, and were diluted in saline prior to injection.

Treatment of cell lines with epigenetic therapy

H1299, H358, H838, A549, and H460 cells were seeded at 2 x 10^5, 1 x 10^6, 3.5x10^5, 3.5 x 10^5, and 2 x 10^5 cells per 75cm^2 culture flask, respectively, and allowed to adhere approximately 20-24h. Cells were then treated with 500nM Aza or mock (1x PBS) in fresh media every 24h for 48h, then treated with 500nM Aza, 50nM entinostat,

combination, or mock (1x PBS) for the final 24h of treatment. All treatments contained a final of 0.025% DMSO for the final 24h treatment. After 72h of treatment, cells were harvested and re-seeded at equal density for all treatment conditions in drug-free media.

Cell viability assays

Following epigenetic treatment, cells were cultured for six days in drug free media. On day 9, cells were seeded in triplicate in opaque walled 96-well plates as follows: H1299 = 1000 cells/well, H358 = 4200 cells/well, H838 = 1700 cells/well, A549 = 1500 cells/well. Approximately 24h later, cells were treated with 17-AAG (3-1000nM, 0.03-10uM for H358), bortezomib (1-300nM), cisplatin (0.03-10uM), docetaxel (0.3-100nM, 0.3-30nM for A549), gemcitabine (1-300nM), or vinorelbine (0.3-100nM) for 72h. Following chemotherapy, ATP content was measured as an indicator of cell viability using the CellTiter-Glo Luminescent Cell Viability Assay (Promega). Cells were incubated with prepared CellTiter-Glo reagent for 10 min at room temperature, and luminescence was read on a SpectraMax M2e plate reader (Molecular Devices). Raw data were corrected for background luminescence, transformed (x=log(x)), and analyzed by nonlinear regression using the equation, log(inhibitor) vs. response with variable slope in GraphPad Prism 5 to obtain IC50 values, 95% confidence intervals, and R^2. IC50 was considered not determined if the value calculated by Prism was ambiguous. Transformed data were then normalized to untreated controls within each pretreatment group for a given chemotherapy to generate log dose response curves. Experiments were repeated at least twice to ensure consistent results, with the exception of vinorelbine for H358 and H1299, since no differences were observed. Results from representative experiments are shown.

Matrigel™ Colony formation assays

Following epigenetic treatment, cells were cultured for six days in drug free media. On day 9, cells were seeded 96-well plates on a 40uL layer of solidified Matrigel™, with 4-5 replicates per pretreatment condition, as follows: H358 = 2000 cells/well, A549 = 1000 cells/well. Approximately 24h later, H358 cell were treated with 10nM gemcitabine, 10nM 17-AAG, or 20nM 17-AAG. A549 cells were treated with 600nM cisplatin, 6nM bortezmib, 10nM 17-AAG, 30nM 17-AACG, or 1nM docetaxel. After 72h, chemotherapy was removed, cells were rinsed once with 1x PBS, and drug free media was added. Colonies were grown an additional 2-4 days, stained with MTT reagent, and imaged and counted on the GelCount™ colony counter (Oxord Optronix). Colony number was normalized to untreated control within a given pretreatment group to determine % colony formation after chemotherapy.

Methylcellulose colony formation assay

Following epigenetic treatment, mock and combination pretreated H1299 cells were cultured for seven days in drug free media. On day 10, cells were treated for 72h with 300nM cisplatin, 600nM cisplatin, or 3nM bortezomib. Cells were then harvested, counted, and seeded in Methocult™ methylcellulose medium at 1000 cells per dish, in triplicate. After incubation for two weeks, colonies of greater than 30 cells were counted under an inverted microscope. Colony number was normalized to untreated control within a given pretreatment group to determine % colony formation after chemotherapy.

Animal xenografts studies

Protocols for all animal experiments were approved by the John Hopkins University Animal Care and Use Committee and were strictly followed. All xenografts were established from cells injected subcutaneously into the right hind flank of 5-7 week old female mice, in a total volume of 100uL, consisting of a 50:50 mix of 1x PBS and Matrigel^{TM}. Tumor volume measurements were calculated as $(L \times W^2)/2$. Aza was administered subcutaneously at 0.5mg/kg. Entinostat was administered intraperitoneally at 1mg/kg. All other chemotherapeutics were administered intraperitoneally. Vehicle for entinostat was 90% saline/10% DMSO. All other vehicle injections were saline. Injection volume was 5mL/kg for all drugs.

Xenografts established from pretreated cells

Following epigenetic treatment, mock and combination pretreated A549 and H460 cells were cultured for seven days in drug free media. On day 10, cells were harvested and counted, and 6.5×10^5 (A549) and 2.75×10^5 (H460) cells were injected into NOD/SCID. Tumors were grown to a starting size of $250mm^3$ (+/- 20%), then added to study. A549 bearing mice were treated with 2mg/kg cisplatin (days 2,9,16), 10mg/kg irinotecan (days 2,5,9,12,16,19), or vehicle (days 2,5,9,12,16,19). H460 bearing mice were treated with 2.5mg/kg docetaxel (q4d x 2) escalated to 5mg/kg docetaxel (q4d x 2), 10mg/kg irinotecan (q4d x 4) or vehicle, starting on day 1.

H358 xenografts and therapeutic administration of epigenetic therapy

Treatment naïve H358 cells were injected nu/nu mice (8×10^5 cells/mouse) and tumors were grown to a starting size of $110mm^3$ (+/- 25%). Mice were treated each week with

0.5mg/kg Aza (days 1-5) and 1mg/kg entinostat (day 5), or vehicle, for four one-week cycles. Beginning week five, mice received 2mg/kg cisplatin (day 2), 10mg/kg irinotecan (days 2 & 5), or vehicle (days 2 & 5), weekly for four weeks.

Patient-derived primary xenografts experiments

Treatment naïve LX14 and LX7 cells collected from freshly grown tumors were injected into NOD/SCID mice (10^6 cells/mouse). LX14 tumors were grown to a starting size of 115mm^3 (+/- 30%). Mice were then treated with vehicle or epigenetic therapy consisting of Aza (days 1-5) and entinostat (day 5) for three weeks. On day 20, representative vehicle tumors were harvested and pooled, single cells suspensions were generated, and $7.5x10^5$ cells/mouse were immediately injected into new NOD/SCID mice. On day 22, all epigenetic tumors were harvested and pooled, single cell suspensions were generated and $5x10^5$ cells/mouse were immediately injected into new NOD/SCID. Vehicle and epigenetic pretreated tumors were allowed to reach approximately 250mm^3 (+/- 20%) and randomized to recieve 30mg/kg gemcitabine or vehicle every third day for five injections. LX7 tumors were grown to a starting size of approximately 160mm^3 (+/- 25%). Mice were randomized to receive vehicle or Aza (days 1-3, 6-10, 13-17) and entinostat (days 3, 10, 17). On day 16 and 17, representative vehicle and epigenetic treated tumors, respectively, were harvested and pooled. Single cell suspensions were generated and frozen at -80°C in 90% FBS/10% DMSO for later use. Cells were later thawed on the same day, and 1.3 x 10^6 cells/mouse for both pretreatment conditions were injected into NOD/SCID mice. Once tumors reached approximately 140mm^3 (+/- 15%), mice were

treated with 2mg/kg cisplatin (days 1,8), 10mg/kg irinotecan (days 1,5,9 and 32,36,40), or vehicle (days 1,5,9).

IV. Conclusions and Future Directions

Using a mouse model to assess tumorigenicity of NSCLC cell lines following their treatment *in vitro* with Aza and entinostat, we have demonstrated that epigenetic based therapies can produce striking anti-tumor effects in select xenografts independent of apparent cytotoxicity in these cell lines *in vitro*. Growth of H358 and H1299 xenografts was significantly impaired following Aza treatment *in vitro*, despite the lesser degree of cytotoxicity in short term viability experiments observed in these compared several other cell lines. While we observed impaired proliferation with concordant increased cell death cell in Aza and combination treated H358 cells for several days following treatment, these cells were indistinguishable from control cells by the day of tumor cell injection into mice. Furthermore, despite antagonistic effects on cell viability in combination matrix assays, and only minor effects on proliferation post treatment, *in vitro* treatment with combination of Aza and entinostat profoundly inhibited growth of H1299 xenografts. Conversely, for cell lines exhibiting the highest degree of cytotoxicity in short term viability assays, and substantial decreases in cell viability and colony formation after treatment, epigenetic therapy exerted only minimal (H2170) to modest (H460) effects on tumorigenicity.

These data clearly indicate that the effects of Aza and entinostat on tumorigenicity of NSCLC cell lines do not directly correlate with acute cytotoxicity resulting from treatment with these agents. This strongly suggests that the anti-tumor effects we observed were due, at least in part, to alteration of the epigenome. Studies using similar models of leukemia and breast tumorigenicity have associated Aza-induced epigenomic changes with anti-tumor efficacy [86], but we have yet to demonstrate this in our NSCLC

models. Similar epigenomic reprogramming following Aza and entinostat treatment *in vivo* has been demonstrated using a rat orthotopic model of NSCLC, however these studies did not address the effects of entinostat alone [109]. Therefore, it is important that our future work address the epigenomic changes resulting from Aza and entinostat treatment in our NSCLC cell line panel.

To that end, we have sampled cells at the end of treatment, one week, and two weeks after treatment, to assess methylation of >485,000 sites using the Illumina Infinium HumanMethylation450 BeadChip array and expression of >41,000 genes using the Agilent 44K Gene Expression array. While some studies have associated epigenetic changes with response to demethylating agents and HDAC inhibitors in the clinic, this has been particularly challenging to clearly demonstrate [80, 110, 111, 114]. Therefore, it is important that we determine whether subsets of genes can be correlated with response in our tumorigenicity models. In addition, we aim to identify changes in protein expression in cells collected one week after treatment using iTRAQ technology. These studies are limited to assessment of proteins present in whole-cell extract, and therefore will omit insoluble membrane proteins, but provide a means of assessing changes in a large number of proteins, and may provide critical insight to the relevance of many of the transcript changes observed in the gene expression analysis.

Our data in a small panel of NSCLC cell lines shows that only select xenografts are significantly affected by epigenetic therapy, which agrees with the results from the phase I/II trial of Aza and entinostat in heavily pretreated patients with advanced stage NSCLC where only a small percentage of patients benefited substantially from combinatorial epigenetic therapy. It remains to be seen whether this therapy will have

greater utility in patients with earlier stage disease who have undergone fewer prior therapies. Preclinically, it is important to extend this work to a greater number of cell lines to better define an overall response rate in these models, and to more accurately associate epigenomic changes with response to therapy. While cell line models certainly have limitations with respect to biomarker discovery, these studies may help provide a candidate gene signature for assessment as clinical biomarkers predictive of patient response. Ongoing preclinical and clinical work to define relevant biomarkers will be essential for the proper determination of a target patient population.

It should also be acknowledged that our data highlight the limitations of using standard *in vitro* cytotoxicity assays to assess sensitivity of cell lines to epigenetic agents. The most profound response achieved in our tumorigenicity model occurred in using a cell line (H1299) that exhibited little to no evidence of sensitivity to combinatorial epigenetic therapy in shorter term *in vitro* assays. This exemplifies, preclinically, the gradual nature and durability of response to epigenetic therapy in patients treated with lower, less toxic doses of these agents, and differs substantially from the rapid, but generally short-lived responses achieved with conventional cytotoxic therapy administered near the MTD.

In addition to the effects on tumorigenicity, we found that combinatorial epigenetic therapy can alter sensitivity of NSCLC both cell line and patient derived xenografts to subsequent irinotecan chemotherapy. However, results with other chemotherapeutic agents were disappointing, with little to no improvement in chemosensitivity noted in our *in vitro* and *in vivo* models. Overall, these data suggest that the fraction of NSCLC tumors that exhibit altered sensitivity to subsequent chemotherapy

may only represent a small fraction of patients. However, we acknowledge that our model systems encompassed a limited number of NSCLC lines and chemotherapeutic agents. Expansion of this work to cover additional lines and relevant therapies, both cytotoxic and targeted (such as EGFR inhibitors, for example) may yield different conclusions. In addition, our in vitro dosing of Aza and entinostat was fixed, and may not represent the optimal dosing strategies to augment chemotherapeutic efficacy in these model systems, and exploration of additional dosing regimens will be important in defining the value of epigenetic priming in preclinical models. Ultimately, it is essential to specifically address this priming strategy in the clinic, and to that end, a randomized phase II clinical trial in patients with advanced lung cancer has been initiated at Johns Hopkins to formally test this.

Still, preclinical studies of epigenetic priming like the work presented here may prove valuable. While we observed sensitization of A549 and LX7 xenografts to irinotecan following combinatorial epigenetic therapy, we have yet to address the mechanisms responsible. Assessment of gene expression changes before and after irinotecan therapy may provide inside into the pathways altered by epigenetic therapy that may invoke enhanced sensitivity to irinotecan. Identification of candidate genes would allow for more specific mechanistic studies involving manipulation of gene expression or pathway activation. In addition, it is important that we assess whether A49 and H460 respond similarly *in vitro* to the active metabolite of irinotecan, SN38, following epigenetic therapy, as this would enable detailed mechanistic studies using our existing model systems.

While there are key differences between efficacy in our preclinical models and clinical outcome in patients, including pharmacokinetics, the tumor microenvironment, and the involvement of the patient's immune system, comparative data from the clinical trial in progress and the preclinical work presented here will help define the relevance of these models to the treatment of NSCLC.

V. References

1. Jemal A, Bray F, Center MM, et al. Global cancer statistics. CA Cancer J Clin 2011;61(2):69-90.
2. Siegel R, Naishadham D, Jemal A. Cancer statistics, 2013. CA Cancer J Clin 2013;63(1):11-30.
3. Pao W, Miller V, Zakowski M, et al. EGF receptor gene mutations are common in lung cancers from "never smokers" and are associated with sensitivity of tumors to gefitinib and erlotinib. Proceedings of the National Academy of Sciences of the United States of America 2004;101(36):13306-11.
4. Sequist LV, Martins RG, Spigel D, et al. First-line gefitinib in patients with advanced non-small-cell lung cancer harboring somatic EGFR mutations. Journal of clinical oncology : official journal of the American Society of Clinical Oncology 2008;26(15):2442-9.
5. Camidge DR, Bang YJ, Kwak EL, et al. Activity and safety of crizotinib in patients with ALK-positive non-small-cell lung cancer: updated results from a phase 1 study. Lancet Oncol 2012;13(10):1011-9.
6. Rekhtman N, Paik PK, Arcila ME, et al. Clarifying the spectrum of driver oncogene mutations in biomarker-verified squamous carcinoma of lung: lack of EGFR/KRAS and presence of PIK3CA/AKT1 mutations. Clin Cancer Res 2012;18(4):1167-76.
7. Engelman JA, Janne PA. Mechanisms of acquired resistance to epidermal growth factor receptor tyrosine kinase inhibitors in non-small cell lung cancer. Clin Cancer Res 2008;14(10):2895-9.

8. Choi YL, Soda M, Yamashita Y, et al. EML4-ALK mutations in lung cancer that confer resistance to ALK inhibitors. NEnglJMed 2010;363(18):1734-39.
9. Katayama R, Shaw AT, Khan TM, et al. Mechanisms of acquired crizotinib resistance in ALK-rearranged lung Cancers. Sci Transl Med 2012;4(120):120ra17.
10. Jones PA, Baylin SB. The fundamental role of epigenetic events in cancer. Nature reviews Genetics 2002;3(6):415-28.
11. Esteller M. Cancer epigenomics: DNA methylomes and histone-modification maps. Nature reviews Genetics 2007;8(4):286-98.
12. Jones PA, Baylin SB. The epigenomics of cancer. Cell 2007;128(4):683-92.
13. Daskalos A, Nikolaidis G, Xinarianos G, et al. Hypomethylation of retrotransposable elements correlates with genomic instability in non-small cell lung cancer. International journal of cancer Journal international du cancer 2009;124(1):81-7.
14. Ehrlich M. DNA hypomethylation in cancer cells. Epigenomics 2009;1(2):239-59.
15. Wolff EM, Byun HM, Han HF, et al. Hypomethylation of a LINE-1 promoter activates an alternate transcript of the MET oncogene in bladders with cancer. PLoS genetics 2010;6(4):e1000917.
16. Fraga MF, Ballestar E, Villar-Garea A, et al. Loss of acetylation at Lys16 and trimethylation at Lys20 of histone H4 is a common hallmark of human cancer. Nature genetics 2005;37(4):391-400.
17. Wen B, Wu H, Shinkai Y, et al. Large histone H3 lysine 9 dimethylated chromatin blocks distinguish differentiated from embryonic stem cells. Nature genetics 2009;41(2):246-50.

18. Irizarry RA, Ladd-Acosta C, Wen B, et al. The human colon cancer methylome shows similar hypo- and hypermethylation at conserved tissue-specific CpG island shores. Nature genetics 2009;41(2):178-86.

19. Hansen KD, Timp W, Bravo HC, et al. Increased methylation variation in epigenetic domains across cancer types. Nature genetics 2011;43(8):768-75.

20. Keshet I, Schlesinger Y, Farkash S, et al. Evidence for an instructive mechanism of de novo methylation in cancer cells. Nature genetics 2006;38(2):149-53.

21. Ohm JE, McGarvey KM, Yu X, et al. A stem cell-like chromatin pattern may predispose tumor suppressor genes to DNA hypermethylation and heritable silencing. Nature genetics 2007;39(2):237-42.

22. Widschwendter M, Fiegl H, Egle D, et al. Epigenetic stem cell signature in cancer. Nature genetics 2007;39(2):157-8.

23. Schlesinger Y, Straussman R, Keshet I, et al. Polycomb-mediated methylation on Lys27 of histone H3 pre-marks genes for de novo methylation in cancer. Nature genetics 2007;39(2):232-6.

24. Gal-Yam EN, Egger G, Iniguez L, et al. Frequent switching of Polycomb repressive marks and DNA hypermethylation in the PC3 prostate cancer cell line. Proceedings of the National Academy of Sciences of the United States of America 2008;105(35):12979-84.

25. Easwaran H, Johnstone SE, Van Neste L, et al. A DNA hypermethylation module for the stem/progenitor cell signature of cancer. Genome Res 2012;22(5):837-49.

26. Baylin SB, Jones PA. A decade of exploring the cancer epigenome - biological and translational implications. Nature reviews Cancer 2011;11(10):726-34.

27. Bachman KE, Park BH, Rhee I, et al. Histone modifications and silencing prior to DNA methylation of a tumor suppressor gene. Cancer cell 2003;3(1):89-95.

28. Mutskov V, Felsenfeld G. Silencing of transgene transcription precedes methylation of promoter DNA and histone H3 lysine 9. The EMBO journal 2004;23(1):138-49.

29. Strunnikova M, Schagdarsurengin U, Kehlen A, et al. Chromatin inactivation precedes de novo DNA methylation during the progressive epigenetic silencing of the RASSF1A promoter. Molecular and cellular biology 2005;25(10):3923-33.

30. Coolen MW, Stirzaker C, Song JZ, et al. Consolidation of the cancer genome into domains of repressive chromatin by long-range epigenetic silencing (LRES) reduces transcriptional plasticity. Nature cell biology 2010;12(3):235-46.

31. Esteller M, Corn PG, Baylin SB, et al. A gene hypermethylation profile of human cancer. Cancer research 2001;61(8):3225-9.

32. Zochbauer-Muller S, Fong KM, Virmani AK, et al. Aberrant promoter methylation of multiple genes in non-small cell lung cancers. Cancer research 2001;61(1):249-55.

33. Belinsky SA. Gene-promoter hypermethylation as a biomarker in lung cancer. Nature reviews Cancer 2004;4(9):707-17.

34. Hanahan D, Weinberg RA. Hallmarks of cancer: the next generation. Cell 2011;144(5):646-74.

35. Nuovo GJ, Plaia TW, Belinsky SA, et al. In situ detection of the hypermethylation-induced inactivation of the p16 gene as an early event in oncogenesis. Proceedings

of the National Academy of Sciences of the United States of America 1999;96(22):12754-9.

36. Licchesi JD, Westra WH, Hooker CM, et al. Promoter hypermethylation of hallmark cancer genes in atypical adenomatous hyperplasia of the lung. Clin Cancer Res 2008;14(9):2570-8.

37. Licchesi JD, Westra WH, Hooker CM, et al. Epigenetic alteration of Wnt pathway antagonists in progressive glandular neoplasia of the lung. Carcinogenesis 2008;29(5):895-904.

38. Sterlacci W, Tzankov A, Veits L, et al. A comprehensive analysis of p16 expression, gene status, and promoter hypermethylation in surgically resected non-small cell lung carcinomas. Journal of thoracic oncology : official publication of the International Association for the Study of Lung Cancer 2011;6(10):1649-57.

39. Brock MV, Hooker CM, Ota-Machida E, et al. DNA methylation markers and early recurrence in stage I lung cancer. The New England journal of medicine 2008;358(11):1118-28.

40. Baylin SB, Ohm JE. Epigenetic gene silencing in cancer - a mechanism for early oncogenic pathway addiction? Nature reviews Cancer 2006;6(2):107-16.

41. Selamat SA, Chung BS, Girard L, et al. Genome-scale analysis of DNA methylation in lung adenocarcinoma and integration with mRNA expression. Genome Res 2012;22(7):1197-211.

42. Toyota M, Ahuja N, Ohe-Toyota M, et al. CpG island methylator phenotype in colorectal cancer. Proceedings of the National Academy of Sciences of the United States of America 1999;96(15):8681-6.

43. Shinjo K, Okamoto Y, An B, et al. Integrated analysis of genetic and epigenetic alterations reveals CpG island methylator phenotype associated with distinct clinical characters of lung adenocarcinoma. Carcinogenesis 2012;33(7):1277-85.

44. Lockwood WW, Wilson IM, Coe BP, et al. Divergent genomic and epigenomic landscapes of lung cancer subtypes underscore the selection of different oncogenic pathways during tumor development. PLoS One 2012;7(5):e37775.

45. Jeong S, Liang G, Sharma S, et al. Selective anchoring of DNA methyltransferases 3A and 3B to nucleosomes containing methylated DNA. Molecular and cellular biology 2009;29(19):5366-76.

46. Jones PA, Liang G. Rethinking how DNA methylation patterns are maintained. Nature reviews Genetics 2009;10(11):805-11.

47. Rhee I, Jair KW, Yen RW, et al. CpG methylation is maintained in human cancer cells lacking DNMT1. Nature 2000;404(6781):1003-7.

48. Rhee I, Bachman KE, Park BH, et al. DNMT1 and DNMT3b cooperate to silence genes in human cancer cells. Nature 2002;416(6880):552-6.

49. Jair KW, Bachman KE, Suzuki H, et al. De novo CpG island methylation in human cancer cells. Cancer research 2006;66(2):682-92.

50. Kim H, Kwon YM, Kim JS, et al. Elevated mRNA levels of DNA methyltransferase-1 as an independent prognostic factor in primary nonsmall cell lung cancer. Cancer 2006;107(5):1042-9.

51. Lin RK, Hsu HS, Chang JW, et al. Alteration of DNA methyltransferases contributes to 5'CpG methylation and poor prognosis in lung cancer. Lung cancer 2007;55(2):205-13.

52. Lin RK, Wu CY, Chang JW, et al. Dysregulation of p53/Sp1 control leads to DNA methyltransferase-1 overexpression in lung cancer. Cancer research 2010;70(14):5807-17.

53. Tang YA, Lin RK, Tsai YT, et al. MDM2 overexpression deregulates the transcriptional control of RB/E2F leading to DNA methyltransferase 3A overexpression in lung cancer. Clin Cancer Res 2012;18(16):4325-33.

54. Iorio MV, Piovan C, Croce CM. Interplay between microRNAs and the epigenetic machinery: an intricate network. Biochimica et biophysica acta 2010;1799(10-12):694-701.

55. Fabbri M, Garzon R, Cimmino A, et al. MicroRNA-29 family reverts aberrant methylation in lung cancer by targeting DNA methyltransferases 3A and 3B. Proceedings of the National Academy of Sciences of the United States of America 2007;104(40):15805-10.

56. Garzon R, Liu S, Fabbri M, et al. MicroRNA-29b induces global DNA hypomethylation and tumor suppressor gene reexpression in acute myeloid leukemia by targeting directly DNMT3A and 3B and indirectly DNMT1. Blood 2009;113(25):6411-8.

57. Agoston AT, Argani P, Yegnasubramanian S, et al. Increased protein stability causes DNA methyltransferase 1 dysregulation in breast cancer. The Journal of biological chemistry 2005;280(18):18302-10.

58. Zhou Q, Agoston AT, Atadja P, et al. Inhibition of histone deacetylases promotes ubiquitin-dependent proteasomal degradation of DNA methyltransferase 1 in human breast cancer cells. Molecular cancer research : MCR 2008;6(5):873-83.

59. Wang J, Hevi S, Kurash JK, et al. The lysine demethylase LSD1 (KDM1) is required for maintenance of global DNA methylation. Nature genetics 2009;41(1):125-9.

60. Sasaki H, Moriyama S, Nakashima Y, et al. Histone deacetylase 1 mRNA expression in lung cancer. Lung cancer 2004;46(2):171-8.

61. Minamiya Y, Ono T, Saito H, et al. Expression of histone deacetylase 1 correlates with a poor prognosis in patients with adenocarcinoma of the lung. Lung cancer 2011;74(2):300-4.

62. Lv T, Yuan D, Miao X, et al. Over-expression of LSD1 promotes proliferation, migration and invasion in non-small cell lung cancer. PLoS One 2012;7(4):e35065.

63. Wang L, Wang J, Sun S, et al. A novel DNMT3B subfamily, DeltaDNMT3B, is the predominant form of DNMT3B in non-small cell lung cancer. International journal of oncology 2006;29(1):201-7.

64. Wang J, Walsh G, Liu DD, et al. Expression of Delta DNMT3B variants and its association with promoter methylation of p16 and RASSF1A in primary non-small cell lung cancer. Cancer research 2006;66(17):8361-6.

65. Kim MS, Kim YR, Yoo NJ, et al. Mutational analysis of DNMT3A gene in acute leukemias and common solid cancers. Acta Pathologica, Microbiologica, et Immunologica Scandinavica 2013;121(2):85-94.

66. Gao Q, Steine EJ, Barrasa MI, et al. Deletion of the de novo DNA methyltransferase Dnmt3a promotes lung tumor progression. Proceedings of the National Academy of Sciences of the United States of America 2011;108(44):18061-6.

67. Wu H, Coskun V, Tao J, et al. Dnmt3a-dependent nonpromoter DNA methylation facilitates transcription of neurogenic genes. Science 2010;329(5990):444-8.

68. Challen GA, Sun D, Jeong M, et al. Dnmt3a is essential for hematopoietic stem cell differentiation. Nature genetics 2012;44(1):23-31.

69. Lister R, Pelizzola M, Dowen RH, et al. Human DNA methylomes at base resolution show widespread epigenomic differences. Nature 2009;462(7271):315-22.

70. Marks PA. Histone deacetylase inhibitors: a chemical genetics approach to understanding cellular functions. Biochimica et biophysica acta 2010;1799(10-12):717-25.

71. Lane AA, Chabner BA. Histone deacetylase inhibitors in cancer therapy. Journal of clinical oncology : official journal of the American Society of Clinical Oncology 2009;27(32):5459-68.

72. Bartling B, Hofmann HS, Boettger T, et al. Comparative application of antibody and gene array for expression profiling in human squamous cell lung carcinoma. Lung cancer 2005;49(2):145-54.

73. Osada H, Tatematsu Y, Saito H, et al. Reduced expression of class II histone deacetylase genes is associated with poor prognosis in lung cancer patients. International journal of cancer Journal international du cancer 2004;112(1):26-32.

74. Schuster-Bockler B, Lehner B. Chromatin organization is a major influence on regional mutation rates in human cancer cells. Nature 2012;488(7412):504-7.

75. Jones PA, Taylor SM. Cellular differentiation, cytidine analogs and DNA methylation. Cell 1980;20(1):85-93.

76. Santi DV, Norment A, Garrett CE. Covalent bond formation between a DNA-cytosine methyltransferase and DNA containing 5-azacytosine. Proceedings of the National Academy of Sciences of the United States of America 1984;81(22):6993-7.

77. Ferguson AT, Vertino PM, Spitzner JR, et al. Role of estrogen receptor gene demethylation and DNA methyltransferase.DNA adduct formation in 5-aza-2'deoxycytidine-induced cytotoxicity in human breast cancer cells. The Journal of biological chemistry 1997;272(51):32260-6.

78. Christman JK. 5-Azacytidine and 5-aza-2'-deoxycytidine as inhibitors of DNA methylation: mechanistic studies and their implications for cancer therapy. Oncogene 2002;21(35):5483-95.

79. Patel K, Dickson J, Din S, et al. Targeting of 5-aza-2'-deoxycytidine residues by chromatin-associated DNMT1 induces proteasomal degradation of the free enzyme. Nucleic acids research 2010;38(13):4313-24.

80. Issa JP, Kantarjian HM. Targeting DNA methylation. Clin Cancer Res 2009;15(12):3938-46.

81. Juttermann R, Li E, Jaenisch R. Toxicity of 5-aza-2'-deoxycytidine to mammalian cells is mediated primarily by covalent trapping of DNA methyltransferase rather than DNA demethylation. Proceedings of the National Academy of Sciences of the United States of America 1994;91(25):11797-801.

82. Oka M, Meacham AM, Hamazaki T, et al. De novo DNA methyltransferases Dnmt3a and Dnmt3b primarily mediate the cytotoxic effect of 5-aza-2'-deoxycytidine. Oncogene 2005;24(19):3091-9.

83. Palii SS, Van Emburgh BO, Sankpal UT, et al. DNA methylation inhibitor 5-Aza-2'-deoxycytidine induces reversible genome-wide DNA damage that is distinctly influenced by DNA methyltransferases 1 and 3B. Molecular and cellular biology 2008;28(2):752-71.

84. Flotho C, Claus R, Batz C, et al. The DNA methyltransferase inhibitors azacitidine, decitabine and zebularine exert differential effects on cancer gene expression in acute myeloid leukemia cells. Leukemia 2009;23(6):1019-28.

85. Hagemann S, Heil O, Lyko F, et al. Azacytidine and decitabine induce gene-specific and non-random DNA demethylation in human cancer cell lines. PLoS One 2011;6(3):e17388.

86. Tsai HC, Li H, Van Neste L, et al. Transient low doses of DNA-demethylating agents exert durable antitumor effects on hematological and epithelial tumor cells. Cancer cell 2012;21(3):430-46.

87. Momparler RL, Ayoub J. Potential of 5-aza-2'-deoxycytidine (Decitabine) a potent inhibitor of DNA methylation for therapy of advanced non-small cell lung cancer. Lung cancer 2001;34 Suppl 4:S111-5.

88. Schrump DS, Fischette MR, Nguyen DM, et al. Phase I study of decitabine-mediated gene expression in patients with cancers involving the lungs, esophagus, or pleura. Clin Cancer Res 2006;12(19):5777-85.

89. Kelly TK, De Carvalho DD, Jones PA. Epigenetic modifications as therapeutic targets. Nature biotechnology 2010;28(10):1069-78.

90. Yoshida M, Kijima M, Akita M, et al. Potent and specific inhibition of mammalian histone deacetylase both in vivo and in vitro by trichostatin A. The Journal of biological chemistry 1990;265(28):17174-9.

91. Bolden JE, Peart MJ, Johnstone RW. Anticancer activities of histone deacetylase inhibitors. Nature reviews Drug discovery 2006;5(9):769-84.

92. Miyanaga A, Gemma A, Noro R, et al. Antitumor activity of histone deacetylase inhibitors in non-small cell lung cancer cells: development of a molecular predictive model. Molecular cancer therapeutics 2008;7(7):1923-30.

93. Brazelle W, Kreahling JM, Gemmer J, et al. Histone deacetylase inhibitors downregulate checkpoint kinase 1 expression to induce cell death in non-small cell lung cancer cells. PLoS One 2010;5(12):e14335.

94. Gilbert J, Baker SD, Bowling MK, et al. A phase I dose escalation and bioavailability study of oral sodium phenylbutyrate in patients with refractory solid tumor malignancies. Clin Cancer Res 2001;7(8):2292-300.

95. Sandor V, Bakke S, Robey RW, et al. Phase I trial of the histone deacetylase inhibitor, depsipeptide (FR901228, NSC 630176), in patients with refractory neoplasms. Clin Cancer Res 2002;8(3):718-28.

96. Ryan QC, Headlee D, Acharya M, et al. Phase I and pharmacokinetic study of MS-275, a histone deacetylase inhibitor, in patients with advanced and refractory solid tumors or lymphoma. Journal of clinical oncology : official journal of the American Society of Clinical Oncology 2005;23(17):3912-22.

97. Gore L, Rothenberg ML, O'Bryant CL, et al. A phase I and pharmacokinetic study of the oral histone deacetylase inhibitor, MS-275, in patients with refractory solid tumors and lymphomas. Clin Cancer Res 2008;14(14):4517-25.

98. Schrump DS, Fischette MR, Nguyen DM, et al. Clinical and molecular responses in lung cancer patients receiving Romidepsin. Clin Cancer Res 2008;14(1):188-98.

99. Siu LL, Pili R, Duran I, et al. Phase I study of MGCD0103 given as a three-times-per-week oral dose in patients with advanced solid tumors. Journal of clinical oncology : official journal of the American Society of Clinical Oncology 2008;26(12):1940-7.

100. Vansteenkiste J, Van Cutsem E, Dumez H, et al. Early phase II trial of oral vorinostat in relapsed or refractory breast, colorectal, or non-small cell lung cancer. Investigational new drugs 2008;26(5):483-8.

101. Traynor AM, Dubey S, Eickhoff JC, et al. Vorinostat (NSC# 701852) in patients with relapsed non-small cell lung cancer: a Wisconsin Oncology Network phase II study. Journal of thoracic oncology : official publication of the International Association for the Study of Lung Cancer 2009;4(4):522-6.

102. Ramalingam SS, Kummar S, Sarantopoulos J, et al. Phase I study of vorinostat in patients with advanced solid tumors and hepatic dysfunction: a National Cancer Institute Organ Dysfunction Working Group study. Journal of clinical oncology : official journal of the American Society of Clinical Oncology 2010;28(29):4507-12.

103. Ramalingam SS, Maitland ML, Frankel P, et al. Carboplatin and Paclitaxel in combination with either vorinostat or placebo for first-line therapy of advanced

non-small-cell lung cancer. Journal of clinical oncology : official journal of the American Society of Clinical Oncology 2010;28(1):56-62.

104. Witta SE, Jotte RM, Konduri K, et al. Randomized phase II trial of erlotinib with and without entinostat in patients with advanced non-small-cell lung cancer who progressed on prior chemotherapy. Journal of clinical oncology : official journal of the American Society of Clinical Oncology 2012;30(18):2248-55.
105. Cameron EE, Bachman KE, Myohanen S, et al. Synergy of demethylation and histone deacetylase inhibition in the re-expression of genes silenced in cancer. Nature genetics 1999;21(1):103-7.
106. Boivin AJ, Momparler LF, Hurtubise A, et al. Antineoplastic action of 5-aza-2'-deoxycytidine and phenylbutyrate on human lung carcinoma cells. Anti-cancer drugs 2002;13(8):869-74.
107. Zhu WG, Lakshmanan RR, Beal MD, et al. DNA methyltransferase inhibition enhances apoptosis induced by histone deacetylase inhibitors. Cancer research 2001;61(4):1327-33.
108. Belinsky SA, Klinge DM, Stidley CA, et al. Inhibition of DNA methylation and histone deacetylation prevents murine lung cancer. Cancer research 2003;63(21):7089-93.
109. Belinsky SA, Grimes MJ, Picchi MA, et al. Combination therapy with vidaza and entinostat suppresses tumor growth and reprograms the epigenome in an orthotopic lung cancer model. Cancer research 2011;71(2):454-62.

110. Gore SD, Baylin S, Sugar E, et al. Combined DNA methyltransferase and histone deacetylase inhibition in the treatment of myeloid neoplasms. Cancer research 2006;66(12):6361-9.

111. Fandy TE, Herman JG, Kerns P, et al. Early epigenetic changes and DNA damage do not predict clinical response in an overlapping schedule of 5-azacytidine and entinostat in patients with myeloid malignancies. Blood 2009;114(13):2764-73.

112. Lin J, Gilbert J, Rudek MA, et al. A phase I dose-finding study of 5-azacytidine in combination with sodium phenylbutyrate in patients with refractory solid tumors. Clin Cancer Res 2009;15(19):6241-9.

113. Braiteh F, Soriano AO, Garcia-Manero G, et al. Phase I study of epigenetic modulation with 5-azacytidine and valproic acid in patients with advanced cancers. Clin Cancer Res 2008;14(19):6296-301.

114. Juergens RA, Wrangle J, Vendetti FP, et al. Combination epigenetic therapy has efficacy in patients with refractory advanced non-small cell lung cancer. Cancer discovery 2011;1(7):598-607.

115. Glasspool RM, Teodoridis JM, Brown R. Epigenetics as a mechanism driving polygenic clinical drug resistance. British journal of cancer 2006;94(8):1087-92.

116. Plumb JA, Strathdee G, Sludden J, et al. Reversal of drug resistance in human tumor xenografts by 2'-deoxy-5-azacytidine-induced demethylation of the hMLH1 gene promoter. Cancer research 2000;60(21):6039-44.

117. Wu J, Hu CP, Gu QH, et al. Trichostatin A sensitizes cisplatin-resistant A549 cells to apoptosis by up-regulating death-associated protein kinase. Acta pharmacologica Sinica 2010;31(1):93-101.

118. Sharma SV, Lee DY, Li B, et al. A chromatin-mediated reversible drug-tolerant state in cancer cell subpopulations. Cell 2010;141(1):69-80.

119. Cooper SJ, von Roemeling CA, Kang KH, et al. Reexpression of tumor suppressor, sFRP1, leads to antitumor synergy of combined HDAC and methyltransferase inhibitors in chemoresistant cancers. Molecular cancer therapeutics 2012;11(10):2105-15.

120. Candelaria M, Gallardo-Rincon D, Arce C, et al. A phase II study of epigenetic therapy with hydralazine and magnesium valproate to overcome chemotherapy resistance in refractory solid tumors. Annals of oncology : official journal of the European Society for Medical Oncology / ESMO 2007;18(9):1529-38.

121. Fu S, Hu W, Iyer R, et al. Phase 1b-2a study to reverse platinum resistance through use of a hypomethylating agent, azacitidine, in patients with platinum-resistant or platinum-refractory epithelial ovarian cancer. Cancer 2011;117(8):1661-9.

122. Matei D, Fang F, Shen C, et al. Epigenetic resensitization to platinum in ovarian cancer. Cancer research 2012;72(9):2197-205.

123. Lehar J, Krueger AS, Avery W, et al. Synergistic drug combinations tend to improve therapeutically relevant selectivity. Nature biotechnology 2009;27(7):659-66.

124. Berenbaum MC. What is synergy? Pharmacological reviews 1989;41(2):93-141.

125. Lehar J, Zimmermann GR, Krueger AS, et al. Chemical combination effects predict connectivity in biological systems. Molecular systems biology 2007;3:80.

126. Hauschild A, Trefzer U, Garbe C, et al. Multicenter phase II trial of the histone deacetylase inhibitor pyridylmethyl-N-{4-[(2-aminophenyl)-carbamoyl]-benzyl}-

carbamate in pretreated metastatic melanoma. Melanoma research 2008;18(4):274-8.

127. Herman JG, Graff JR, Myohanen S, et al. Methylation-specific PCR: a novel PCR assay for methylation status of CpG islands. Proceedings of the National Academy of Sciences of the United States of America 1996;93(18):9821-6.

128. Zinn RL, Pruitt K, Eguchi S, et al. hTERT is expressed in cancer cell lines despite promoter DNA methylation by preservation of unmethylated DNA and active chromatin around the transcription start site. Cancer research 2007;67(1):194-201.

129. Moffat J, Grueneberg DA, Yang X, et al. A lentiviral RNAi library for human and mouse genes applied to an arrayed viral high-content screen. Cell 2006;124(6):1283-98.

130. Brzezianska E, Dutkowska A, Antczak A. The significance of epigenetic alterations in lung carcinogenesis. Molecular biology reports 2013;40(1):309-25.

131. Steele N, Finn P, Brown R, et al. Combined inhibition of DNA methylation and histone acetylation enhances gene re-expression and drug sensitivity in vivo. British journal of cancer 2009;100(5):758-63.

132. Zeller C, Dai W, Steele NL, et al. Candidate DNA methylation drivers of acquired cisplatin resistance in ovarian cancer identified by methylome and expression profiling. Oncogene 2012;31(42):4567-76.

133. Daniel VC, Marchionni L, Hierman JS, et al. A primary xenograft model of small-cell lung cancer reveals irreversible changes in gene expression imposed by culture in vitro. Cancer research 2009;69(8):3364-73.

VI. Biographical Sketch

Frank P. Vendetti III

Born July 10, 1982 in Franklin, Pennsylvania

Education

University of Pittsburgh	2000-2004	BSc	Biological Science
Johns Hopkins University	2005-Present	PhD	Pharmacology and Molecular Sciences

Personal Statement

I am particularly interested in the study of novel approaches to the treatment of cancer. As a graduate student in the laboratory of Dr. Charles Rudin, I studied the effects of epigenetic based therapies, including demethylating agents and histone deacetylase inhibitors, in a variety of preclinical models of non-small cell lung cancer (NSCLC). My postdoctoral research in the laboratory of Dr. Chris Bakkenist will focus on investigating the therapeutic utility of ATM kinase and ATR kinase inhibition, with or without ionizing radiation or DNA-damaging agents, in models of lung, breast, and ovarian cancer.

Research Experience

Graduate (Jan 2006-Oct 2013)

Advisor: Charles M. Rudin, M.D., Ph.D.

Title: Assessing epigenetic therapy in preclinical models of non-small cell lung cancer

Undergraduate (May 2003- Dec 2004)

Advisor: Jeffrey D. Hildebrand, Ph.D.

Title: Analysis of Shroom function in epithelial cell architecture and analysis of Apxl-actin interactions.

Academic Awards and Honors

Howard Hughes Medical Institute (HHMI) Research Fellowship, Aug 2003-Apr 2004

University of Pittsburgh Academic Scholarship, August 2000-April 2004

William Binder Zeder Memorial Scholarship, August 2003

National Society of Collegiate Scholars, inducted October 2001

Outstanding Freshman in Biological Sciences Award, September 2001

Publications

1. Vendetti FP, Rudin CM. Epigenetic therapy in non-small-cell lung cancer: targeting DNA methyltransferases and histone deacetylases. Expert Opin Biol Ther. 2013 Sep;13(9):1273-85. (PMCID not available)
2. Juergens RA, Wrangle J, Vendetti FP, et al. Combination epigenetic therapy has efficacy in patients with refractory advanced non-small cell lung cancer. Cancer Discov. 2011 Dec;1(7):598-607. (PMCID:PMC3353724)
3. Dietz ML, Bernaciak TM, Vendetti F, et al. Differential actin-dependent localization modulates the evolutionarily conserved activity of Shroom family proteins. J Biol Chem. 2006 Jul 21;281(29):20542-54. (PMCID not available)